

**THIS MICROFILM MAY NOT BE FULLY
DISTRIBUTED IN ANY WAY WITHOUT
IN EACH INSTANCE, PROCURED THROUGH
LIBRARIES, MASSACHUSETTS INSTITUTE OF TECHNOLOGY**

ADAPTIVE ESTIMATION AND CONTROL FOR
NUCLEAR POWER PLANT LOAD CHANGES

by

ROBERT L. MOORE, JR.

S.B., University of Michigan
(1964)

M.S., Massachusetts Institute of Technology
(1965)

E.E., Massachusetts Institute of Technology
(1966)

SUBMITTED IN PARTIAL FULFILLMENT OF THE
REQUIREMENTS FOR THE DEGREE OF
DOCTOR OF PHILOSOPHY

at the

MASSACHUSETTS INSTITUTE OF TECHNOLOGY

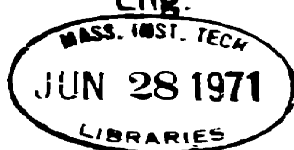
May, 1971



Signature of Author
Department of Electrical Engineering, May 21, 1971

Certified by
Thesis Supervisor

Accepted by
Chairman, Departmental Committee on Graduate Students
Eng.



ADAPTIVE ESTIMATION AND CONTROL FOR
NUCLEAR POWER PLANT LOAD CHANGES

by

Robert L. Moore, Jr.

Submitted to the Department of Electrical Engineering on May 21, 1971 in partial fulfillment of the requirements for the degree of Doctor of Philosophy.

ABSTRACT

The problem being considered is the control of power load changes in a nuclear power plant. In particular, the problem is that of making large and fast load changes without causing serious disturbances to the plant operation. In order to make such load changes, a control strategy is designed to coordinate two major plant inputs - the reactor control rods and the turbine load. However, to be viable the control must overcome several kinds of variation and uncertainty in plant behavior. Some variations are due to slow physical changes in the plant. Other variations in behavior are due to unmeasured current plant conditions and to random disturbances. These variations, together with the inadequacy of simple models to describe the plant, lead to uncertainty in the plant behavior. The major contribution of this thesis is to provide means for overcoming the problems of variation and uncertainty, so that large and fast power load changes can be made.

The control developed in this study makes use of a stochastic model. A low order state variable form stochastic model is used to represent the plant. The parameters of this model are identified from measurement data records, using a maximum likelihood identification technique. The stochastic model is then used in a state estimator which gives estimates of important unmeasured plant variables. The stochastic model is also used to adjust control constraints and to predict the plant performance during the load change for display and monitoring purposes. In the event that the plant behavior deviates from the model predictions, the model is adapted to be consistent with the plant performance. These techniques together overcome the difficulties of variation and uncertainty in the nuclear plant behavior, thus permitting large, fast load changes to be made without upsetting the plant operation.

A nuclear power plant was not available for experimentation; therefore, a detailed and realistic high order simulation of a plant was used. The simulated plant included nonlinear effects, disturbances and measurement

noise. The simulation was run on an analog computer which was treated as an actual plant by the digital control computer. The experiments performed in this study clearly demonstrate the feasibility of control of large and fast load changes on a nuclear power plant, and these can be made much more smoothly than the conventional control of small load changes. The experiments also demonstrate the feasibility of detecting and adapting to plant variation, and the feasibility of control in the presence of uncertainty.

Thesis Supervisor: Fred C. Schweppe
Title: Associate Professor of Electrical Engineering

ACKNOWLEDGEMENTS

This study would not have been possible without the active encouragement and support of numerous people and organizations. On the organization level, thanks are given to the New England Electric Company for allowing a load change on the Connecticut Yankee Reactor to be observed from the control room and for allowing reactor operators to be interviewed. Thanks are also given the Westinghouse Electric Corporation for discussions on nuclear power plant control. A special thanks is given to The Foxboro Company for granting the extensive use of their simulation and computer control facilities for the experimental portion of this thesis, and for their financial support of this work.

The study was actively supported and encouraged by all three members of the thesis committee. Dr. Fred Schweppe, thesis supervisor, developed many of the identification techniques used in this study, and he provided valuable advice in the area of power systems behavior. Dr. Elias Gyftopoulos, Professor of Nuclear Engineering, contributed substantially to the understanding of nuclear reactor behavior and the causes of reactor control problems. Dr. Leonard Gould, Professor of Electrical Engineering, provided valuable advice in the area of process control and in the interpretation of the control and hypothesis test techniques developed in the study. All three members of the committee gave willingly of their time to analyze and review the work in progress. Their criticisms and comments were useful and many of them have been integrated into the final thesis. Their help and advice are gratefully acknowledged.

One of the more time-consuming phases of this study was the design, construction and verification of the analog simulation. This was greatly aided by Hans Dik, an employee of The Foxboro Company, who had previous extensive experience with nuclear plant simulations.

Finally, thanks are due to the author's wife, Christine, and to his three boys Robert, David and Thomas. They have been very understanding during these last few years.

TABLE OF CONTENTS

	<u>Page</u>
List of Figures	8
Chapter 1 Introduction	10
1.1 The Load Change Problem	10
1.2 The Scope of the Study	14
1.3 Related Studies	20
1.4 The Contribution of this Study	23
Chapter 2 The Nuclear Plant	26
2.1 Plant Description	26
2.2 Plant Behavior During Transients	32
Chapter 3 The Model Identification	43
3.1 Introduction to the Identification Problem	43
3.2 The Deterministic Model	44
3.3 The Stochastic Model	50
3.4 Initial Parameter Estimates	54
3.5 Maximum Likelihood Identification	60
3.6 Hypothesis Test	65
3.7 Results of Model Identification	67
Chapter 4 The Deterministic Control	78
4.1 Definition of the Control Problem	78
4.2 Input and State Constraints	80
4.3 Control Which Balances Reactor and Turbine Power	92

TABLE OF CONTENTS (Continued)

	<u>Page</u>
4.4 Control for Rapid Load Changes	97
4.5 Examples of Load Changes	101
4.6 Load Following Control	104
Chapter 5 Control in the Presence of Variation and Uncertainty	111
5.1 Introduction to the Problem	111
5.2 Behavior of the Stochastic Model	113
5.3 Modification of the Constraints	118
5.4 Prediction of Measurement Bands	121
5.5 On-line Hypothesis Testing	127
5.6 Parameter Adaptation	132
Chapter 6 Summary	137
6.1 Problem Restatement	137
6.2 Results of this Study	138
6.3 Extensions	141
References	144
Appendix A The Nuclear Plant Simulation	149
Appendix B The Kalman Filter	168
Biographical Note	173

LIST OF FIGURES

		<u>Page</u>
2.1-1	A Pressurized Water Nuclear Power Plant	27
2.2-1	Plant Simulation Structure	34
2.2-2	Response of the Plant to Rod Withdrawal	36
2.2-3	Response of the Plant to Load Increase Without Rod Movement	37
2.2-4	A 10% Load Increase Under Analog Control, Large Moderator Coefficient	39
2.2-5	A 10% Load Increase Under Analog Control, Small Moderator Coefficient	40
2.2-6	A 10% Load Increase Under Analog Control, Large Xenon Effect	41
3.3-1	Model Summary	53
3.4-1	A Least Squares Fit	58
3.5-1	A Kalman Filter with Likelihood Calculation Appended	64
3.7-1	Effects of Truncation and Roundoff Errors	74
3.7-2	Experimental Determination of Roundoff Errors	76
4.2-1	Pressurizer Level Deviations for Fast Primary Loop Average Temperature Transients	85
4.2-2	Primary Loop Pressure Deviations for Fast Primary Loop Average Temperature Transients	87
4.4-1	Optimal Reactor Power Trajectories for Different Primary Loop Average Temperature Constraints	99
4.5-1	A 40% Load Change Under Computer Control, Constrained Primary Loop Average Temperature Deviation	102

LIST OF FIGURES (Continued)

		<u>Page</u>
4.5-2	A 40% Load Change Under Computer Control, Zero Desired Primary Loop Average Temperature Deviation	103
4.5-3	A 40% Load Change Under Computer Control, Large Xenon Effect Conditions	105
4.6-1	Overall Control Logic	109
5.2-1	An Interpretation of State Covariance	117
5.3-1	Adjustment of the Constraints	120
5.4-1	Prediction of Measurement Performance Bands	124
5.4-2	Display of Actual vs. Predicted Measurements During Normal Load Changes	125
5.4-3	Display of Actual vs. Predicted Measurements Following a Plant Variation	126
5.5-1	Hypothesis Test Performance Under Normal Conditions	130
5.5-2	Hypothesis Test Performance Following Plant Variation	131
5.6-1	Least Squares Cost Performance Following Plant Variation	134
5.6-2	Display of Actual vs. Predicted Measurements Following Plant Variation and Model Adaptation	135
A-1	Overall Simulation	153
A-2	Physical Simulation Facility	154
A-3	Analog Rod Control	158
A-4	Block Diagram of Heat Exchanger	162
A-5	Turbine Model	165

CHAPTER 1
INTRODUCTION

1.1 The Load Change Problem

A nuclear power plant of the pressurized water type is the subject of this study. About half of the commercial nuclear power plants in the United States are of this type. Some of the newer plants exceed 1000 megawatts in electrical power at full load. Nuclear power plants are rapidly becoming a major source of the nation's power supply. As these nuclear plants become more dominant, it will become necessary to provide improved load change control for them, so that they can be easily used to balance the power load of a network. The balance of power in a network can be upset by customer load changes, by plant failures and by other causes. The restoration of balance in the power network may depend on the ability of power plants to undergo large, fast changes in the power which they produce.

As a preface to the discussion of the load change problem, the basic elements of a pressurized water nuclear power plant are briefly summarized here. The plant consists basically of a reactor which generates thermal power, two circulating water and steam loops to transfer the heat, and a turbine to transform the thermal power into mechanical power which then drives the electrical generators.

A power load change consists of changing the power produced in the reactor and the power delivered by the turbine. This must be done in a

manner which does not seriously disturb the plant operation. Large and fast load changes require a control which provides simultaneous coordinated control for both the reactor control rods and the turbine load setpoint. This is necessary to avoid large deviations in plant variables. Any residual deviations can then be corrected by feedback control. If these inputs are not coordinated, as is the case for typical existing control schemes, a large, fast power load change can cause serious deviations in important plant variables which, in turn, can trigger an automatic emergency plant shutdown.

The design of a control to coordinate the reactor and turbine power changes is made difficult by variation in plant behavior. The variation causes the plant to respond differently to the same inputs at different times. Thus a fixed control system such as conventional analog control systems cannot consistently handle large and fast load changes. This problem is exemplified by the following quote from the system documentation for a large nuclear power plant. [17]

The Reactor Control System is flexible and will try to follow all load changes. However, for a given plant condition, there is a load change magnitude beyond which a reactor trip is likely. Thus, a restriction may be placed on the capability of the plant to follow load demands such as may be requested by the area load control dispatcher.

In fact, the conventional control systems do not adapt to cope with plant variation, and this together with the lack of coordination of the turbine and reactor restrict the capability for large, fast load changes using existing control systems.

Changes in plant conditions, disturbances, measurement noise and unmeasured variables are the major sources of variation and resultant uncertainty in plant behavior. A suitable control for large and fast load changes must overcome the effects of variation and uncertainty, to provide smooth operation under the full range of normal conditions.

The plant variations which occur are now considered in more detail. The variations considered in this study are:

1. Variations in the initial reactor state. The behavior of the plant varies, depending on the initial condition of some unmeasured reactor states. The major instance is the dynamic behavior of the reactor at high power levels. This depends on the unmeasured concentration of certain fission product isotopes. The most important isotopes are Xe^{135} and its precursor I^{135} . The behavior of the reactor is more sluggish before these isotopes accumulate than after. In addition to the effect on dynamic behavior, the initial states of the Xe^{135} and the I^{135} also have an influence on the feasible magnitude and speed of load changes at high power levels which remain within the control capabilities. If the reactor has a high concentration of these isotopes, then the range of allowed load changes must be restricted.

2. Variations in the initial plant states outside the reactor. Initial states outside of the reactor also have a significant influence on whether an acceptable plant deviation will occur during a given load change. For example, the behavior of the primary loop pressure during the load change depends on the initial states of the pressurizer. The pressure may or may not experience large deviations, depending on the initial level and pressure in the pressurizer.

3. Slow physical variations. The plant behavior changes slowly over the fuel cycle, which is about a year. The major effects are due to changes in the composition of the fuel and changes in the concentration of certain chemicals in the moderator water which circulates through the reactor which, in turn, produce significant modifications in the plant behavior. In particular, the magnitude of the effects on the reactor due to variation in the fuel and moderator temperatures change.

4. Apparent variations due to nonlinearity. As the process is operated at different load conditions the nonlinearity of the process leads to apparent behavior changes. These are not true variations since the behavior is repeatable by returning to previous load conditions. If the nature of the nonlinearity is known, then these effects can be predicted. However, if the nature of the nonlinearity is not known, then the effects of it are considered to be plant variations. That is, the plant is behaving differently, just as if a true physical variation as described in item 3 above had occurred.

5. Random variations. The reactor is continually subject to minor disturbances [60] and the measurements are subject to noise. These factors cause some variation of a random nature in the plant behavior.

The above sources of variation in plant behavior, due to variations in initial state, physical plant changes, nonlinearity and randomness, all act to make large and fast load changes a difficult control problem. This problem is solved by using a range of estimation and control techniques which reduce the uncertainty, adapt to the variation and which thereby provide smooth control of large and fast load changes.

1.2 The Scope of the Study

In the previous section the load change problem was defined. To reiterate, the goal is to produce large and fast load changes in a smooth manner without serious disturbances to the plant operation. This requires a control to coordinate two major plant inputs, the reactor control rods and the turbine load setpoint. Due to the complexity of the problem the coordination of these inputs requires a model of the plant so that the coordinating control actions can be calculated. This model is a crude representation of the plant. It has errors which appear as disturbances to the control scheme. In addition, the actual plant is subject to several types of variation, which lend uncertainty to any plant model. The problems of model error, plant variation, and the resultant uncertainty are the major considerations of this study. Means are developed to cope with these effects so that large and fast load changes can be made smoothly.

A number of techniques from modern control and estimation theory are applied in this study to overcome the problems of variation and uncertainty. Techniques of identification, prediction, control and adaptation are used in a set of computer programs for load change control. These programs are experimentally tested on a detailed simulation of a nuclear power plant, which includes the effects of variation, disturbance noise and measurement noise. The simulation is run on an analog computer.¹

¹In this study the word simulation always refers to the analog computer detailed simulation of the plant, while the word model always refers to the crude plant model in the digital computer.

The estimation and control programs are run on a digital computer which treats the analog simulation as if it were a plant. Table 1.2-1 illustrates the experimental part of this study. The plant inputs which are controlled by the digital computer are the reactor control rods and the turbine load setpoint. The plant measurements which are used by the digital computer are the reactor power, primary loop average temperature,¹ turbine power, rod group position measurement and turbine load setpoint measurement.

A model of the plant to be used in the digital computer for estimation and control purposes is developed. The model is stochastic, being composed of a deterministic part and a noise part. The deterministic part of the model contains approximations of the major plant phenomena. There are six states and twelve parameters in this part of the model. The noise portion of the model includes disturbances to the states of the deterministic model and noise added to the measurements. The parameters of both the deterministic and the noise parts of the model are considered initially unknown. Thus, the overall stochastic model has a specified structure, but the parameters are considered initially unknown to be identified to match the model to the measured plant performance.

Values of the parameters of the stochastic model are based on data records from the simulated plant taken during load change. The criterion for choosing the parameter values is maximum likelihood.² A separate

¹The average of two temperature measurements, one each at the reactor inlet and outlet.

²This technique is discussed in Section 3.5.

TABLE 1.2-1

The Experimental Procedure of the Study

1. Analog Computer: used to simulate the plant.
 - A. Coupled nonlinear simulations of the physical processes, including the reactor, heat exchanger, pressurizer, turbine and other parts.
 - B. Disturbance noise and measurement noise added to enhance realism.
2. Analog to Digital Interface: one second scan intervals.
 - A. Measurements:
 - reactor power
 - primary loop average temperature
 - turbine load
 - rod group position
 - turbine load setpoint
 - B. Manipulated control inputs:
 - rod group speed
 - turbine load setpoint
3. Digital Computer: used for calculations and control.
 - A. Stochastic model parameter identification.
 - B. Kalman filtering to give estimates of measured and unmeasured states.
 - C. Prediction of bands of uncertainty.
 - D. Calculation of control inputs.
 - E. Display of predicted plant performance prior to the load change.
 - F. Display of realized vs. predicted performance during the load change.
 - G. On-line hypothesis testing to detect plant variation.
 - H. Adaptation of the model.

hypothesis test technique is used to see if the maximum likelihood identification is successfully producing a stochastic model consistent with the plant data records.¹

After the stochastic model has been identified, it is used in a number of separate applications. One of these is the design of a state estimator to provide estimated values of the plant states. The type of state estimator used in this study is a Kalman filter. This state estimator, which is discussed more fully in Appendix B, is designed automatically by the computer once the stochastic model parameters are known. The use of a state estimator provides estimated values of the important unmeasured states. For example, the concentrations of fission product isotopes in the reactor are estimated in this way for use in the control strategy. Other uses of the stochastic model are discussed shortly, after the following presentation of the control strategy.

To guarantee smooth operation during the load change, the control which is proposed must keep the plant within certain specified and calculated control constraints, and it must make the load change subject to limited control capabilities. The directly specified constraints considered here are the conventional deviation limits on primary loop temperature, primary loop pressure, pressurizer level, available control reactivity, rate of control rod motion, and reactor and turbine power rate of change constraints. In addition to these directly specified constraints, the control also observes certain indirectly specified or

¹This technique is discussed in Section 3.6.

calculated constraints on power changes due to the initial states in the reactor, e.g., Xenon effects. These constraints are all observed to ensure smooth plant operation during and after load change.

The control equations are based on the deterministic portion of the model. This control is modified, as described later, to operate in the presence of uncertainty. The control coordinates two major plant inputs which directly affect the reactor and the turbine to keep the plant within specified and calculated constraints during the load change. The plant load is changed in minimum time subject to the constraints.

The control constraints are adjusted to provide for uncertainty by use of the stochastic model. The nominal¹ state behavior is predicted for the load change, together with the state covariance about the nominal. This covariance is used as a measure of the variation which might be expected in performance, considering the fact that the process is stochastic rather than deterministic. A band of uncertainty about the nominal trajectory is defined based on this covariance representing the 99.7% probability, a priori, that the state will be within the band at a given time.

The calculated band of uncertainty is used to adjust the state constraints - to make them more restrictive. Thus the nominal plant behavior is well within the actual constraints and in fact the entire 99.7% probability band of expected plant behavior lies within the actual constraints. Thus, the control can operate in the presence of uncertainty,

¹The nominal trajectory is the result of prediction using the deterministic model only. In other words, the disturbance is assumed to be zero for the nominal predicted trajectory.

even though the control equations are based on the deterministic portion of the model.

In addition to the direct control applications of adjusting the constraints and estimating the states, the stochastic model is also used to aid in the monitoring of the plant during the load change. To accomplish this, the calculated 99.7% probability performance bands of the plant measurements¹ about the nominal trajectory are calculated and are displayed prior to the start of the load change. As the load change progresses, the realized plant measurements are superposed on this display, so that the plant operator can monitor the actual vs. predicted performance. The reactor power and the primary loop average temperature were chosen for this display purpose to illustrate the prediction capability.

The plant performance during the load change is automatically monitored by the computer using two distinct criteria. The first criterion makes use of the predicted measurement performance bands discussed above. The load change can be aborted if these bands are violated. (However since an occasional noise spike on the measurements can cause a bounds violation, it is desirable to abort only if several points are outside the bounds.) The other criterion makes use of a statistical test called a hypothesis test. For the test used in this study,² it is found that when the plant behavior is different from that predicted by the stochastic model, the hypothesis test quickly detects this error. The hypothesis

¹The predicted measurement bands consider both the disturbance and the measurement noise, while the predicted state bands consider the disturbance noise only.

²See Section 5.5.

test consistently detects plant variation before the observed plant performance under the control is noticeably deviating from the predicted measurement bands. Thus, of the two criteria, the hypothesis test is more sensitive to plant variation.

Variation in the plant is detected by the measurement bands test and the hypothesis test discussed above. In the event of a variation, the load change is stopped and the model of the plant is adapted, based on the data acquired during the abortive load change. This procedure proves capable of adapting to plant variation and of producing a model which is once again consistent with the plant data.

In summary, the scope of this study involves the application of several techniques from modern system theory to the load change problem. These techniques include the identification of a stochastic model of the plant, and the use of this model for state estimation and prediction. Bands of predicted performance are used to adjust the control constraints. Bands of predicted measurements are used for display and monitoring. A hypothesis test is used to determine if the model is consistent with the plant data. The result of all these techniques is to provide smooth, fast and large load changes in the presence of plant variation and uncertainty.

1.3 Related Studies

This investigation brings together a number of techniques to provide control in the presence of variation and uncertainty, and to thereby provide improved control of the nuclear power plant during load changes.

Prior work of a theoretical nature has provided the groundwork for this study.

The identification technique used here is maximum likelihood. This technique was developed by R. A. Fisher [24]. The technique has been previously used for identification of the parameters of dynamic systems, particularly by Astrom [5]. The theoretical convergence properties of maximum likelihood techniques for special forms of state variable models have been considered by Kashyap [36]. The form of maximum likelihood technique used in this study, with general form state variable stochastic models, was developed by Schweppe [58].

Techniques other than maximum likelihood have been used for identification of the parameters of stochastic models. These techniques, generally called adaptive filtering, use the errors in on-line state estimators to make corrections in the parameters of a stochastic model. Jazwinski [32] considers dealing with variations by adapting a disturbance noise covariance matrix in a manner which requires some assumptions on the form of the covariance matrix. Bryson and Ho [13] adapt the magnitude of a factor multiplying the measurement covariance matrix. Mehra [46] develops a technique for identifying noise covariance matrices, given the deterministic part of the model. He uses a hypothesis test to see if the hypothesis of a correct model should be rejected. Anderson et al. [2] consider the estimation of the deterministic and the noise parameters of a model for the special case where all states are measured. None of the above adaptive filtering approaches has the generality of the maximum likelihood technique used in this study. With this method, it is

possible to identify parameters in the deterministic and the noise portions of a state variable stochastic model without the necessity for measurements of all states. The maximum likelihood identification technique thus ranks as the most general of the available techniques for identifying the parameters of a stochastic model.

The specific problem of identifying parameters in a nuclear reactor model has been previously studied. Habegger [27] estimates parameters in a model by considering them as states in a state estimator. Sage and Masters [55] use a least squares approach to identify parameters in a reactor model. Ciechanowicz and Bogumil [16] use spectral techniques to identify parameters in a simple linear model of a reactor. None of these previous reactor identification studies has the generality of this study, which identifies the parameters of both the deterministic and the stochastic portions of a sixth order nonlinear model of the nuclear power plant.

A number of previous studies have considered the optimal control of the nuclear reactor for power changes. All of the prior studies consider low power operation, where the plant to reactor coupling is negligible. At high power operation, the plant coupling via temperature feedback of the circulating moderator water can rapidly affect the reactor behavior. Thus the plant coupling due to this circulating water is a major consideration in the reactor behavior for high power operation. Some of the prior studies make the lower power operation restriction explicit, such as Marciniak [45], while others effectively assume low power operation by setting the coupling to zero before deriving results as in Duncombe and Rathbone [21].

The prior studies have generally considered constraints on the reactor and the control rods. However, the constraints on the remainder of the plant, particularly the primary loop pressure, have been neglected in prior studies. This is not a problem for low power operation, where the plant coupling is small, but it is a major consideration at high power operation.

Some previous investigations have considered the effects of Xenon for the reactor shutdown problem. The effect of Xenon on load changes at high power is also important, although it has not been considered in most prior studies. This is another case of an effect which can be neglected at low power levels, where natural Xenon decay dominates Xenon burnoff, but which is important at high power levels.

None of the prior studies for optimal control of the nuclear plant during power changes are valid for high power operation. There are several studies valid for low power operation, in particular, those of Marciniak [45], Monta [47], Duncombe and Rathbone [21] and Weaver [64]. There are also numerous prior studies on the somewhat related problem of optimal shutdown to minimize Xenon poisoning, in particular the studies of Ash [3], Lewens et al. [43], Roberts et al. [52], [53], and Rosztoczy [54]. However, this is the first study to consider the important effects which occur at high power operation.

1.4 The Contribution of this Study

The practical applications of modern control and estimation theory usually require low order models of processes. Many processes, in

particular nuclear power plants, are complex nonlinear processes which can only be crudely described by low order models. The errors which occur due to using a crude model are similar to the errors produced by disturbances, and to some extent model errors can be handled by using a stochastic model which allows for disturbances. This study considers maximum likelihood identification of the parameters of both the deterministic and the stochastic parts of a low order nonlinear model as a means of coping with some inaccuracy in the low order model. The resulting model is then used for estimation, prediction and control of a realistic simulated plant. A contribution of this study is that it provides a means for using modern control and estimation theory in a realistic environment where the available models are low order, but where the actual process is more complex.

The nuclear power plant is subject to the types of variations common to many processes. This study provides a number of techniques for coping with such variations. The parameters of a stochastic model are identified by a maximum likelihood technique to provide a model consistent with the plant data. The model adequacy is monitored by means of a hypothesis test to detect plant variation. In the event of variation, the model parameters are adapted. The control of the plant is based on calculated state constraints, which consider the estimated initial condition of the plant. These constraints are then modified - made more restrictive - to take into account the uncertainty predicted by the stochastic model. The control is based on the state estimates provided by an on-line state estimator. These techniques, taken together, provide a means for control

in the presence of the variation and uncertainty which normally occur in a nuclear power plant, as well as in many other processes.

The unique problems of high power operation of nuclear power plants make prior work on low power reactor operation of little relevance to this problem. Further, this study is the first to consider the optimal control problem for the overall plant as opposed to the reactor alone. This problem includes consideration of the coupling between the reactor and the remainder of the plant. The results of this study should be directly applicable to actual pressurized water nuclear power plants, providing the capability for large, fast and smooth load changes. Thus, in addition to proving the usefulness of several theoretical techniques, this study also makes a contribution in that it provides a practical solution to the load change problem which is demonstrated on a detailed simulated plant.

CHAPTER 2

THE NUCLEAR PLANT

2.1 Plant Description

A brief description of the pressurized water nuclear power plant is presented here. The details of the physical processes are discussed further in the simulation summary, Appendix A. The effects described here are considered in the design of the nuclear plant control.

Figure 2.1-1 shows the major parts of the nuclear power plant, which includes the reactor, the primary loop, the pressurizer, the heat exchanger, the secondary loop, the throttle valves, and the turbine-generator unit.

The energy flow through the plant is accomplished by the water circulating around the primary and secondary loops. Heat is produced in the reactor by nuclear fission. As Figure 2.1-1 illustrates, the primary loop contains water which carries heat energy from the reactor to the heat exchanger, where the heat is transferred to the secondary loop. The water in the secondary loop boils in the heat exchanger, producing steam. The throttle valves admit steam to the turbine. The turbine produces shaft power from the expansion of the steam. The generator, driven by the shaft, produces electric power.

The reactor is now considered in more detail. During normal operation the nuclear fission process is in critical steady state. In general, each fission is caused by an interaction between a neutron at thermal energy and an atom of U^{235} . A fission produces on the average more than two

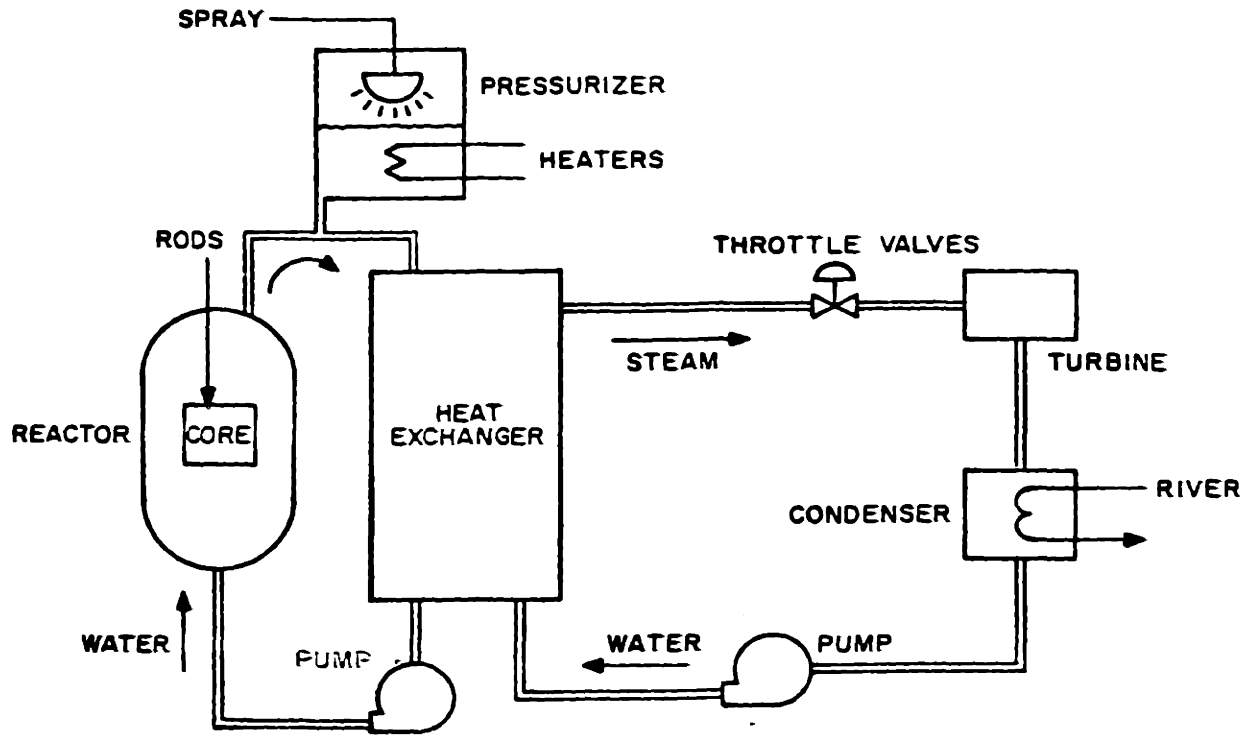


FIGURE 2.1-1 A Pressurized Water Nuclear Power Plant

neutrons. Some of these neutrons are absorbed or leak from the reactor. At critical steady state there remains a net of one neutron which enters into additional fission, and thus steady state is maintained.

A small fraction of the neutrons produced by a fission are not produced immediately. This small fraction, called delayed neutrons, results from the decay of certain fission products. Delayed neutrons effectively slow down the reactor fission dynamics during a transient.

The reactor can be controlled by control rods which absorb neutrons. When the reactor is in a critical steady state, the control rod absorption together with all other absorptions and leakage of neutrons result in a net of one neutron available for fission for each neutron that caused fission. As the control rods are inserted, a larger fraction of neutrons are absorbed in each generation and the reactor power decreases. As control rods are withdrawn, a lower fraction of neutrons are absorbed and the reactor power increases.

Boron compounds are put into the water which flows through the reactor. Boron acts as an absorber of neutrons as a control rod does. Thus the concentration of boron in the reactor can be manipulated to affect the state of the reactor. In general, this concentration is only adjusted slowly, whereas the fast control of the reactor is handled by the control rods.

The water which flows through the reactor core serves as a moderator. The high energy neutrons from fission are slowed down or moderated in the water. This is necessary because neutrons slowed to low energy have a much higher probability of interaction with fuel atoms to cause fission.

Water provides a good moderator because the collision of neutrons with light atoms, such as hydrogen in the water, is more effective in slowing down the neutrons than collision with relatively heavy metal atoms.

The water also serves as a means of transferring heat. Nearly all of the heat produced by fission comes from the kinetic energy of the fission fragments and it appears in the fuel. The heat is transferred to the flowing water, which moves through the reactor core in a time on the order of seconds.

The reactor transient behavior will now be considered. The role of the control rods in changing the reactor power or fission rate has been discussed previously. There are several other major variables which also affect the dynamic behavior of the reactor. These include temperature changes which may occur in the fuel and the moderator water and changes in the concentration of certain isotopes which absorb neutrons, such as Xe^{135} .

As the moderator and fuel temperatures rise, there are various physical changes in material dimensions, material densities, neutron energy spectrum, and other effects in the reactor. As temperatures vary, these effects generally cause a change in the balance between production and destruction of neutrons. These effects are called moderator and fuel temperature feedback effects. In a pressurized water reactor these feedback effects are generally negative and they help to stabilize the reactor.

The moderator water in the primary loop may have its temperature disturbed due to turbine load changes. These temperature disturbances

then influence the reactor. Thus plant load changes can influence the reactor behavior, and the overall plant must be considered in discussing the behavior of the reactor.

Because of the moderator temperature effect, the power changes at the turbine can initiate a transient in the reactor. This effect is generally a stabilizing influence on the plant, as the temperature transient caused by a turbine power change will tend to change the reactor power in the same direction as the turbine power change. The size of this effect varies over the fuel cycle (about a year) as the concentration of Boron in the moderator is changed.

The transient behavior of the reactor depends strongly on the concentration of certain isotopes which absorb neutrons. The major effect is due to Xe^{135} , which is a strong absorber of neutrons. The concentration of Xe^{135} is negligible during a reactor startup, but the concentration builds up slowly during steady high power operation, due to the creation of Xe^{135} from the decay of certain products of fission. At equilibrium at high power levels, this creation of Xe^{135} and the loss of Xe^{135} , mostly due to neutron absorption, are in balance. The concentration of Xe^{135} can change significantly in a period of minutes if the reactor power is changed. This gives the effect of a significant change in the fraction of neutrons which are absorbed. The effect of Xe^{135} at high power levels is a destabilizing influence. A rise in reactor power produces an initial transient decrease in the Xe^{135} , which tends to make reactor power increase still more. However, the steady state effect of a reactor power increase is a larger Xe^{135} concentration. That is, the initial fast transient is

in the opposite direction to the steady state change. This complex phenomenon, which involves other isotopes as well as Xe^{135} , is discussed in further detail in Section 3.2.

The other portions of the nuclear power plant are now considered. As Figure 2.1-1 illustrates, the pressurizer is a surge tank with heaters and sprays to provide pressure control for the primary loop. A transient change in the primary loop average water temperature will cause a surge flow into or out of the pressurizer, as the primary loop water expands or contracts. This surge flow will cause a pressure transient. Thus both the pressure and the level in the pressurizer are disturbed when the primary loop average temperature changes.

As Figure 2.1-1 illustrates, a heat exchanger couples the primary and secondary loops. The heat exchanger is a shell and tube type. The secondary side of the exchanger contains boiling water. The steam is separated and goes to the turbine. The boiling temperature and the heat transfer are influenced by secondary loop pressure, and thus the primary loop is strongly coupled to pressure changes in the secondary loop. A set of throttle valves admits steam to the turbine. The turbine reacts rapidly to changes in steam flow. A common approximation is that the load on the plant is proportional to steam flow.

A discussion of the plant should include some mention of the measurements and controls which are typically present. A plant may have hundreds of variables monitored for safety and other purposes. However, only a few major measurements are of interest in the load change problem. These include reactor power, primary loop pressure, temperatures of the hot and

cold legs in the primary loop, pressurizer level, rod group positions, steam flow to the turbine, and electric load on the plant. All of these measurements are considered available for use in the control strategy. A typical analog control system uses these measurements to control the major plant inputs: the rods, the pressurizer heaters and sprays, the secondary loop feedwater pumps, and the throttle valves. Table 2.1-1 shows a typical analog control configuration for these major plant inputs.

This completes the brief discussion of the major parts of a pressurized water nuclear power plant. In the next section the behavior of the plant under transient conditions is considered.

2.2 Plant Behavior During Transients

In this study a detailed simulation of a pressurized water nuclear power plant was used for experimentation. This simulation is described in detail in Appendix A. The simulation includes the major parts of the plant discussed in Section 2.1 and shown in Figure 2.1-1. In addition to the simulation of the various physical parts of the plant, the simulation also includes disturbance noise and noise on the measurements. The overall simulation does not represent plant behavior exactly, but it does have sufficient detail to illustrate the plant behavior during transients. The structure of the simulation is shown in Figure 2.2-1. As this figure illustrates, the analog controls for the pressurizer, the turbine, and the reactor were part of the simulation.

A number of response tests are presented in this section to illustrate the behavior of the plant. The first transient response experiment, shown

TABLE 2.1-1
Typical Analog Control Configuration

<u>Description</u>	<u>Measurements</u>	<u>Plant Inputs</u>
Rod Control	- Reactor Power - Turbine Power - Primary Loop Temperature	Control Rods
Pressurizer Control	- Pressurizer Pressure - Pressurizer Level	Heaters Sprays
Heat Exchanger Control	- Steam Flow - Feedwater Flow - Level in Exchanger	Feedwater Pumps or Valves
Turbine Control	- Load Demand - Turbine Power	Throttle Valves

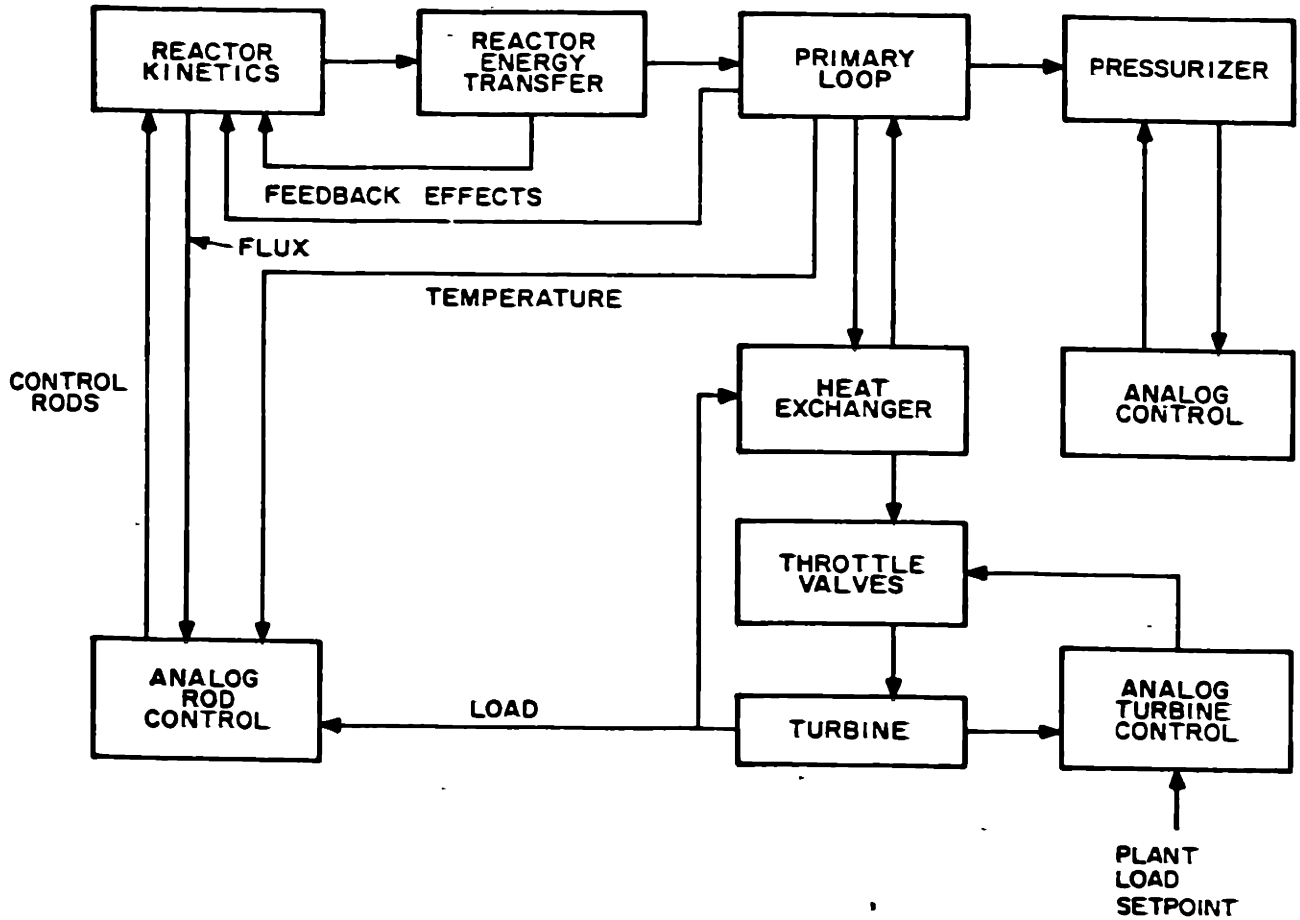


FIGURE 2.2-1 Plant Simulation Structure

in Figure 2.2-2, gives the response to a withdrawal of control rods at the maximum withdrawal rate. As the rods are withdrawn, the reactivity increases, leading to a reactor power increase. The overall behavior of the plant during this transient can be thought of as due to the mismatch between reactor power and turbine power. The extra power is giving rise to the primary loop temperature increase. The transient shown is for a moderator temperature coefficient of $-1 \times 10^{-4} \Delta K/^{\circ}F$ and for the case of no Xenon poisoning. A smaller moderator temperature coefficient or more Xenon would lead to more severe transients than those shown.

The transient response shown in Figure 2.2-3 shows the effect of a step change in the load setpoint. The analog turbine control system manipulates the throttle valves to accomplish the load change. The analog rod control system has been disconnected for this experiment to show the behavior of the reactor in the absence of rod motion. Eventually, a new steady state is reached, in the absence of rod motion, where the moderator temperature is lower and where the reactor power is higher. If the rod control system had been used also, a desired primary loop average temperature can be adjusted without changing plant load, just as in the first experiment described above. The behavior shown in Figure 2.2-3 is for the same conditions of Xenon and moderator temperature coefficient as in Figure 2.2-2.

Experiments performed under the normal analog control of the plant are now discussed. In particular, the behavior of the plant for different moderator temperature coefficients and for different Xenon concentration

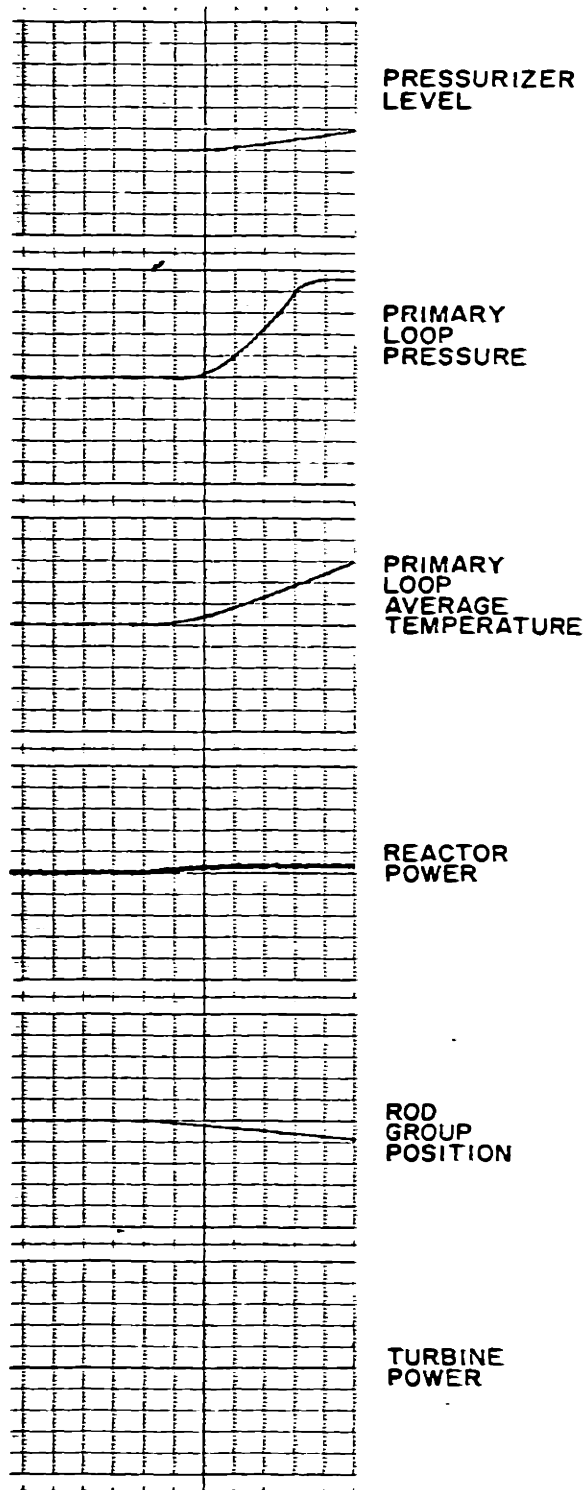


FIGURE 2.2-2 Response of the Plant to Rod Withdrawal

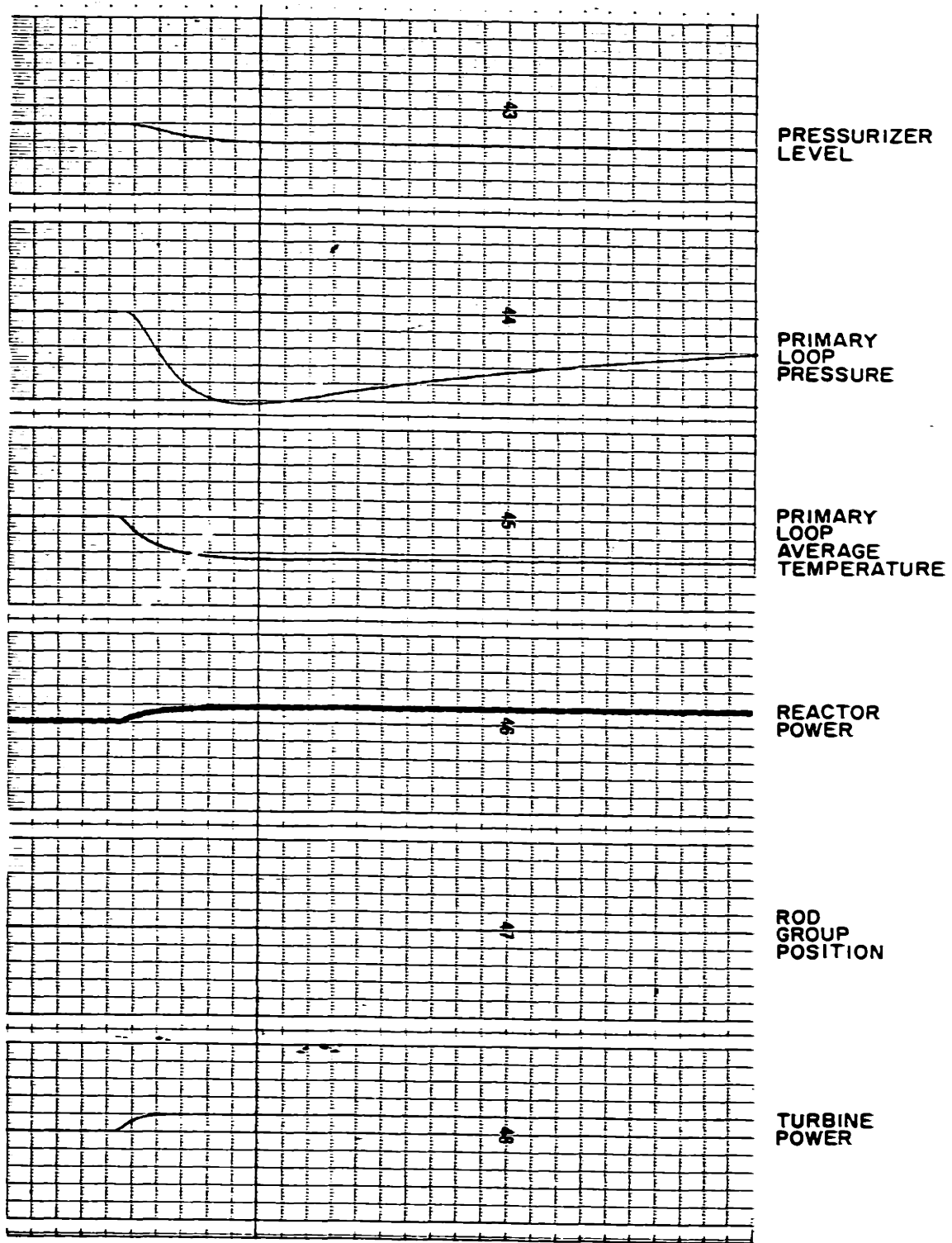


FIGURE 2.2-3 Response on the Plant to Load Increase Without Rod Movement

is considered. Figure 2.2-4 shows the plant transient response to a step in plant load setpoint under conditions of a large moderator feedback effect, $-1 \times 10^{-4} \Delta K/^\circ F$ and no Xenon. The transient change in reactor power is due both to the effect of the control rods and the effect of the transient in moderator temperature. The primary loop pressure and the pressurizer level both experience significant variations as the primary loop temperature changes.

Figure 2.2-5 shows the plant response to the same 10% step in plant load setpoint, but for the case of a much smaller moderator temperature coefficient, $-1 \times 10^{-5} \Delta K/^\circ F$. The temperature transient in this case is more severe, leading to larger transients in pressure and in pressurizer level.

Figure 2.2-6 shows the plant response for a 10% step in plant load setpoint for the case of an initial high Xenon concentration, corresponding to a load change after a period of high power operation. The effect of the Xenon is to make the reactor power change occur more rapidly, which reduces the initial temperature transient. However, the Xenon effect continues, leading to a tendency for reactor power to rise. The rising primary loop temperature and the power mismatch are detected by the analog control system, which drives the rods to counter these effects.

For the load changes considered in this section (10% load changes) the analog control system performs acceptably. A number of variables are disturbed during the load change, particularly the primary loop pressure, but the deviations are within acceptable bounds. However, the undesirable

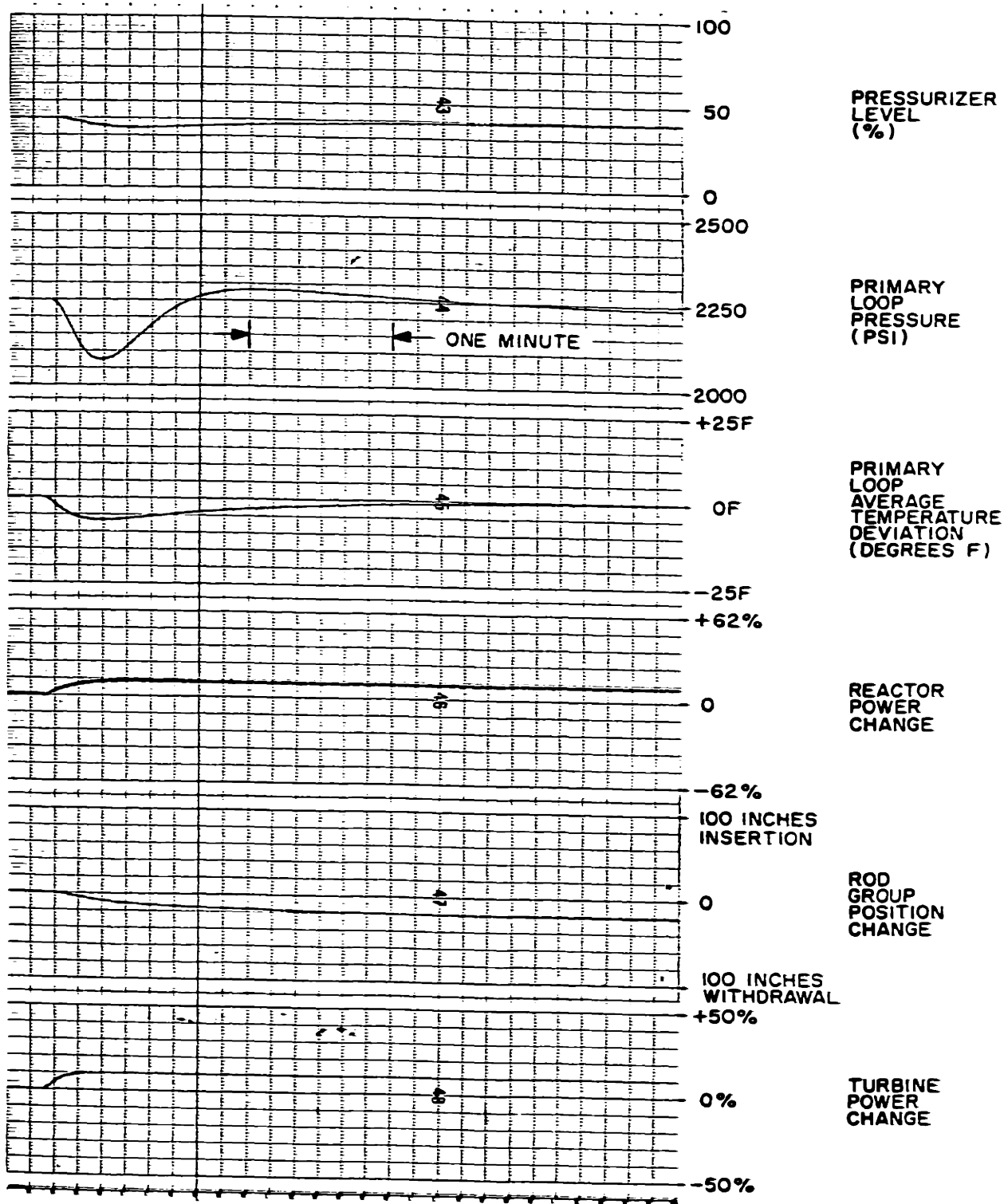


FIGURE 2.2-4 A 10% Load Increase Under Analog Control, Large Moderator Coefficient

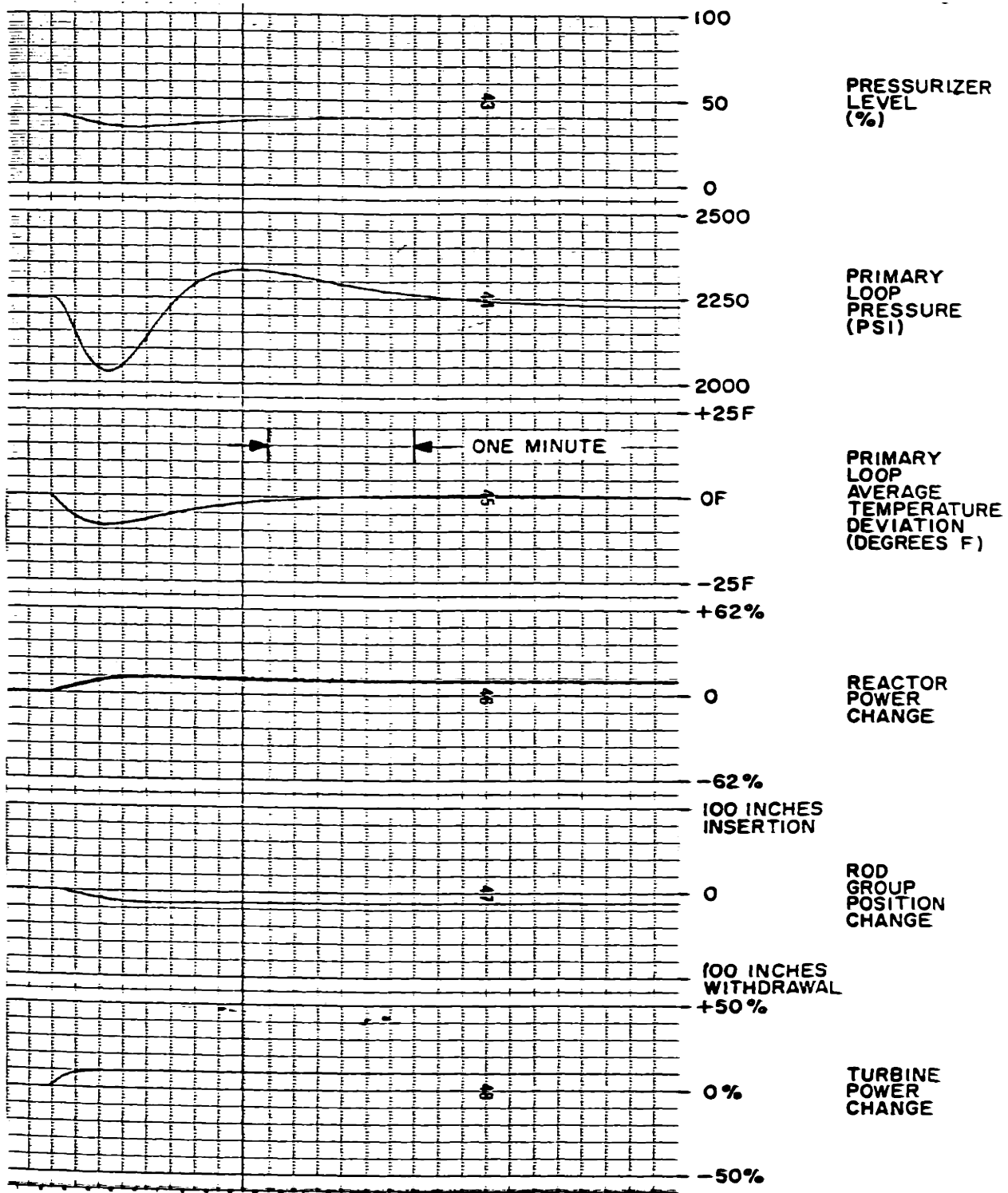


FIGURE 2.2-5 A 10% Load Increase Under Analog Control, Small Moderator Coefficient

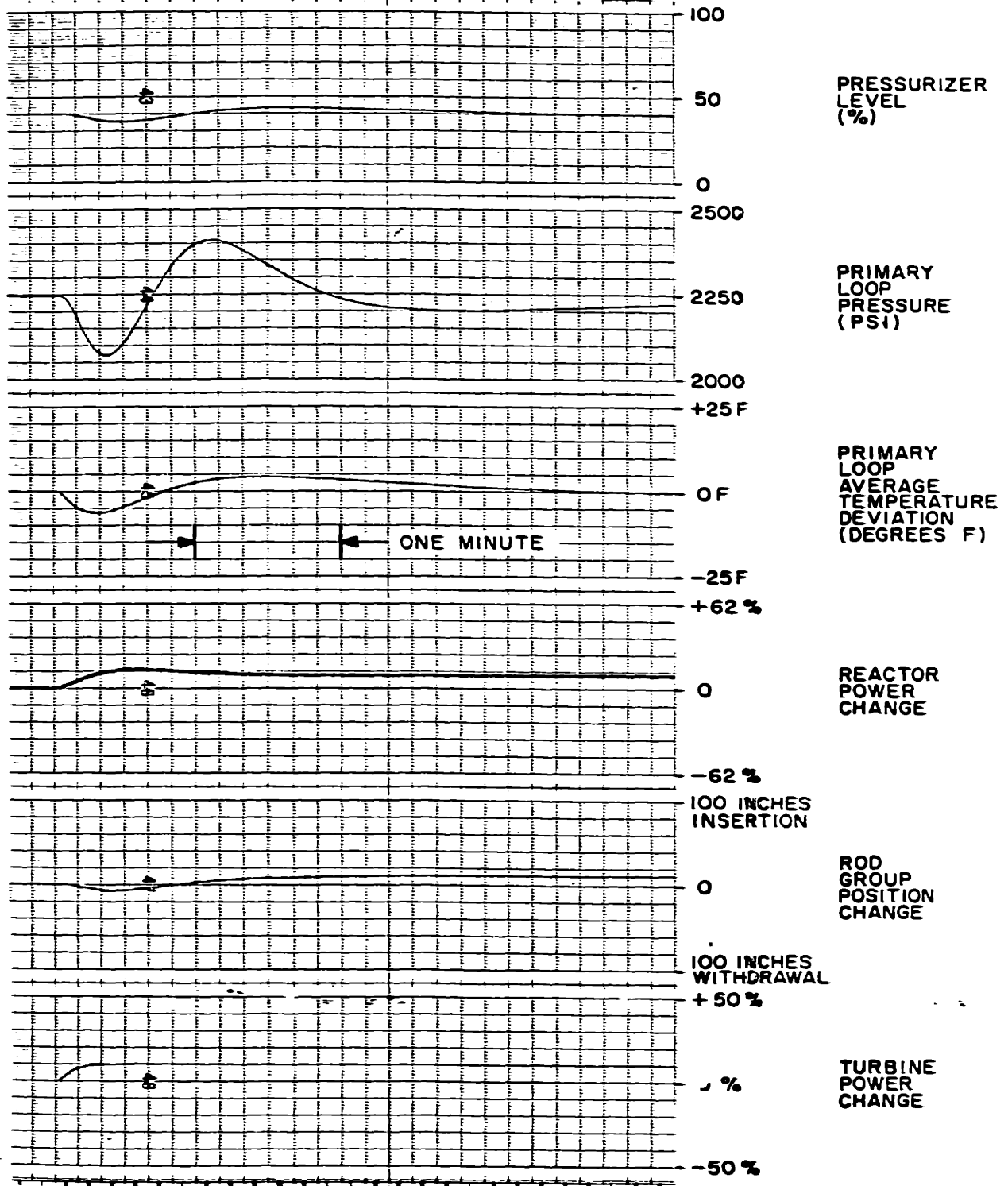


FIGURE 2.2-6 A 10% Load Increase Under Analog Control, Large Xenon Effect

deviations in pressure and other variables get worse as larger load change steps are attempted with the analog control system. Thus the analog control system is limited to small step load changes. In contrast, the computer control developed in this study is capable of large, fast load changes, with less deviation in the pressure and some other important transient variables than is produced by the analog control for the small load change experiments described in this section.

CHAPTER 3

THE MODEL IDENTIFICATION

3.1 Introduction to the Identification Problem

In this study a load change control is developed for the nuclear power plant. The control is based on a model of the plant. However the nuclear plant is a complex process. The types of simple low order models which are required for control purposes can only approximate the actual plant. There are several methods used in this study which compensate for part of the approximation and which allow a low order model to be useful in the control of the complex plant. The methods used include deterministic modeling of the major physical phenomena, modeling of the disturbance and measurement noise effects, and identification of the parameters of the overall model.

The model considered in this study is a stochastic model, that is, a model which contains a deterministic part and which also contains a representation of disturbance noise and measurement noise. The use of a stochastic model allows a means of coping with the random behavior of the process. In addition to this, the use of a stochastic model compensates for some model errors. This occurs because the effect of model errors is that the state does not behave quite as predicted - which is the same effect which a disturbance noise produces. Thus the disturbance noise portion of the model represents random disturbances and also a certain amount of model error. The result of using a stochastic model is that

means are provided to cope with both random process variations and with some model error.

The stochastic model has a number of parameters which are not assumed to be known. In the deterministic part of the model the structure is determined by physical laws, but the coefficients or parameters of the model are assumed to be varying or unknown. In the noise part of the model, the parameters of the disturbance noise and the measurement noise are also assumed to be unknown. The parameters of the stochastic model are identified to find the closest fit of the stochastic model behavior to the observed plant behavior.

The criteria for identification of the parameters of the overall stochastic model, comprised of the deterministic and the noise models, is that of maximum likelihood. This technique involves the choice of parameters to maximize the conditional probability of the observed data for the set of parameters. The technique involves a direct search over the parameters to find the maximum likelihood fit.

To sum up, the problem is identification of the parameters of a state variable stochastic model using plant data records. The solution to this identification problem, using the maximum likelihood criterion, has been developed theoretically by Schweppe [58] in the general form used here. This work represents the application to a process of this general state variable stochastic model parameter identification technique.

3.2 The Deterministic Model

The deterministic portion of the model is considered first. The basic procedure for constructing the model was to represent the major

energy storage, generation, and energy output phenomena in terms of simple lumped models. Thus the known plant structure was used in defining the model structure. The alternative procedure, to consider the plant unknown except for model order, was rejected due to the large number of unknown parameters which would result.

The nuclear reactor is represented by one group of delayed neutrons with a prompt jump approximation:

$$\frac{dD}{dt} = b_4 P_R \gamma \quad (3.2-1)$$

$$P_R = \frac{D}{1-\gamma} \quad (3.2-2)$$

where:

D is delayed neutron precursor density

P_R is reactor power

γ is normalized reactivity

b_4 is a parameter which is identified and adapted.

The above equations are widely used as a simple model for the reactor. This study also considers a number of effects which influence the reactivity γ . The model used for the reactivity about a nominal operating point is:

$$\gamma = -b_1(P_R - P_{R_0}) - b_2(T_{AV} - T_{AV_0}) + b_3(R - R_0) - b_8(X - X_0) \quad (3.2-3)$$

where:

T_{AV} is primary loop average temperature

R is control rod group position

X is Xe^{135} concentration or poisoning

The zero subscript denotes operating point values. The parameters which give the magnitudes of the reactivity effects, b_1 , b_2 , b_3 , and b_8 , are all identified and adapted.

The reactivity effects are now discussed in more detail. The parameter b_1 in equation (3.2-3) for the reactor power feedback effect on reactivity represents the fuel coefficient. The use of reactor power rather than modeling a separate fuel temperature is equivalent to assuming a fast thermal time constant for fuel temperature.

The primary loop average temperature feedback effect, b_2 in equation (3.2-3), represents the moderator temperature coefficient. An unsuccessful model which lumped the fuel and moderator feedback effects was also tested. The fuel and moderator effects tend to act together during rod reactivity experiments. However, during disturbances arising from load changes, the fuel and primary loop moderator water temperatures tend to move in opposite directions. Thus both effects must be included in a load change model.

A Xenon (Xe^{135}) effect on reactivity, represented by the parameter b_8 in equation (3.2-3), is included since Xenon effects can produce serious transients for power changes at high power levels. The fact that Xenon production changes slowly, while at high power levels Xenon burnoff changes directly with reactor power, leads to the significant Xenon transients at high power levels. Nearly all of the Xe^{135} is created by I^{135} decay. The Xe^{135} is destroyed by natural decay at low power levels, but a burnoff of Xenon due to reactor flux dominates at high power levels. An approximate model is:

$$\frac{dX}{dt} = b_{11} I - b_{10} X - b_9 P_R X \quad (3.2-4)$$

where:

b_9 is a parameter which is identified and adapted. The parameters b_{10} and b_{11} , associated with very slow effects, were not identified in this study. These parameters were set to theoretical values. They could be identified by analysis of long term data records if desired.

The I^{135} concentration in the reactor has a significant effect on high power operation because of the role of I^{135} in producing Xe^{135} . The I^{135} can be approximately represented as being created by fission and destroyed by natural decay. The equations for this are

$$\frac{dI}{dt} = b_{12} P_R - b_{11} I \quad (3.2-5)$$

where I is the concentration of I^{135} . This is a slow process which takes hours to experience significant transients. For this reason the parameters b_{11} and b_{12} are not identified or adapted in this study, but are set to theoretical values.

The control rods are modeled as an incrementally linear reactivity effect, represented by the parameter b_3 in equation (3.2-3). This is recognized as an approximation. The effect of nonlinear incremental rod worth appears as a reactivity disturbance and the later inclusion of disturbance noise in the model copes with this effect.

The rod control is modeled as:

$$\frac{dR}{dt} = u_1 \quad (3.2-6)$$

where u_1 , the rod rate of withdrawal, is a manipulated input of the plant.

In most plants the control rods are under an analog control system which is complex and nonlinear. In this study it is assumed that this analog control is replaced by digital control, thus the rod control is a plant input included in the model and available for control.

The model for the remainder of the plant, external to the reactor, is now considered. The primary loop is modeled as an energy storage.

$$\frac{dT_{AV}}{dt} = b_5(P_R - P_{Ro}) - b_6(P_T - P_{To}) \quad (3.2-7)$$

where:

T_{AV} is primary loop average temperature

P_R is reactor power

P_T is turbine power

The parameters b_5 and b_6 are identified and adapted.

The turbine and its control system constitute a dynamic system with a time constant on the order of seconds. The plant load is not directly adjustable, so that in adjusting load via the analog control setpoint this dynamic system must be considered. The turbine and its analog control system are modeled as a first order system

$$\frac{dP_T}{dt} = b_7 u_2 - b_7 P_T \quad (3.2-8)$$

where:

P_T is the turbine power

u_2 is the plant load setpoint, a manipulated input of the plant.

The parameter b_7 is identified and adapted.

The deterministic model developed in this section can be expressed as:

$$\frac{dx}{dt} = \underline{f}(\underline{x}, \underline{u}, \underline{b}) \quad (3.2-9)$$

where:

\underline{x} is a six dimensional vector of plant states

\underline{u} is a two dimensional vector of plant inputs

\underline{b} is a twelve dimensional vector of parameters

\underline{x} is taken as

$$\underline{x} = \begin{bmatrix} D \\ T_{AV} \\ P_T \\ R \\ X \\ I \end{bmatrix} \quad (3.2-10)$$

The nominal measurements are considered as

$$\underline{y} = \underline{h}(\underline{x}, \underline{u}, \underline{b}) \quad (3.2-11)$$

where

$$\underline{y} = \begin{bmatrix} P_R \\ T_{AV} \\ P_T \\ R \\ u_2 \end{bmatrix} \quad (3.2-12)$$

3.3 The Stochastic Model

A stochastic model of the plant is defined by allowing for disturbances and measurement noise models in addition to the deterministic model. The data from the plant consist of samples which are corrupted by noise. The noise is assumed to be added to the nominal measurement, equation (3.2-11), to give

$$z_K = h(x_K, u_K, b) + w_K \quad (3.3-1)$$

where the subscripts K refer to the sampled values at a time labeled K. w_K , the measurement sensor noise, is assumed to be zero mean white Gaussian noise with covariance W.

$$(w_K \ w_K') = W \quad (3.3-2)$$

The covariance matrix W is assumed to be unknown, to be identified from the data records.

The stochastic model allows for disturbance noise driving the model states. This noise represents random plant disturbances and model errors, which appear as disturbances. The result of allowing for disturbance inputs to the model is that the model states are described by probability distributions at a particular time. These distributions evolve through time. In order to consider the way in which these distributions evolve, a model linearized about the nominal expected state at each time K is formed. Small deviations from the expected state propagate approximately according to this linearized model. It is assumed that the probability distribution about the nominal state evolves according to this model also.

The system is linearized about the nominal trajectory $\underline{x}^*(t)$. In order to derive this trajectory, the continuous time differential equations must be integrated. The initial state \underline{x}_{K-1}^* is the initial condition for the integration. The effect of the input is approximated as

$$\underline{u}^*(t) = \underline{u}_{K-1} + \frac{t}{\Delta} (\underline{u}_K - \underline{u}_{K-1}) \quad (3.3-3)$$

where

$$\Delta = t_K - t_{K-1} \quad (3.3-4)$$

This approximation is not necessary when the inputs are under computer control, since the inputs then change only at times t_K .

The deviations from the nominal trajectory \underline{x}_K^* are:

$$\tilde{\underline{x}}_K = \underline{x}_K - \underline{x}_K^* \quad (3.3-5)$$

$$\tilde{\underline{x}}_K = A_{K-1} \tilde{\underline{x}}_{K-1} + G \underline{v}_K \quad (3.3-6)$$

where A_{K-1} is the solution at time t_K of

$$\frac{d\phi}{dt} = \frac{\partial \underline{f}(\underline{x}, \underline{u}, \underline{b})}{\partial \underline{x}} \bigg|_{\substack{\phi \\ \underline{x}^*, \underline{u}^*, \underline{b}}} \quad (3.3-7)$$

with initial condition

$$\phi(t_{K-1}) = I \quad (3.3-8)$$

The vector \underline{v}_K , representing the disturbance noise, is assumed to be zero mean, white Gaussian noise with identity covariance. The matrix G is

assumed to be unknown, to be identified. This structure allows the number of disturbance inputs to be chosen as a model parameter, and the number of identified stochastic parameters can be thus varied to meet the needs of the problem without necessarily requiring large numbers of unknown parameters.

The linearized model for the measurements about the nominal trajectory gives the nominal measurements:

$$\tilde{y}_K = \underline{h}(\underline{x}_K, \underline{u}_K^*, \underline{b}) - \underline{h}(\underline{x}_K^*, \underline{u}_K^*, \underline{b}) \quad (3.3-9)$$

so approximately

$$\tilde{y}_K = C_K \tilde{x}_K \quad (3.3-10)$$

where:

$$C_K = \left. \frac{\partial \underline{h}(\underline{x}, \underline{u}, \underline{b})}{\partial \underline{x}} \right|_{\underline{x}_K^*, \underline{u}_K^*, \underline{b}} \quad (3.3-11)$$

and the noisy measurements are

$$\tilde{z}_K = \tilde{y}_K + w_K \quad (3.3-12)$$

This completes the description of the stochastic model of the plant. This model is used for a variety of purposes in the study.

The model is summarized in Figure 3.3-1. The major manipulated inputs are the reactor control rods rate of movement and the turbine load setpoint. The model has a stochastic structure to allow for model errors, disturbances to the states, and measurement noise. The basic behavior of

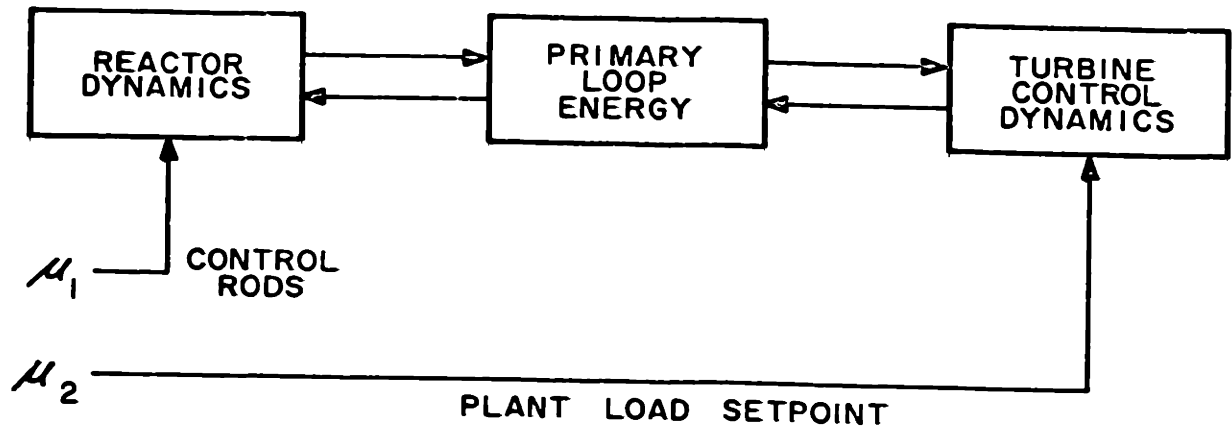


FIGURE 3.3-1 Model Summary

the model can be understood in terms of reactor power, turbine power and energy storage. There are dynamics associated with both the reactor power and the turbine power. If these two powers are somehow maintained equal, then the plant energy is constant and the stored energy in the plant is not seriously disturbed even if the power is rapidly changing. If the reactor power and the turbine are mismatched, then the plant energy is changing.

3.4 Initial Parameter Estimates

The identification technique requires a search over the parameters to determine, at least locally, the maximum likelihood estimates. This search is expedited by making some reasonable initial guesses on the parameters. The initial guess on the deterministic parameters was found by a fast least squares fit of the deterministic model to the data which were acquired from the simulated plant. The initial guesses for the stochastic noise model were made by a simple analysis of the noise in the simulated plant data records. The procedures used to generate these initial guesses are now considered in more detail.

A least squares identification was used to obtain tentative values for \underline{b} , the parameters of the deterministic model. The cost function was of the form:

$$J(\underline{b}) = \sum_{K=1}^N \sum_{i=1}^3 c_i (z_i - y_i)^2 \quad (3.4-1)$$

where:

y represents model predictions

z represents measurement data

c represents weighting factors

The rod position and load setpoint values are taken from the data records and used as if they were deterministic for this calculation. The measurements being considered in the cost function are:

- z_1 reactor power measurement
- z_2 primary loop average temperature measurement
- z_3 turbine power measurement.

The data was taken at one second intervals. The length of the data records varied from 100 to 300 seconds during which the plant was in a transient load change condition. The reactor power measurement was quite noisy with standard deviation on the order of 2 to 3% of the total signal, while the other measurements were less noisy. This was intended to match actual plant measurement conditions [60]. The costs were chosen so that equal costs were assessed for a 1% reactor power error, a 1% turbine power error, and a 1°F primary loop average temperature error.

The search technique was a modified Davidon-Fletcher-Powell [19], [25]. This method starts as a steepest descent search. As the search proceeds and information is gathered from the search, the method approaches Newton's method in efficiency. For quadratic cost functions this is a conjugate directions search, like the conjugate gradients method, and it converges in the same number of steps as the number of parameters being identified. In comparison, Newton's method converges in one step for quadratic cost functions, but it requires considerable computation. The Davidon-Fletcher-

Powell method combines the best features of both conjugate gradients and Newton's methods, and it is a powerful technique for minimizing functions which approximate a quadratic at the minima, the usual case. There are other good search techniques which could have been used [11], [31], but the Davidon-Fletcher-Powell method was chosen due to its excellent convergence properties.

The starting point $\underline{b} = 0$ was originally chosen for the search to test the possibility of identification with no a-priori guesses of parameter values. This resulted in local minima which were poor fits. This problem was resolved by starting from a crude guess of the values in \underline{b} , which were based on guesses of the time constants and magnitudes of the effects represented by these parameters. A local grid search using 3 values of each parameter was conducted about the crude guess. The search was then initiated from the best point on the grid search. The search generally converged after 2K to 3K directional searches, where K is the number of parameters identified. Each directional search requires K+1 evaluations to determine the gradient and an average of 4 evaluations along the search direction. The total number of cost function evaluations was thus generally 2K(K+5) to 3K(K+5). The computer time for this search was 2 to 5 minutes, depending on the number of parameters, length of data record, and number of directional searches. This time could undoubtedly be reduced in practice by more efficient programming. A typical run identifying 9 parameters and using 200 seconds of data with one second sample intervals takes 4 minutes for the least squares identification on an IBM 360-50 computer.

Figure 3.4-1 shows a data record which was taken from the simulated plant. The deterministic predictions of the model are superposed on this figure to illustrate the model fit. The initial estimates of the deterministic parameters, derived from the least squares fit procedure, were used to make the predictions.

In addition to initial estimates of the deterministic model parameters, it is also necessary to derive initial estimates of the noise model parameters. The estimate for the covariance of the measurement noise is taken directly from the measurement data records. The measurement covariance W is estimated from successive differences, making use of the theoretical relationship

$$E \left((z_K - z_{K-1}) [z_K - z_{K-1}]' \right) = 2R_0 - 2R_{-1} + 2W \quad (3.4-2)$$

where

$$R_0 = E (y_K y_K') \quad (3.4-3)$$

$$R_{-1} = E (y_K y_{K-1}') \quad (3.4-4)$$

are autocorrelation matrices for the process outputs.

For a process with time constants long compared to the sample time R_0 and R_{-1} are close in value and if the measurement noise covariance W dominates the difference, then approximately

$$W = \frac{1}{2} \langle (z_K - z_{K-1}) (z_K - z_{K-1})' \rangle \quad (3.4-5)$$

where $\langle \rangle$ indicates time average and where W is assumed stationary. Thus a simple technique for estimating the measurement noise directly from the

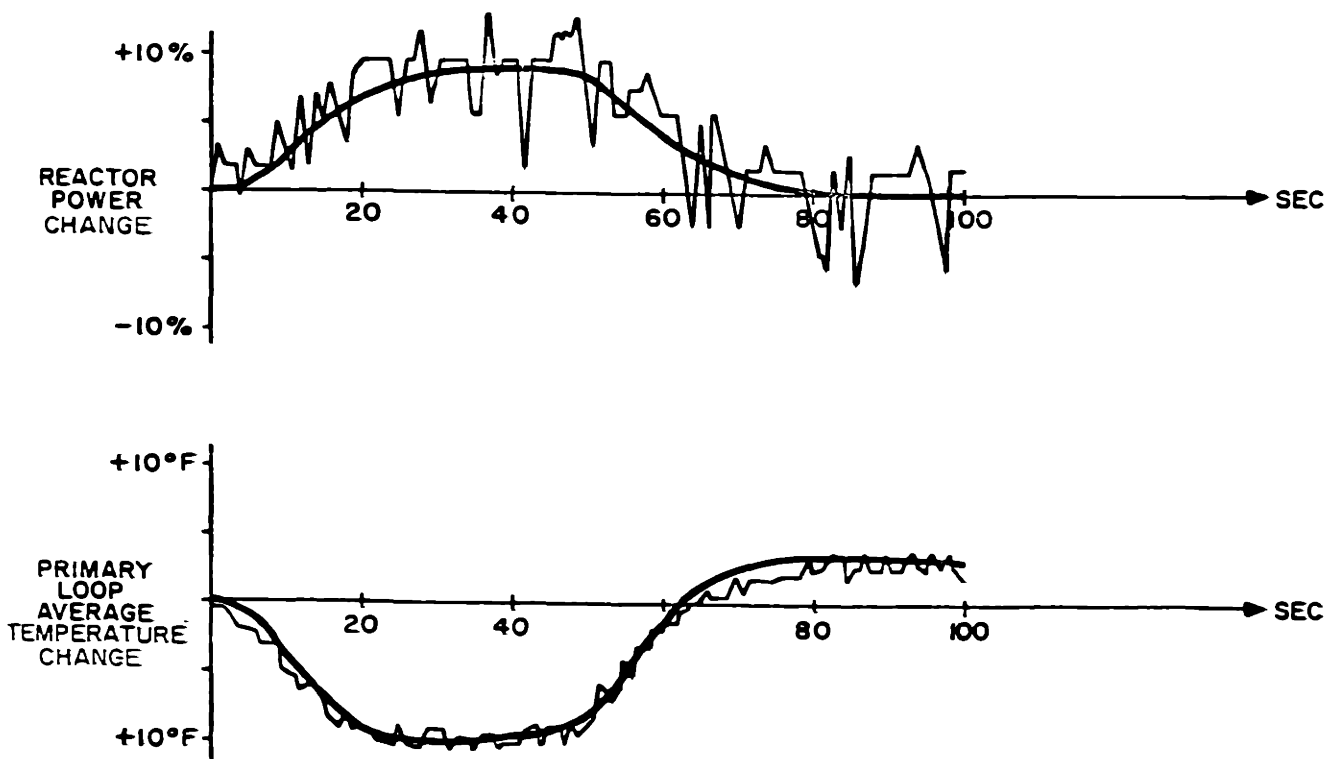


FIGURE 3.4-1 A Least Squares Fit

data records has been developed. Since this measurement noise covariance estimation is so straightforward and logical, this was chosen as the final estimation technique for the measurement noise parameters W .

An initial guess on the disturbance noise input matrix G was derived to provide a starting point for the search for the identification of the disturbance parameters. This guess was made to match the model covariance to the covariance produced by the noise on the measurements of the inputs operating through the linearized input matrix:

$$B = \frac{\partial f(\underline{x}, \underline{u}, \underline{b})}{\partial \underline{u}} \bigg|_{\underline{x}_0^*, \underline{u}_0^*, \underline{b}} \quad (3.4-6)$$

If the measurements of the inputs have a covariance U (estimated as in the case of the process measurements), then the matrix G_0 is chosen so that

$$G_0 G_0' = B U B' \quad (3.4-7)$$

Since G_0 is just an initial guess, the procedure is simplified by retaining only the diagonal elements of U in U_0 and by setting

$$G_0 = B \sqrt{U_0} \quad (3.4-8)$$

Procedures have been described for the initial estimates or guesses for the parameters of the model, the deterministic parameters \underline{b} and the stochastic matrix parameters W and G . The parameters \underline{b} and G are further identified by maximum likelihood techniques, while the initial estimate of W is retained as is. The further identification of \underline{b} generally produced small changes, however the further identification of G gives a much

different final identification. The initial guesses on the parameters do not satisfy a statistical hypothesis test, described later, while the final maximum likelihood estimates do give a model which is statistically consistent with the plant. Thus the initial guesses developed in this section cannot be accepted as final, and a further maximum likelihood identification is necessary.

3.5 Maximum Likelihood Identification

The likelihood function is formed from the conditional probability function of the observations given the parameters by considering the latter as if the parameters were unknown and the observations known. The likelihood function is:

$$L_N(\underline{\alpha}) = p(\{\underline{z}_k\}_N | \underline{\alpha}) \quad (3.5-1)$$

where the parameters $\underline{\alpha}$ include the deterministic parameters \underline{b} and the parameters of the noise model in the matrix G . The data record $\{\underline{z}_k\}_N$ is a set of N measurement vectors which are taken from the plant. If $\underline{\alpha}$ were given then the probability density function for any set $\{\underline{z}_k\}_N$ is given a-priori by $p(\{\underline{z}_k\}_N | \underline{\alpha})$, the conditional probability density function. If the data $\{\underline{z}_k\}_N$ is given and $\underline{\alpha}$ is unknown, then the same function is viewed as a likelihood function.

The maximum likelihood estimate of the parameters $\underline{\alpha}$ is the estimate which maximizes the likelihood function, or equivalently which maximizes the log likelihood function. The latter function is easily computed using a Kalman filter which is described in Appendix B. An important

property of the Kalman filter is used in this method. The Kalman filter produces the conditional mean and covariance of the states and residuals at time K. For Gaussian probability distributions these are sufficient statistics to produce the conditional probability functions. The Kalman filter can thus be used to generate the conditional probability density function $p(\underline{z}_N | \{\underline{z}_K\}_{N-1}, \underline{\alpha})$. This function is used in a manner described later in this section to determine the likelihood function. Thus the calculation of the likelihood function for the stochastic state variable problem makes use of properties of the Kalman filter.

The model at hand is a nonlinear one, so it is linearized at each time step about the estimated state. This gives the effect of a time varying linear model. The estimates of the states are defined as:

$\hat{\underline{x}}_K$, the a-priori estimate of \underline{x}_K , before observing \underline{z}_K

\underline{x}_K^* , the a-posteriori estimate of \underline{x}_K , after observing \underline{z}_K

The nominal trajectory, and the linearization are as described in Section 3.3.

The extended Kalman filter for the system is described by the equations for the propagation of the mean and the covariance:

$$\underline{x}_K^* = \hat{\underline{x}}_K + \Gamma_K C_K' [C_K \Gamma_K C_K' + W]^{-1} (\underline{z}_K - \underline{h}(\hat{\underline{x}}_K, \underline{u}_K, \underline{b})) \quad (3.5-2)$$

$$\Gamma_{K+1} = A_K P_K A_K' + GG' \quad (3.5-3)$$

$$P_K = \Gamma_K - \Gamma_K C_K' (C_K \Gamma_K C_K' + W)^{-1} C_K \Gamma_K \quad (3.5-4)$$

where P_K is the covariance matrix for the a-posteriori state estimates

$$P_K = \mathcal{E} [(\underline{x}_K^* - \underline{x}_K)(\underline{x}_K^* - \underline{x}_K)'] \quad (3.5-5)$$

and where Γ_K is the covariance matrix for the a-priori state estimates.

$$\Gamma_K = \mathcal{E} [(\hat{x}_K - x_K)(\hat{x}_K - x_K)'] \quad (3.5-6)$$

The a-priori estimate \hat{x}_{K+1} is found by integrating the nonlinear differential equations from the state x_K^* . An initial state and covariance, x_0^* and P_0 , must be specified.

The residuals of the Kalman filter are of particular interest, these residuals represent the difference between model prediction and observations.

$$r_K = z_K - h(\hat{x}_K, u_K, b) \quad (3.5-7)$$

which according to the linearized model is

$$r_K = C_K \tilde{x}_K + w_K \quad (3.5-8)$$

The residuals are theoretically a zero mean white Gaussian process with covariance matrix:

$$R_K = C_K \Gamma_K C_K' + W \quad (3.5-9)$$

The fact that for a correct model the residuals are a white noise process, that is, uncorrelated in time, is used in the hypothesis test. An incorrect model will produce correlated residuals and the hypothesis test is designed to be sensitive to correlation to detect this.

The manner in which the likelihood function is maximized, making use of the extended Kalman filter, is now considered. The probability function $p(\{z_K\}_N | \alpha)$ is defined as the likelihood function. The value of α which

maximizes this function is called the maximum likelihood estimate. This value of $\underline{\alpha}$ also maximizes the log of the likelihood function

$$\xi_N(\underline{\alpha}) = \log[p(\{z_K\}_N | \underline{\alpha})] \quad (3.5-10)$$

Now by Bayes rule

$$p(\{z_K\}_N | \underline{\alpha}) = p(\{z_K\}_{N-1} | \underline{\alpha}) p(z_N | \{z_K\}_{N-1}, \underline{\alpha}) \quad (3.5-11)$$

Thus, the log likelihood function can be calculated recursively.

$$\xi_N(\underline{\alpha}) = \xi_{N-1}(\underline{\alpha}) + \log[p(z_N | \{z_K\}_{N-1}, \underline{\alpha})] \quad (3.5-12)$$

The probability term is known from the covariance matrices propagated by the Kalman filter.

$$p(z_N | \{z_K\}_{N-1}, \underline{\alpha}) = [(2\pi)^{K_2} |\det R_N|]^{-1/2} \exp\{-\frac{1}{2} \underline{r}_N' R_N^{-1} \underline{r}_N\} \quad (3.5-13)$$

where R_N is the covariance matrix of the residuals \underline{r}_N . K_2 is the dimension of \underline{r}_K . Taking logs, the propagation equation is

$$2 \xi_N(\underline{\alpha}) = 2 \xi_{N-1}(\underline{\alpha}) - \ln |\det R_N| - K_2 \ln 2\pi - \underline{r}_N' R_N^{-1} \underline{r}_N \quad (3.5-14)$$

This equation can be appended to the extended Kalman filter to generate the log likelihood function. The filter is rerun over data with a new parameter set $\underline{\alpha}$ to evaluate the likelihood function for the new $\underline{\alpha}$. An efficient search procedure, described previously in Section 3.4, is used to find the maximum likelihood values of the parameters $\underline{\alpha}$. Figure 3.5-1 shows the Kalman filter with the likelihood calculation appended.

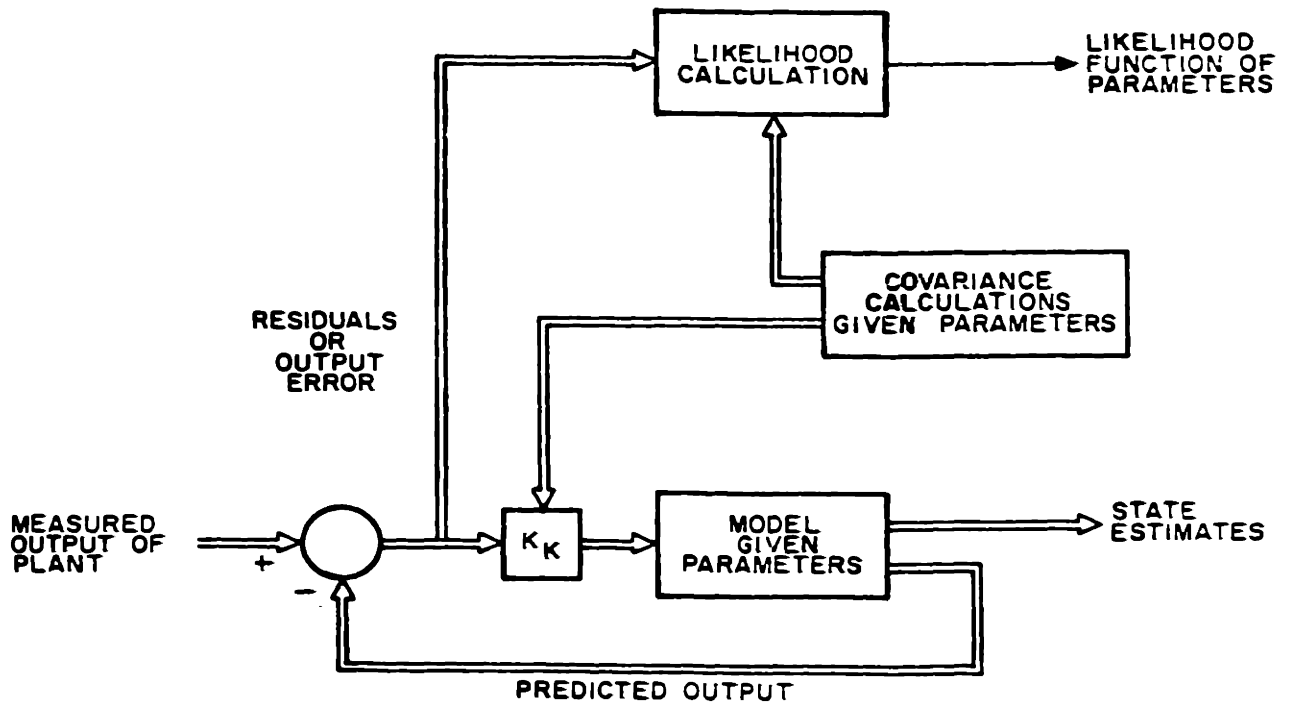


FIGURE 3.5-1 A Kalman Filter with Likelihood Calculation Appended

3.6 Hypothesis Test

The time required for a re-identification makes it desirable to continue to use a model so long as it adequately represents plant behavior. To evaluate this, a hypothesis test is used.

The residuals of the extended Kalman filter are considered. The null hypothesis H_0 is that these residuals are a white sequence of Gaussian distributed independent random vectors:

$$\underline{r}_1, \underline{r}_2, \dots, \underline{r}_N$$

with zero mean and covariance which is propagated by the filter equations:

$$R_K = C_K \Gamma_K C_K^t + W \quad (3.6-1)$$

The desired form of the hypothesis test is a single statistic, which under the null hypothesis has a known distribution and which is also sensitive in some sense to an alternative hypothesis. The alternative hypothesis H_1 is that the sequence of vectors $\{\underline{r}_K\}$ is serially correlated. The statistic which is considered is a simple extension to multiple variables of the Mean Square Successive Difference Test which is used by statisticians for the same purpose [12]. The principle of the test is to estimate the covariance from the samples in two different ways, one of which is sensitive to serial correlation. The required calculations are:

$$\bar{\underline{r}} = \frac{1}{N} \sum_{K=1}^N \underline{r}_K \quad (3.6-2)$$

$$S = \frac{1}{N-1} \sum_{K=1}^N (\underline{r}_K - \bar{\underline{r}})(\underline{r}_K - \bar{\underline{r}})' \quad (3.6-3)$$

$$D = \frac{1}{2(N-1)} \sum_{K=1}^{N-1} (r_{K+1} - r_K)(r_{K+1} - r_K)' \quad (3.6-4)$$

If the model is correct, then the residuals are uncorrelated and S and D are both unbiased estimates of R. If R_K is not stationary, but if the model is correct, then S and D should still be approximately equal, and they will be estimates of the average of R_K .

The statistic D is insensitive to serial correlation, while the statistic S is not. Thus if the model is correct and the residuals are white, then D and S will be comparable, while if the model is incorrect and the residuals are correlated they will tend to be different.

The test is simplified by considering the diagonal elements of R. If s_L and d_L are the L-th diagonal elements, then

$$\mu_L = \frac{\frac{d_L}{s_L} - 1}{\sqrt{\frac{N-2}{N^2-1}}} \quad (3.6-5)$$

is approximately unit normal under the hypothesis H_0 for large N.

Brownlee [12] states that this is a good approximation for N as small as 10.

In order to incorporate all the diagonal elements in the hypothesis test, a statistic is calculated:

$$T = \underline{\mu}' \underline{\mu} \quad (3.6-6)$$

Since the μ_L are theoretically unit normal under hypothesis H_0 , T is

theoretically Chi-squared with K_2 degrees of freedom, where K_2 is the dimension of $\underline{\mu}$. Table 3.6-1 shows the theoretical variation with dimension and level of significance.

This hypothesis test proved to be very sensitive to model error, as is desired. The statistic T performs about as expected under hypothesis H_0 when the model fit is good. However, if the plant is varied the statistic gets large quickly, giving a forewarning of model error. This occurs because the statistic is sensitive to correlation in the residuals, and in the case of correlated residuals the statistic tends to grow as N gets larger. The hypothesis test thus provides the means of judging the acceptability of model fit, both for the initial maximum likelihood identification, and also for the on-line performance tests.

3.7 Results of Model Identification

The uncertain parameters of the model were identified by a maximum likelihood procedure. Initial estimates of the parameters of the deterministic portion of the model were first found using the techniques described in Section 3.4. With these initial guesses the time required for a maximum likelihood identification was about 10 minutes of IBM 360-50 computer time per 100 seconds of data for 10 undetermined parameters. In practice, this identification time could be improved by orders of magnitude depending on program efficiency, approximation in the calculations, and the speed of the computer. There was no effort to minimize this computer time in this study.

TABLE 3.6-1
Chi-Squared Probability Table

$\underline{\mu}$ is a vector of theoretically unit normal components

$T = \underline{\mu}'\underline{\mu}$ is a Chi-squared distributed random variable

p is the probability that $T \leq E$

Dimension of Vector Values of E for Specific Probabilities

	$p = .999$	$p = .95$	$p = .9$	$p = .5$
1	10.8	3.84	2.71	.455
2	13.8	5.99	4.61	1.39
3	16.3	7.81	6.25	2.37
4	18.5	9.49	7.78	3.36
5	20.5	11.1	9.24	4.35

The identifications were made using data taken with and without analog control. The experiments support the following conclusions:

1. Different short data records from the same plant yield somewhat different parameter values. These values are consistent with the search started at two different initial points.
2. A plant variation (decrease of moderator feedback by a factor of 10) followed by a re-identification yields a successful model fit.
3. All identifications were successful starting from a crude guess of parameters. These crude guesses varied in error from a factor of 2 to a factor of 10.
4. Data taken under analog control, for three different experiments and for various load changes from 10% to 40%, tended to give mutually consistent parameter values. Data taken without analog control gave a somewhat different set of parameter values. The models of each, when evaluated for the other type, gave fair model fits. It is thus considered acceptable to perform the initial identification using data taken with the plant under analog control.

The maximum likelihood identifications were done on a plant startup model with no equilibrium Xenon. The results of identifications for four separate data sets are shown in Table 3.7-1. In general the deterministic model parameters do not vary much for good fits, while the stochastic model parameters vary considerably, indicating local minima or non-unique minima. All of these identifications provide acceptable model fits. The hypothesis test indicates that the models are consistent with the data. The

TABLE 3.7-1

Results of Maximum Likelihood Identifications

<u>Deterministic</u>	<u>PARAMETERS</u>				
	<u>Initial</u>	<u>Run A</u>	<u>Run B</u>	<u>Run C</u>	<u>Run D</u>
b_1	+2.	+1.9968	+2.0026	+2.1947	+2.0003
b_2	+2.	+2.0004	+1.9992	+2.2279	+1.9997
b_3	+1.	+1.0036	+ .9982	+1.0363	+1.1998
b_4	.01	.0103	.0108	.0088	.0043
b_5	.2	.2031	.1994	.2087	.1954
b_6	.175	.1751	.1758	.1973	.1793
<u>Stochastic</u>					
ϵ_1	0.	- .0024	- .0039	.0000	.0004
ϵ_2	0.	- .0010	.0035	- .0002	.0008
ϵ_3	0.	.0009	.0004	- .0011	.0014
ϵ_4	.007217	- .0016	- .0001	- .0004	- .0005

Other Results:

Negative Log Likelihood:

<u>Run A</u>	<u>Run B</u>	<u>Run C</u>	<u>Run D</u>
-.1887.75	-1884.23	-1859.68	-1901.64

Hypotheses Test Vector (Elements theoretically are unit normal if model fits):

<u>Run A</u>	<u>Run B</u>	<u>Run C</u>	<u>Run D</u>
-.8251	-.8650	-.8961	-.8612
.7151	.1431	-1.6352	-.2553

TABLE 3.7-1 (Continued)

Hypothesis Test Statistic (Theoretically Chi-squared with 2 degrees of freedom if model fits):

<u>Run A</u>	<u>Run B</u>	<u>Run C</u>	<u>Run D</u>
1.192	.769	3.477	.8069

Probability of a test statistic worse than the observed, given a correct model:

<u>Run A</u>	<u>Run B</u>	<u>Run C</u>	<u>Run D</u>
55%	68%	17%	67%

corresponding results for a model with Xenon, identifying 9 deterministic parameters and 10 stochastic parameters, is given in Table 3.7-2.

One search was performed using the hypothesis test as the performance criteria rather than the negative log likelihood. The best fit models under these two criteria are not precisely the same; however, the two criteria do have a very strong tendency to move together, and the likelihood function and hypothesis test statistic values were not significantly different using the alternate criteria.

The numerical solution techniques were found to be an important factor in the validity of the maximum likelihood search. The numerical gradient calculations in particular, involving differences of numbers which are the end result of extensive calculations, are a critical factor. There are two major sources of error: truncation error, which results from using approximations to solve the differential equations, and accumulated roundoff error, which results from the roundoff which occurs in representing every number at every calculation by a finite computer word. These effects, if they are recognized, can be compensated. Truncation error can be reduced by using more accurate integration methods, and roundoff can be reduced by using double precision arithmetic or by changing to another computer with a greater word length. This situation is conceptually shown in Figure 3.7-1.

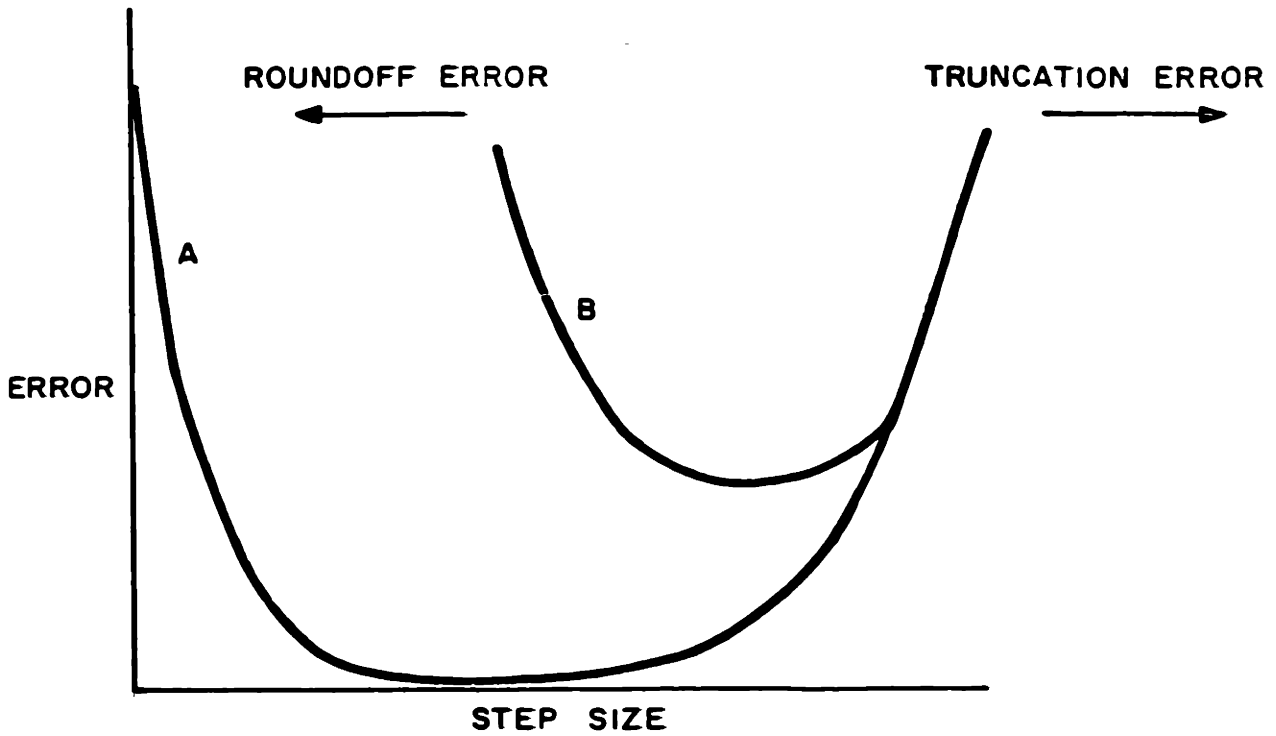
An experiment was employed in this study to detect these errors by repetitive calculation of a gradient at a point near the minimum of the search, with a smaller step at each gradient calculation. Actually each parameter had an individual step size, in ratio to its magnitude, and this

TABLE 3.7-2

Results of Identification for a Larger Model with Xenon Effects

Deterministic Parameters		Stochastic Parameters	
b_1	1.59	ε_1	.00010
b_2	2.00	ε_2	.00156
b_3	.21	ε_3	-.00269
b_4	.05	ε_4	.00045
b_5	.31	ε_5	.00113
b_6	.23	ε_6	.00265
b_7	.13	ε_7	-.00111
b_8	.52	ε_8	.00004
b_9	3.12	ε_9	-.00012
		ε_{10}	.00001

Hypothesis Test Result: Probability of a worse test statistic if the model is correct: 47%.



- A. SUFFICIENT WORD LENGTH IN COMPUTER
- B. INSUFFICIENT WORD LENGTH IN COMPUTER

FIGURE 3.7-1 Effects of Truncation and Roundoff Errors

ratio was the adjusted value. The first use of this method showed no convergence, indicating that a program change to reduce truncation or roundoff error was necessary. The integration technique was changed from Euler to fourth order Runge-Kutta at a cost of nearly 50 percent in the total computation time. This reduced truncation error.

The effect of roundoff error is more difficult to correct. The effect of finite computer word size is to add a term similar to pseudo-random noise to the performance function.

$$J(\underline{\alpha} + \underline{\Delta}) = J^*(\underline{\alpha} + \underline{\Delta}) + w_1 \quad (3.7-1)$$

where J^* is the accurate value and where w_1 represents pseudo-random noise due to computer roundoff. When the noisy performance functions are used to calculate gradients, the result is approximately the true gradient plus a noise term

$$\underline{g}(\underline{\alpha}) = \underline{g}^*(\underline{\alpha}) + \frac{1}{\Delta} (w_1 - w_2) \quad (3.7-2)$$

As the step size used for the gradient approximation gets small, the gradient does not converge to the true $\underline{g}^*(\underline{\alpha})$, but rather it becomes more noise dominated.

The gradients at a value of $\underline{\alpha}$ near the minimum are shown in Figure 3.7-2. This shows that computational or roundoff noise definitely exists and that it limits the resolution severely for the maximum likelihood technique. The noise can be reduced by multiple sampling (at small separations) or by using a computer with a larger word size.

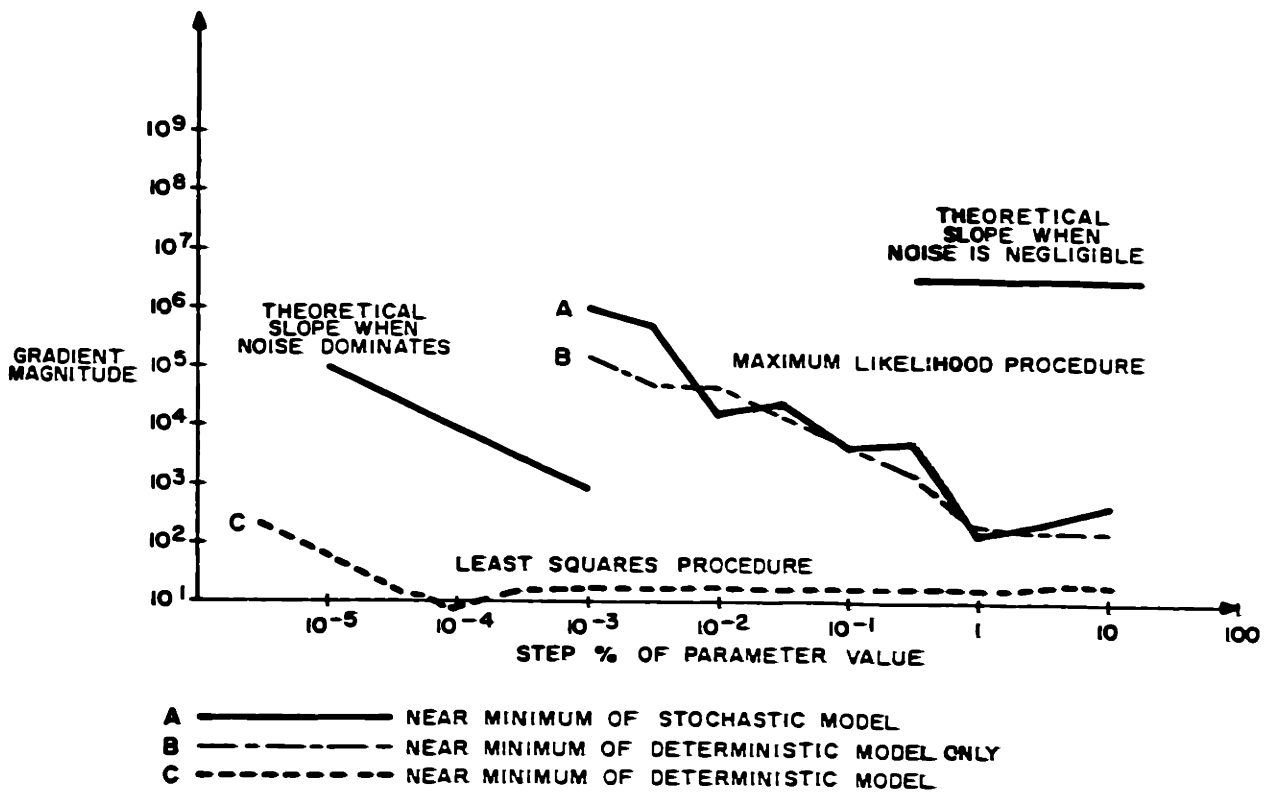


FIGURE 3.7-2 Experimental Determination of Roundoff Errors

On the basis of the identification results and the roundoff error tests, some conclusions can be drawn. The maximum likelihood technique seems most useful in identifying the parameters of the noise portion of the model, particularly the parameters of the disturbance noise. On the other hand, for the deterministic model parameters, the maximum likelihood has poor resolution and a much longer computing time relative to the least squares technique.

The procedure followed in this study was to perform the maximum likelihood search off-line on data records to arrive at a stochastic model. The parameters of the noise portion of the model were then assumed constant, and the on-line adaptation was of the deterministic model parameters only, using the least squares technique. In a plant application it would be desirable to put the maximum likelihood identification on line as well to provide on-line adaptation of the disturbance noise parameters.

The identification or model adaptation need be repeated only when a hypothesis test indicates that the model validity is degraded. This model adaptation may be done between load changes, using data acquired during the load change. This was the procedure used in the demonstration of the identification in this study.

CHAPTER 4

THE DETERMINISTIC CONTROL

4.1 Definition of the Control Problem

A goal of this study is to provide a control scheme which can make large and fast load changes without serious disturbances to the nuclear plant. This control must operate in the presence of variation and uncertainty. The problem is attacked in two parts. The first part, discussed in Chapter 4, deals with the deterministic control problem, which involves the control of the deterministic model alone with no consideration of variation or uncertainty. The second part, discussed in Chapter 5, presents the modifications which are made to cope with plant variation and with uncertainty.

The goal of the control strategy developed here is to provide rapid load changes which keep the plant within specified constraints. The operator can choose some of these constraints to ensure smooth plant operation. Other constraints are calculated based on plant capabilities and on the initial plant state. Altogether the constraints define regions of operation within which a load change can be made without serious upsets to the plant.

If there were no constraints, then a large fast load change would be no problem. The turbine power would simply be changed to provide the new load as fast as possible, with no consideration as to the effect on the plant, and the rods would be used to try to restore plant equilibrium.

This is the way that small step load changes are made by a typical analog control system. However, this procedure is inadequate for a large fast load change, where it would seriously disturb the plant and cause considerable deviations in some variables which should not be disturbed. Sizable load changes should be made in a manner which does not disturb the plant beyond some chosen constraints. This requires a coordinated control strategy for the turbine and the reactor. The inputs to the plant are calculated, based on a model of the plant and on the current estimated plant state. The model used for derivation of the control was presented in Section 3.3. The strategy developed in this study is intended to provide a rapid load change without violating the chosen plant constraints.

In the language of control theory, the plant constraints are of two types: input constraints and state constraints. The input constraints to the problem are discussed more fully in the next section. These input constraints are on the rate and extent of rod movement and on the turbine power rate of change, which is related to an input.

The state constraints are due to a combination of chosen constraints and calculated constraints. These are considered in detail in the following section. The plant constraints considered include primary loop pressure deviations, pressurizer level deviations, and primary loop average temperature deviations.

In addition to the general rapid load change problem, the special case where the constraint on the primary loop average temperature is reduced to zero deviation is considered. This corresponds to balancing

reactor power and turbine power throughout the load change, thereby not disturbing the stored energy in the primary loop or, equivalently, not disturbing the average temperature in the primary loop. This strategy produces a somewhat slower load change, but it has the advantage of eliminating the undesirable plant variations in primary loop pressure and in pressurizer level. This strategy is explained more fully in Section 4.3.

In summary, the deterministic part of the control problem is to take the plant, without yet considering uncertainty, through a specified load change rapidly, subject to certain constraints. The load change would be trivial and also impractical if there were no constraints. Some of the constraints are hard constraints, due to physical limitations or deviation limits. Other constraints, such as turbine power rate of change, are available as control parameters. The control problem, in the face of all the constraints, is to provide sufficiently smooth plant behavior and to still make fast load changes.

4.2 Input and State Constraints

The constraints on the inputs of the model are a limit on rate of rod group motion u_1 and a limit on plant load setpoint u_2 . There is another effective input constraint, which is the constraint on maximum allowed rate of turbine power change. The rate of change of turbine power, $\frac{dP_T}{dt}$ can be considered to be effectively an input to the plant, since it is controlled directly by adjustments in the plant load setpoint

u_2 . The control strategy is designed as if $\frac{dP_T}{dt}$ were directly controlled, and then in implementation the desired $\frac{dP_T}{dt}$ is used to calculate adjustments in the actual input u_2 . This was the strategy used in the computer control demonstration.

For the reasons discussed above, the constraints on the inputs are expressed as rod rate and turbine power rate constraints

$$\left| \frac{dR}{dt} \right| \leq M_1 \quad (4.2-1)$$

$$\left| \frac{dP_T}{dt} \right| \leq M_2 \quad (4.2-2)$$

The constraint on rod movement $\frac{dR}{dt}$ is a hard constraint, due to physical limitations on the rate at which a rod group can be moved. The value for the rod rate constraint used in this study was 45 inches per minute, corresponding to typical existing plants.

The constraint on the turbine power rate of change $\frac{dP_T}{dt}$ is less rigid. The physical limitation on turbine power rate of change depends on the rate at which the analog turbine control system moves the throttle valves. The value of the turbine power rate constraint used in this study was 1% per second, which is well within the capacity of a typical plant. A more restrictive rate may be specified to reduce turbine blade stress or to force slower load changes. Thus the turbine power rate of change constraint acts as a parameter of the control scheme, which can be set at a conservative value to slow down the load change if desired.

The reactor power rate of change is also restricted. The control strategy developed here generally balances the turbine and reactor power

rates of change so that only one of these needs to be constrained. The reactor power rate of change constraint is phrased in terms of the turbine power constraint M_2 in this study, so that the reactor constraint is

$$\left| \frac{dP_R}{dt} \right| \leq \frac{b_6}{b_5} M_2 \quad (4.2-3)$$

The fundamental constraint could be expressed in terms of reactor power rate of change if desired, without affecting the results of the study.

The exact values of the rod rate and turbine power rate constraints are not important to the conclusions of the study. These constraints can be chosen as control parameters if desired, so long as the chosen values lie within the plant capability. The control strategy simply remains within the constraints, whatever they are.

The state constraints which are used in the study are due to plant conditions which must be considered during the load change. Some of these plant conditions are pre-specified deviation limits, which will trigger a plant shutdown if they are violated.* Examples of these are the limits on primary loop pressure, pressurizer level, and primary loop average temperature.

Other plant conditions which must not be violated are considered here, which are dependent on unmeasured variables. The effect of Xenon puts a limit on the manner in which a large load change can be made.

*An automatic emergency plant shutdown is commonly referred to as a plant "trip". The reactor shutdown is colorfully called a "scram". In the cases considered here, at high power operation, reactor scrams and plant trips occur together.

These limits also depend on the amount of available rod reactivity and on the rate at which rod reactivity can be applied.

The plant state constraints are now considered in more detail. The explicit constraints on primary loop pressure, pressurizer level, and primary loop average temperature are considered first. These are the constraints which are first violated, barring accidents, in the event of a poor load change control for high power operation conditions.

The pressurizer level is considered first. During transient plant conditions the pressurizer level changes as water surges into or out of the pressurizer. These surges are due to changes in the primary loop average temperature, and the resulting expansion or contraction of water. Thus pressurizer level deviations can be related directly to deviations in primary loop average temperature.

Let

V_T = pressurizer total volume (fixed)

V_S = steam volume

V_L = liquid volume (level is measured)

P = pressure (measured)

ΔT = primary loop average temperature deviation from equilibrium

The pressurizer level deviation limits are transformed into constraints on primary loop temperature. Let:

V_1 = low liquid volume limit

V_2 = high liquid volume limit

S = total surge

Then
$$\Delta T_1 = \frac{V_1 - V_L}{S} \quad (4.2-4)$$

$$\Delta T_2 = \frac{V_2 - V_L}{S} \quad (4.2-5)$$

ΔT_1 , ΔT_2 are low and high limits on primary loop average temperature which will cause a violation of the pressurizer level limit. These calculated state constraints ΔT_1 and ΔT_2 depend on the current liquid volume V_L .

Figure 4.2-1 shows the relationship between pressurizer level deviations and temperature deviations for a nominal plant with a 1000 ft.³ pressurizer and with 5000 ft.³ of water in the primary loop. It is clear that the limits on pressurizer level can be respected by observing calculated constraints on the primary loop average temperature.

The effect of primary loop pressure deviations is analyzed by considering the pressure in the pressurizer. An approximation is made that the pressurizer controls are too slow to affect the results of a fast load change. This is a conservative approximation which is not far wrong.* As a worst case approximation flashing and condensation are neglected and the pressurizer is analyzed as a simple surge tank.

The total surge into the tank is due to the change in primary loop average temperature, and the resulting expansion or contraction of water. Thus the approach is to relate pressure transients under worst case

*On the nominal plant for this study, a 100 ft.³ total surge out corresponding to 12°F primary loop average temperature drop would cause a pressure transient which would require about 300 seconds to correct with a 1 Megawatt heater input. Flashing is neglected in this approximation.

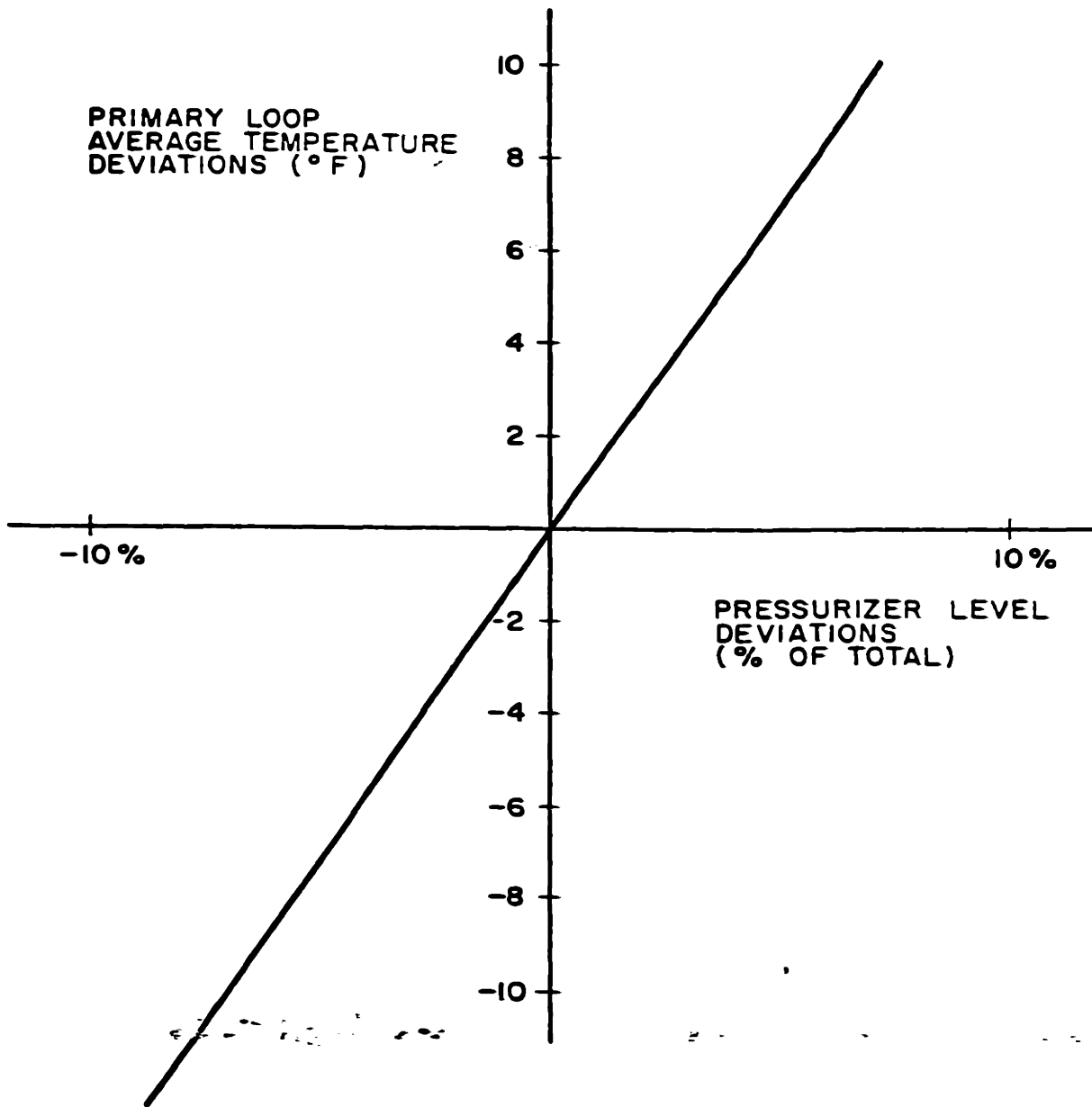


FIGURE 4.2-1 Pressurizer Level Deviations for Fast Primary Loop Average Temperature Transients

conditions to the total surge, which is in turn related to primary loop average temperature deviations.

The pressure in the pressurizer during fast transients can be approximately related to total surge if a gas law is assumed. The gas law is assumed to have the general form:

$$PV_S^\delta = \text{Constant}. \quad (4.2-6)$$

The exponent δ varies from 1.0 for an isothermal ideal gas process to higher values for adiabatic processes. A value of 1.2 is used in this study corresponding to a process intermediate between isothermal and adiabatic.

If the pressure constraints are defined:

P_1 low pressure limit

P_2 high pressure limit

then the equivalent liquid volume constraints V_1' and V_2' are found in terms of these limits on pressure and in terms of the current pressure P and liquid volume V_L .

$$P_1 (V_T - V_1')^\delta = P (V_T - V_L)^\delta \quad (4.2-7)$$

$$P_2 (V_T - V_2')^\delta = P (V_T - V_L)^\delta \quad (4.2-8)$$

The state constraints on the primary loop average temperature $\Delta T_1'$ and $\Delta T_2'$ due to the liquid volume limits V_1' and V_2' are found using equations (4.2-4) and (4.2-5). Thus state constraints $\Delta T_1'$ and $\Delta T_2'$ have been derived from a worst case analysis of pressure deviations. Figure 4.2-2 shows this relationship for the nominal plant considered in this study.

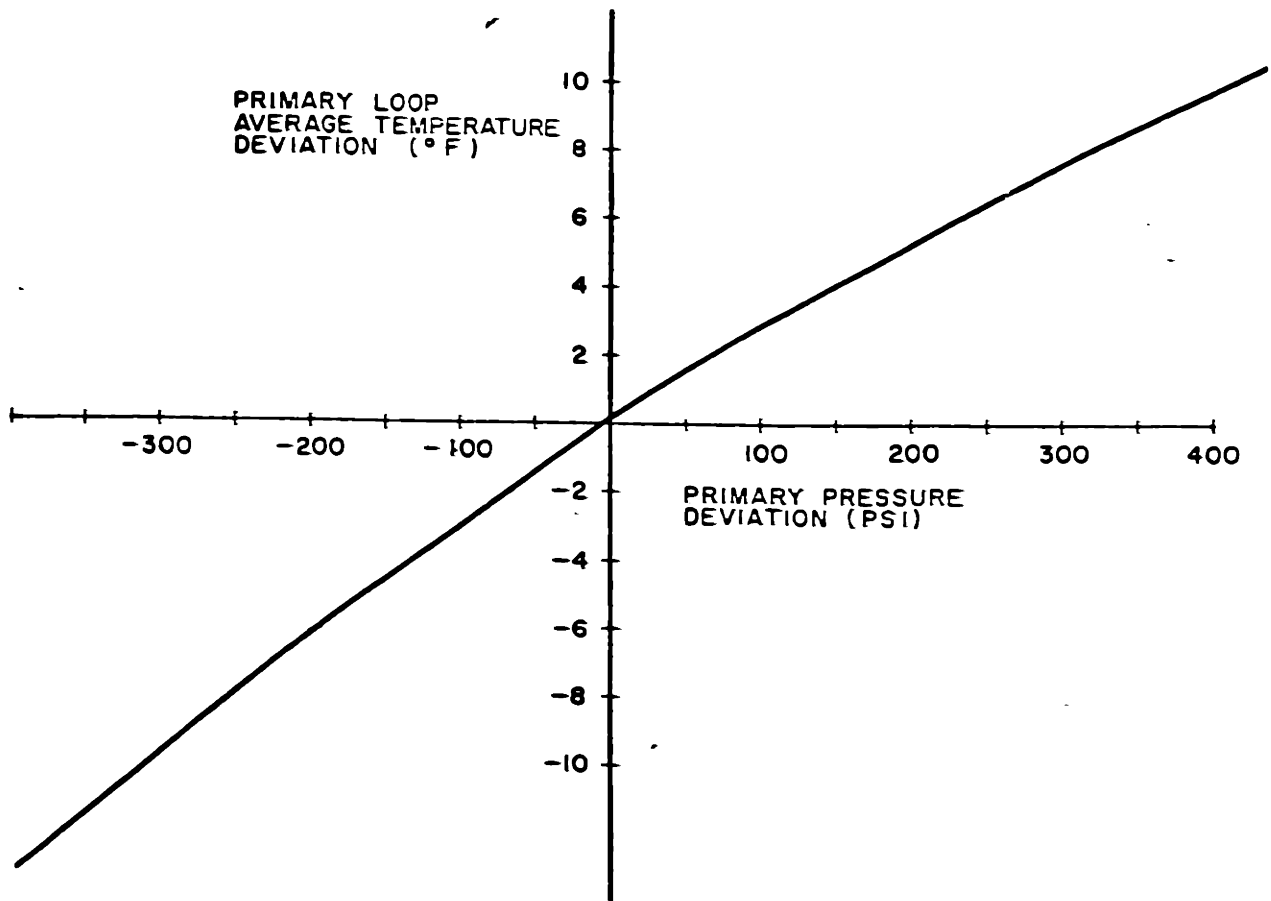


FIGURE 4.2-2 Primary Loop Pressure Deviations for Fast Primary Loop Average Temperature Transients

In a previous analysis the constraints on pressurizer level were translated into constraints ΔT_1 and ΔT_2 on primary loop average temperature. Similarly constraints on pressurizer pressure, considered for a worst case analysis, were translated into constraints $\Delta T_1'$ and $\Delta T_2'$ on primary loop average temperature. A direct constraint on primary loop average temperature deviations can also be justified in terms of avoiding thermal shock during the load change. Temperature changes cause stresses on the pipes and joints around the plant, and avoidance of large transients can be justified in terms of minimizing these stresses. Constraints $\Delta T_1''$ and $\Delta T_2''$ are assumed to be specified for this reason.

Three constraints on primary loop average temperature have been derived, based on constraints on pressurizer level, pressurizer pressure, and a direct constraint on average temperature. The most restrictive of the constraints is chosen as the actual state constraint. The low deviation constraint is thus:

$$\Delta T_1^* = \max\{\Delta T_1, \Delta T_1', \Delta T_1''\} \quad (4.2-9)$$

while the high deviation constraint is

$$\Delta T_2^* = \min\{\Delta T_2, \Delta T_2', \Delta T_2''\} \quad (4.2-10)$$

The control strategy is designed to maintain primary loop average temperature within the constraints ΔT_1^* and ΔT_2^* .

As a special case, a suboptimal load change strategy which produces slower load changes but less plant variation can be obtained by making the state constraints ΔT_1^* and ΔT_2^* even more restrictive. From the preceding analysis it is clear that an imposed choice of ΔT_1^* and ΔT_2^* equal to zero

will cause no deviations in primary loop pressure or pressurizer level. This is physically due to the fact that there is no total surge into the pressurizer if the primary loop average temperature is maintained constant. This strategy is suboptimal since it leads to longer load changes, but it is attractive in terms of smooth plant operation and so it is considered as a special case of the constrained control problem.

The presence of Xenon, which is significant at high power operation, imposes additional constraints on the problem. The Xenon effect is discussed in Section 3.2. The consequences of Xenon on the control of the plant are serious at high power levels. It is possible to initiate a Xenon transient which causes reactivity to change more than the control reactivity can be changed. This may occur for large fast power changes starting from a high operating power. The problem is familiar for reactor shutdown [3], [43], [52]. For load changes the problem is less severe than for shutdown, but it is still a factor to be considered.

The reactivity transient produced by the Xenon must be countered by control rod motion in order to maintain the overall reactivity constant after the load change. The available control rod travel is defined as:

- + ΔR_1 rod withdrawal capability in inches
- ΔR_2 rod insertion capability in inches

The model is then used to predict the Xenon reactivity transient caused by a change in power level. A worst case approximation is made by assuming that the I^{135} population is constant. This gives the new equilibrium Xenon

$$X = \frac{b_{11} I_0}{b_{10} + b_9 P_R} \quad (4.2-11)$$

The maximum extent of the reactivity transient due to the Xenon is thus

$$\gamma_x = -b_8(X-X_0) = \frac{b_8 b_{11} I_0}{b_{10} + b_9 P_R} + b_8 X_0 \quad (4.2-12)$$

The available control reactivity must be capable of countering this reactivity to ensure that the plant will remain under control throughout the Xenon transient. Another way of looking at this is to say that the reactor power P_R should be constrained so that the Xenon transient effect in the future will not exceed the available control reactivity. This constraint varies as the concentrations of Xe^{135} , I^{135} and the available control reactivity change.

The constraint is found by solving equation (4.2-12) for the limit, with $-\gamma_x$ set to the total available control reactivity. The high limit is

$$P_{R_2} < \frac{b_8 b_{11} I_0}{b_9 b_8 X_0 - b_3 b_8 \Delta R_2} - \frac{b_{10}}{b_9} \quad (4.2-13)$$

If ΔR_2 is sufficiently large, there is no constraint on P_R . The low limit is

$$P_{R_1} > \frac{b_8 b_{11} I_0}{b_9 b_8 X_0 + b_3 b_9 \Delta R_1} - \frac{b_{10}}{b_9} \quad (4.2-14)$$

Reactor power decreases are the more severely limiting case since very large rod withdrawal capability ΔR_1 is needed, as shown in equation (4.2-14), to counter the Xenon transient to reduce P_R to a small fraction of its high power equilibrium without the Xenon causing reactor shutdown.

At this point low and high power constraints on reactor power P_{R_1} and P_{R_2} have been derived. These constraints represent the values that the reactor power must be kept within in order to be sure that the Xenon transient effect will not exceed the total available rod capability. The values for the constraints depend on the current estimated states of the X^{135} and I^{135} concentrations, as well as on the current rod capability.

The Xenon transient causes an additional difficulty in addition to the maximum reactivity transient. The rate of change of reactivity due to Xenon must be countered by the control rods continuously in order to maintain the desired reactor power. Thus the rate at which the control reactivity can be changed is as important as the total available control reactivity. Consideration of the model developed in Section 3.2 shows that the maximum rate of reactivity change due to Xenon, for a step change in reactor power starting from a high power is theoretically

$$\frac{d\gamma_x}{dt} = -b_8 \frac{dX}{dt} = -b_8 [b_{11} I - b_{10} X - b_9 P_R X] \quad (4.2-15)$$

The rod reactivity rate must be fast enough to counter this transient. This gives a constraint on allowed reactor power change in order to not cause a Xenon transient to exceed the rate of rod reactivity capability $b_3 M_1$. The high power constraint is

$$P_{R_2}' < \frac{b_3 M_1 + b_8 b_{11} I_o + b_8 b_{10} X_o}{b_8 b_9 X_o} \quad (4.2-16)$$

and the low power constraint is

$$P_{R_1}' > \frac{-b_3 M_1 + b_8 b_{11} I_o + b_8 b_{10} X_o}{b_8 b_9 X_o} \quad (4.2-17)$$

These constraints are significant, if ever, only at high Xenon concentrations. The constraint is avoidable by designing the reactor for fast rod speed capability M_1 .

The Xenon effects, in summary, give rise to reactivity transients which must be handled by the available control reactivity. Thus a constraint on the allowed reactor power is established to ensure that the Xenon transient does not exceed the control capabilities. Equations (4.2-13) and (4.2-14) give the reactor power constraint considering the total available rod motion. Equations (4.2-16) and (4.2-17) give the constraint in terms of the rate at which rods can be moved. The most restrictive of these constraints must be chosen. It is important to note that the values of the constraints depend on the Xe^{135} and I^{135} concentrations. Values for these unmeasured concentrations can be provided by the on-line state estimation.

4.3 Control which Balances Reactor and Turbine Power

The solution developed in this study provides a rapid load change for the deterministic model, subject to constraints on the inputs and on the states. The theory of optimal control provides some necessary conditions for the optimal control solution for problems of this type. Referring to the equations of Section 3.2, the system being considered is a sixth

order nonlinear one with input and state constraints. The general form for the necessary conditions for the solution of such problems can be found in Denham [20]. The solution with the aid of the general necessary conditions is a trial and error procedure. The general necessary conditions do not provide a solution, but only some conditions which the solution must satisfy. Some techniques have been used ([7], [9]) to find solutions which satisfy the necessary conditions by trial and error, with the deviation of a trial solution from necessary conditions used as a cost function. In these techniques a search is conducted to try to approach a solution which satisfies the necessary conditions. The examples which are known to have been solved by these techniques are much simpler than the problem at hand.

The problem is approached in this study by a much simpler technique, which takes advantage of the particular model structure and the signs of certain parameters. Strictly speaking, the approach used in this study is not a derivation or a proof of minimum time control. However the development is justified on the basis of physical arguments, specific to this problem, and the resultant control is believed to be the minimum time solution.

The load change control developed in this study consists of one or two parts. In the first part the rods are moving at the maximum constrained rate, producing the fastest possible rate of reactor power change. This strategy continues until the reactor power rate of change reaches the power rate constraint. Thereafter, the load change is at the constrained

rate. This second part of the load change does not always occur.

The analysis of the reactor power behavior must consider the dynamic effects of the delayed neutrons and the Xenon. The analysis is simplified by the fact that these effects lead to reinforcing (but delayed) changes in reactor power. An increase in reactor power, due to rod withdrawal or other reactivity insertion, causes delayed neutrons to increase, which gives rise to a further (but delayed) power increase. Similarly, an increase in reactor power burns off more Xenon, producing a positive reactivity effect similar to a rod withdrawal (but delayed). A similar analysis holds for power decreases. Thus in terms of the effects of delayed neutrons and Xenon, the reactor power is increased more rapidly over the near future if it is made as large as possible at the present time, that is, if rods are withdrawn at the maximum rate. Any other strategy produces lower reactor power, not only at the present time, but also at any time in the near future.

A control strategy is now developed for the case where the primary loop average temperature is subject to a zero deviation constraint. That is, the control strategy attempts, by coordinating the reactor and the turbine, to cause no deviation in the primary loop average temperature. The problem is considered in parts. The first sub-problem is the energy transfer and storage represented by the equations:

$$\frac{dT_{AV}}{dt} = b_5(P_R - P_{R_0}) - b_6(P_T - P_{T_0}) \quad (4.3-1)$$

where

$P_R - P_{R_0}$ = change in reactor power

$P_T - P_{T_0}$ = change in turbine power

T_{AV} = primary loop average temperature.

The primary loop average temperature T_{AV} represents stored energy in the plant. It is evident both from the equations and from physical reasoning that turbine power may be changed at a rate corresponding to the rate of change in reactor power without changing the energy in the plant. Any other load change strategy will change the energy in the plant, changing the primary loop average temperature T_{AV} . Thus the control strategy must act to balance turbine power and reactor power if the primary loop average temperature is to be maintained constant.

In the initial part of a load change, the reactor power is changing more slowly than its constraint, and the problem is to control the turbine to match the reactor power. The desired turbine power rate of change, from equation (4.3-1), is

$$\frac{dP_T}{dt} = \frac{b_5}{b_6} \frac{dP_R}{dt} \quad (4.3-2)$$

The model equations of Section 3.2 are used to express this in terms of the states and inputs. The result applies for the case of constant moderator temperature. The desired turbine power rate of change is

$$\frac{dP_T}{dt} = \frac{b_5}{b_6} \left[\frac{b_4 \gamma D + b_3 D \frac{dR}{dt} - b_8 D (b_{11} I - b_{10} X - b_9 P_R X)}{(1-\gamma)^2 + b_1 D} \right] \quad (4.3-3)$$

The reactivity γ and reactor power P_R are functions of the states and inputs, and they are calculated as part of the state estimation. The rod

rate. This second part of the load change does not always occur.

The analysis of the reactor power behavior must consider the dynamic effects of the delayed neutrons and the Xenon. The analysis is simplified by the fact that these effects lead to reinforcing (but delayed) changes in reactor power. An increase in reactor power, due to rod withdrawal or other reactivity insertion, causes delayed neutrons to increase, which gives rise to a further (but delayed) power increase. Similarly, an increase in reactor power burns off more Xenon, producing a positive reactivity effect similar to a rod withdrawal (but delayed). A similar analysis holds for power decreases. Thus in terms of the effects of delayed neutrons and Xenon, the reactor power is increased more rapidly over the near future if it is made as large as possible at the present time, that is, if rods are withdrawn at the maximum rate. Any other strategy produces lower reactor power, not only at the present time, but also at any time in the near future.

A control strategy is now developed for the case where the primary loop average temperature is subject to a zero deviation constraint. That is, the control strategy attempts, by coordinating the reactor and the turbine, to cause no deviation in the primary loop average temperature. The problem is considered in parts. The first sub-problem is the energy transfer and storage represented by the equations:

$$\frac{dT_{AV}}{dt} = b_5(P_R - P_{R_0}) - b_6(P_T - P_{T_0}) \quad (4.3-1)$$

where

$P_R - P_{R_0}$ = change in reactor power

$P_T - P_{T_0}$ = change in turbine power

T_{AV} = primary loop average temperature.

The primary loop average temperature T_{AV} represents stored energy in the plant. It is evident both from the equations and from physical reasoning that turbine power may be changed at a rate corresponding to the rate of change in reactor power without changing the energy in the plant. Any other load change strategy will change the energy in the plant, changing the primary loop average temperature T_{AV} . Thus the control strategy must act to balance turbine power and reactor power if the primary loop average temperature is to be maintained constant.

In the initial part of a load change, the reactor power is changing more slowly than its constraint, and the problem is to control the turbine to match the reactor power. The desired turbine power rate of change, from equation (4.3-1), is

$$\frac{dP_T}{dt} = \frac{b_5}{b_6} \frac{dP_R}{dt} \quad (4.3-2)$$

The model equations of Section 3.2 are used to express this in terms of the states and inputs. The result applies for the case of constant moderator temperature. The desired turbine power rate of change is

$$\frac{dP_T}{dt} = \frac{b_5}{b_6} \left[\frac{b_4 \gamma D + b_3 D \frac{dR}{dt} - b_8 D (b_{11} I - b_{10} X - b_9 P_R X)}{(1-\gamma)^2 + b_1 D} \right] \quad (4.3-3)$$

The reactivity γ and reactor power P_R are functions of the states and inputs, and they are calculated as part of the state estimation. The rod

rate $\frac{dR}{dt}$ is at its maximum $\pm M_1$ during this part of the load change, where the reactor power is changing more slowly than the power rate constraint. This phase does not last long in the case of a reactor at high power equilibrium with a large concentration of Xe^{135} ; however, this phase is dominant throughout a load change in the case of startup, when Xenon effects are nil.

It is possible for the reactor power rate of change to reach the power rate constraint. In this case the control strategy is to change the reactor power and turbine power according to the maximum constrained rate. This requires a reactor power rate of change.

$$\frac{dP_R}{dt} = \frac{b_6}{b_5} \frac{dP_T}{dt} \quad (4.3-4)$$

The rate of rod movement necessary to make the reactor power obey this equation is found using the model equations of Section 3.2

$$\frac{dR}{dt} = \frac{1}{b_3 D} \left[\frac{b_6}{b_5} ((1-\gamma)^2 + b_1 D) \frac{dP_T}{dt} - b_4 \gamma D + b_8 D (b_{11} I - b_{10} X - b_9 P_R X) \right] \quad (4.3-5)$$

The turbine power rate of change $\frac{dP_T}{dt}$ is at the maximum constrained rate $\pm M_2$ during this phase of the control. The above expression for the rate of rod movement is given in terms of quantities which are calculated by the on-line state estimator.

Small model errors may cause a mismatch in turbine and reactor power, which would cause the primary loop average temperature deviation to drift away from zero. An additional control is proposed, so that the non-limiting

control, either rods or turbine power, is modified to correct for such deviations. The proposed implementation is

$$\Delta\left(\frac{dR}{dt}\right) = -K_1 \Delta T_{AV} \quad (4.3-6)$$

or

$$\Delta\left(-\frac{dP_T}{dt}\right) = K_2 \Delta T_{AV} \quad (4.3-7)$$

where K_i may have different values, depending on which control is non-limiting. This control prevents the average temperature T_{AV} from drifting due to small model errors and small reactor and turbine power mismatch. The gains K_i were found by on-line experimentation in this study.

To summarize the results, a rapid load change control for the case of zero primary loop average temperature deviation requires that turbine power and reactor power rates of change be balanced. Of these two, one rate of change will limit the load change rate, while the other is used to maintain the power balance. The calculation of the correct inputs, or the coordination, requires a model. The crude plant model developed in Section 3.2 is used for this purpose. The proposed implementation uses state estimates to determine the control. This becomes a feedback or closed loop control under this proposed implementation. This was the way the demonstration was handled also.

4.4 Control for Rapid Load Changes

In the previous section a control strategy was derived which maintains a balance between the turbine power and the reactor power throughout the

load change. The more general case is now considered, where the deviation in primary loop average temperature T_{AV} has a non-zero constraint. The negative moderator temperature coefficient, which is the usual situation, gives an increase in reactivity for a decrease in temperature. Thus a mismatch in reactor and turbine power, causing the temperature to drop for load increases or to rise for load decreases, allows an even faster load change. An example of the change in reactor power due to allowing a constrained deviation in primary loop temperature is shown in Figure 4.4-1 for the case of a load increase.

Assuming that the faster load change strategy is desired, the control is modified during the time that the primary loop average temperature is being driven toward its constraint. There are two cases to consider:

Case 1: The reactor power rate of change remains less than the power rate constraint. In this case the control law is to move rods at maximum rate and to change turbine power at maximum rate up to a switch time. The turbine power rate is then set at its minimum (zero in this study) until the reactor power matches turbine power. If the switch time is chosen correctly, this will occur with primary loop average temperature at its constraint. The control thereafter is the same as in the zero average temperature deviation case, and the primary loop average temperature will theoretically stay on its constraint. The switch time is calculated by fast time simulation in this study. An equivalent switch boundary, equal to the primary loop average temperature at the theoretical switch time, is used for the actual control.

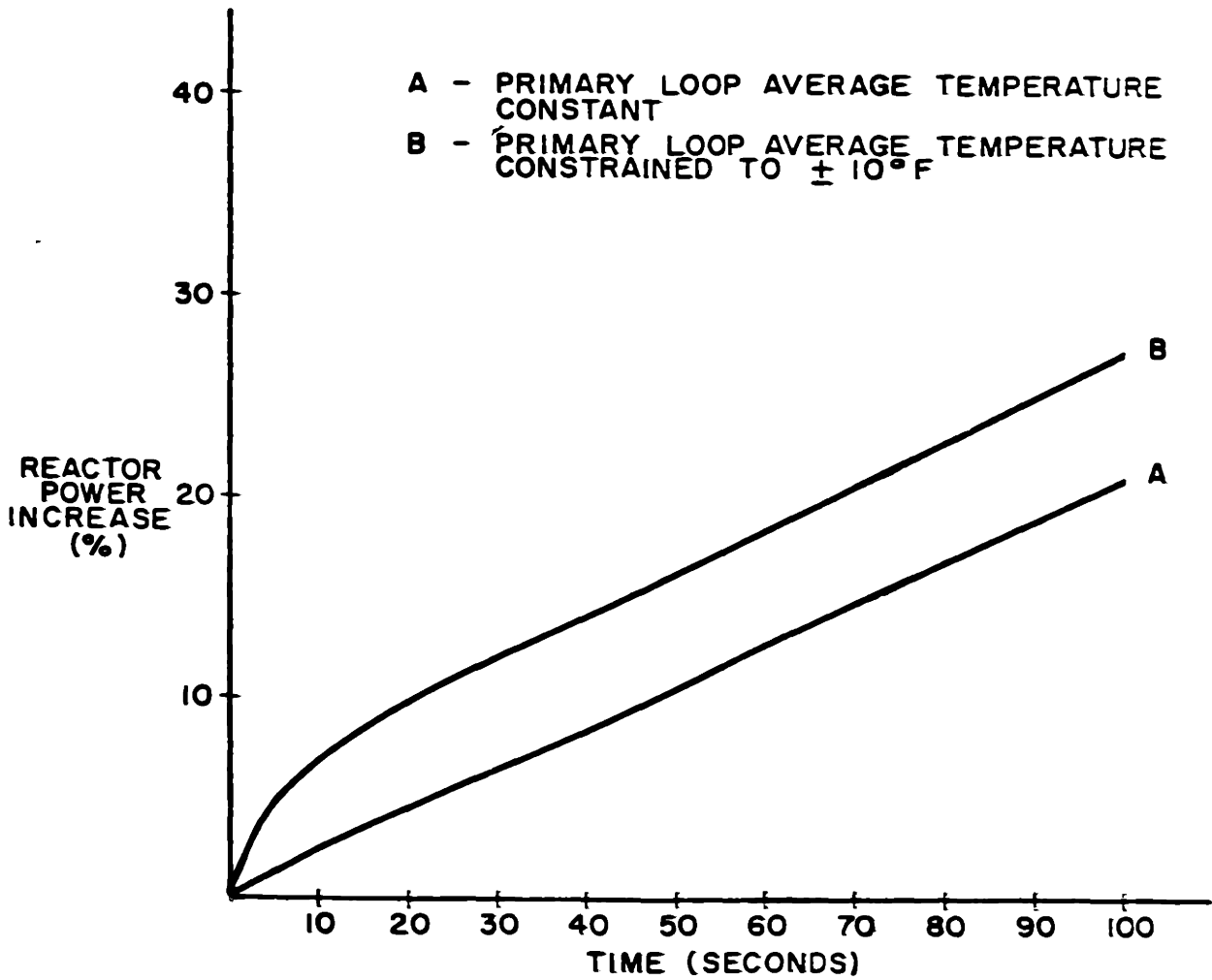


FIGURE 4.4-1 Optimal Reactor Power Trajectories for Different Primary Loop Average Temperature Constraints

Case 2: When attempting the above strategy, the reactor power rate of change matches the power rate constraint before the primary loop average temperature reaches its constraint. This means that even when changing turbine power at the maximum constrained rate, the reactor power rate of change matches it before the primary loop average temperature constraint is violated. The control in this case is to simply change turbine power at its constrained rate throughout the load change, and to move the rods at maximum rate until turbine power and reactor power are matched. Thereafter, the rods are the non-limiting control which is used to match reactor power to turbine power. The occurrence of Case 2 is easily detected in the fast time simulation. Case 2 can arise when load changes are made, starting from high power equilibrium with large concentrations of Xe^{135} and I^{135} in the reactor.

A control strategy has been developed here based on the deterministic model given in Section 3.2. The control strategy is modified in Chapter 5 to allow for uncertainty in the model, and to cope with disturbances and measurement noise. The problem of detecting plant variation and adapting the model is also considered in Chapter 5. Thus the control developed at this point, in Chapter 4, is not a complete description of the load change control.

The various parts of the deterministic control strategy are summarized later in Table 4.6-1. The logic structure used in the implementation is shown in the related Figure 4.6-1.

4.5 Examples of Load Changes

The control strategies developed in Sections 4.3 and 4.4 were tested under a variety of reactor conditions. The load increase problem was considered for two values of moderator temperature coefficient and for high and low Xenon poisoning.

Figure 4.5-1 shows a 40% load change at low Xenon poisoning, as during startup. A moderator temperature coefficient of $-10^{-4} \Delta K/^{\circ}F$ was used. The target surface for primary loop temperature was $-8^{\circ}F$ from equilibrium. Notice that the turbine power or load is initially rising at maximum rate to cause a drop in primary loop temperature. The rods are withdrawn continuously at maximum rate during this load change, as the reactor power is increasing more slowly than the turbine power can be increased. The initial rise in reactor power is due to the reactivity inserted by the lowering of the primary loop temperature. This reactivity insertion is large here due to the large moderator temperature coefficient. When the moderator coefficient is smaller, this initial rise is slight, and the policy of allowing any deviation is hard to justify.

Figure 4.5-2 shows the same load change for the same plant, except the constraint on primary loop water temperature deviation has been reduced to zero deviation. The turbine power or load and the reactor power are in balance throughout the load change. For this example, at low Xenon equilibrium or startup conditions, the control rods are moved at maximum rate throughout the load change. The turbine power rate of increase is controlled, via the load setpoint, to maintain turbine power equal to reactor power.

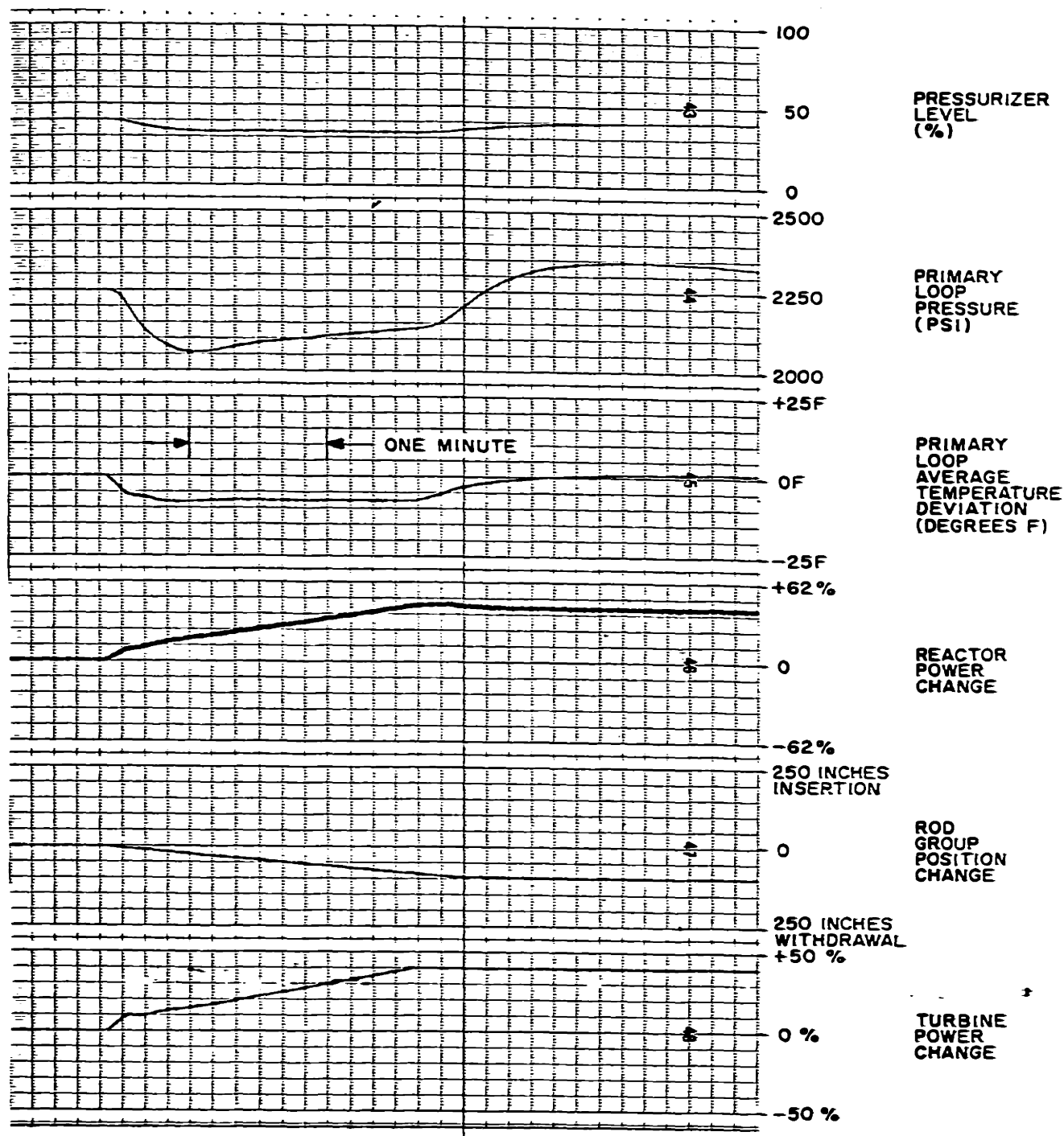


FIGURE 4.5-1 A 40% Load Change Under Computer Control, Constrained Primary Loop Average Temperature Deviation

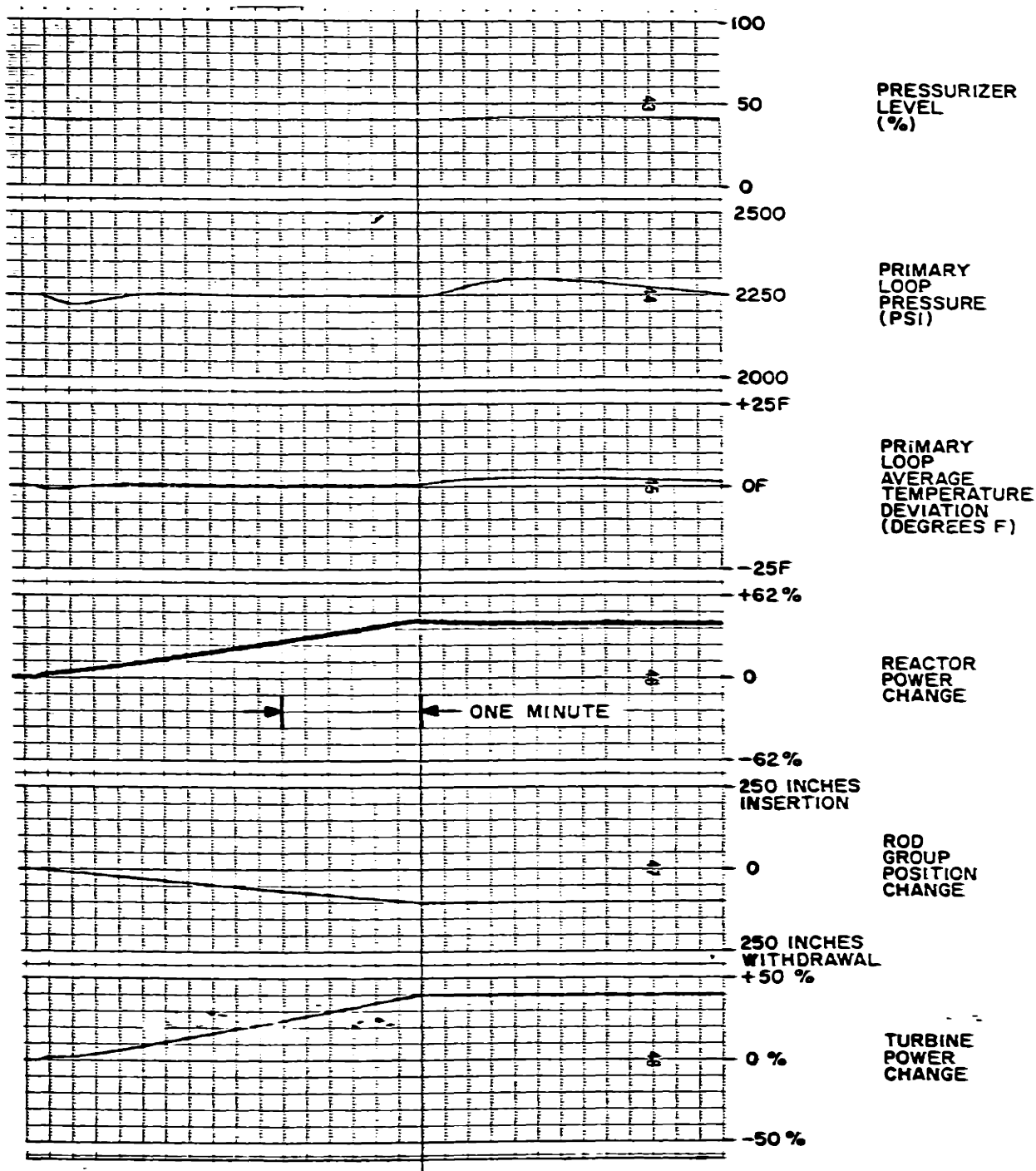


FIGURE 4.5-2 A 40% Load Change Under Computer Control, Zero Desired Primary Loop Average Temperature Deviation

Figure 4.5-3 shows the 40% load change for a plant at high Xenon equilibrium, corresponding to a plant which has been operating at high power for a day or more. Notice in this case that at a point in the load change the reactor power rate of increase matches the turbine power maximum allowed rate of increase, and the control rods become the non-limiting control from this point on.

4.6 Load Following Control

In addition to major load changes, many power plants are used to regulate system frequency by picking up or dropping load as the system frequency varies. Since many plants are presumably in this mode of operation, the load changes involved for a given plant are small. The conventional analog plant control, since it does not adapt to varying plant behavior, may not perform well under all conditions unless it is readjusted.

As part of the load change problem, a model of the plant was developed which can also be used to provide improved regulation between load changes. The theory of optimal control provides some easily implemented results for problems of this type. The basic solution is to separate the problem into two parts. The plant states are estimated to provide values of the states for use by the control. The optimal control is then developed for the model linearized about the current operating point. The optimal controller is designed using the linear system, quadratic cost approach [6], [42]. The entire procedure, including stochastic model parameter identification, Kalman filter state estimator

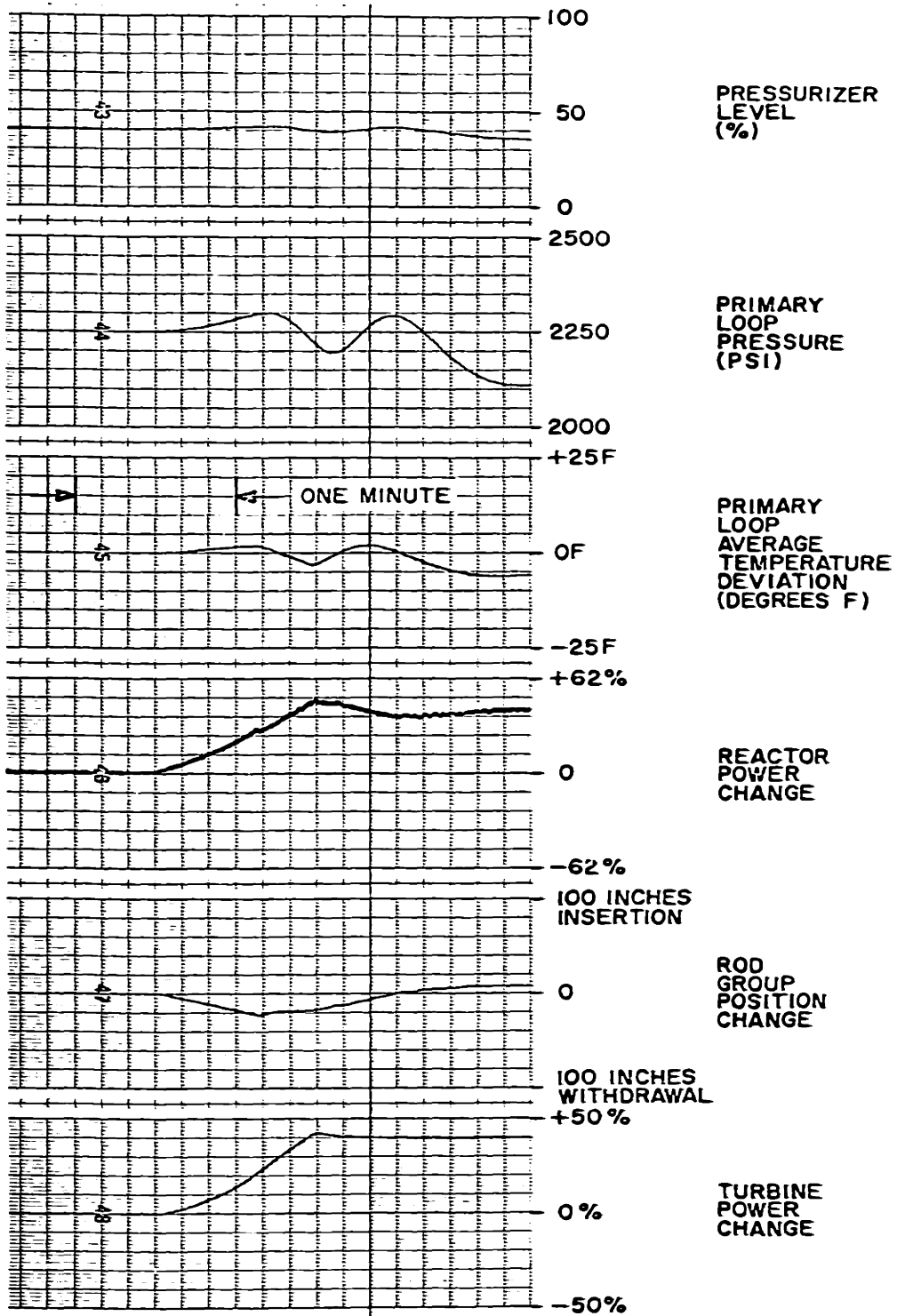


FIGURE 4.5-3 A 40% Load Change Under Computer Control, Large Xenon Effect Conditions

design, and the optimal controller design can be automatically carried out by the computer, and the programs for this were developed as part of this study.

The linear system, quadratic cost control is now considered. The linear system about the operating point is described by the equations

$$\underline{x}_{K+1} = A \underline{x}_K + B \underline{u}_K \quad (4.6-1)$$

$$\underline{y}_K = C \underline{x}_K \quad (4.6-2)$$

where

\underline{x}_K is a K_1 dimensional vector of states

\underline{y}_K is a K_2 dimensional vector of measurements

\underline{u}_K is a K_3 dimensional vector of inputs

A, B, C are constant matrices

The cost function is

$$J = \sum_{K=0}^{N-1} \frac{1}{2} (\underline{y}'_{K+1} Q \underline{y}_{K+1}) + \frac{1}{2} (\underline{u}'_K R \underline{u}_K) \quad (4.6-3)$$

The general solution, as developed by Lee [42], is determined by the equations

$$P_0 = C' Q C \quad (4.6-4)$$

$$M_K = P_{K-1} - P_{K-1} B (B' P_{K-1} B + R)^{-1} B' P_{K-1} \quad (4.6-5)$$

$$P_K = A' M_K A + C' Q C \quad (4.6-6)$$

$$\underline{u}_K = -K_K \underline{x}_K \quad (4.6-7)$$

is the optimal solution with

$$K_{N-K} = [B' P_{K-1} B + R]^{-1} B' P_{K-1} A \quad (4.6-8)$$

Fortunately, the solution is asymptotic for large N under general conditions, so that the equations can be solved recursively until P_K is stationary to within some criteria, and then a single gain matrix K can be calculated. The solution to be implemented, then, is

$$\underline{u}_K = -K \underline{x}_K \quad (4.6-9)$$

For the load following problem, the inputs are the rod rate and the plant load setpoint. The load following demand signal is assumed to be slowly varying with respect to the plant control time constants, so that the problem is to correct small errors in turbine power. Thus if L_D is demand load, then $(P_T - L_D)$ represents a deviation in plant load to be corrected by the load following control. The primary loop average temperature T_{AV} may also experience some deviation to be corrected, as will the reactor power P_R . The problem thus coincides with the previous formulation, with

$$\underline{y} = \begin{bmatrix} P_R \\ T_{AV} \\ P_T \end{bmatrix} \quad (4.6-10)$$

as the measurement vector, where

P_R is reactor power

T_{AV} is primary loop average temperature

P_T is turbine power

and with

$$\underline{u} = \begin{bmatrix} \frac{dR}{dt} \\ u_2 \end{bmatrix} \quad (4.6-11)$$

where

$\frac{dR}{dt}$ is rate of control rod motion

u_2 is setpoint of turbine power control

The control of the plant about a given operating point has been derived in this section. The control makes use of the stochastic model of the plant and the Kalman filter, both of which were developed for the load change problem. Thus normal load following control is a simple and logical extension of the control scheme. The overall control logic is shown in Figure 4.6-1. The different control modes are defined in Table 4.6-1. This control logic provides computer control of the turbine and reactor for the full range of normal conditions.

TABLE 4.6-1
Control Strategy Summary

<u>Mode*</u>	<u>Rod Control</u>	<u>Turbine Power</u>	<u>Primary Temp</u>
1	Maximum rate: withdraw for load increase insert for load decrease	Maximum rate in direction of load change	Moves toward its intended constraint
2	Same as 1 Maximum rate	Zero rate	Rate of change slows as reactor power approaches turbine power
3	Same as 1 Maximum rate	Manipulated to make turbine power balance reactor power	Deviations are used to modify the turbine control
4	Manipulated to make reactor power balance turbine power	Maximum rate in direction of load change	Deviations are used to modify the rod control
5	Multivariable control manipulates rods and turbine power to provide load following for small deviations.		

*The modes may not all occur during a load change. Refer to Figure 4.6-1 for the sequence and conditions under which specific modes occur.

CHAPTER 5

CONTROL IN THE PRESENCE OF VARIATION AND UNCERTAINTY

5.1 Introduction to the Problem

There are a number of sources of variation and uncertainty in the plant. Some of the variations have been considered in previous chapters. The effects of variations in initial state and in available rod reactivity are considered in Chapter 4 as part of the deterministic control problem. In addition to these variations, the plant also appears subject to slow behavior changes and to fast variations due to random disturbances and to model error. These slow and fast variations are considered in this chapter. The slow variations are handled by adaptation, and the fast variations are handled by considering them to be stochastic or uncertain processes.

The unmodeled plant variations, due to slow physical changes, or to nonlinear effects, are handled by adapting the model parameters. There are two methods developed for determining when the model no longer adequately describes the plant. One of these methods is a bounds test, which considers whether the plant variables have exceeded certain bounds which are precalculated based on the stochastic model. The other method is a hypothesis test, which uses a test statistic to determine if the plant behavior is no longer consistent with the stochastic model. Whenever the model no longer represents the plant, the load change can be aborted, and the model parameters are then adapted.

Another method is used to handle the fast variations due to disturbance and measurement noise. The problem here is to control the plant in spite of these inevitable noise effects. From a practical point of view, it is not important whether the noise makes the load change slightly slower or faster, but it is important if the noise makes the plant violate the allowed plant constraints during the load change. Thus the method used to cope with the noise is to adjust the state constraints - make them more conservative - by an amount determined by the stochastic model. The amount of the adjustment is such that the predicted value of a state under the proposed control lies within the constraint with greater than 99.8% probability.

In addition to the adjustment of the constraints, the stochastic model is used to predict performance bands within which the measurements of plant performance are expected to lie. These predicted measurement bands are based on the disturbance noise and the measurement noise, as well as the deterministic model. They represent high and low limits within which the measurements at any time are expected to lie, with about 99.7% probability. These bands are used for two purposes. They are displayed prior to and during the load change, with realized plant measurements superposed, to give the plant operator a reassurance or a warning. The bands and the realized measurements are also automatically monitored, to give the control computer a reassurance or a warning. In the event of violation of the bands, either the computer or the operator can terminate the load change.

In summary, methods are developed which allow the control of the plant in spite of slow or fast variations in the plant. The slow variations are

detected, and the model parameters are adapted based on current plant performance. The fast variations are accepted as inevitable and they are considered in adjusting the state constraints within which the plant should remain. The fast variations are also considered in defining performance bands for monitoring purposes. These techniques allow the control to operate in the presence of variation and uncertainty.

5.2 Behavior of the Stochastic Model

For a given load change, the deterministic model and the deterministic control can be used to predict the expected behavior of the plant. However, the plant is subject to disturbance noise and measurement noise, so its behavior will not match the deterministic predictions. For this reason a stochastic model, derived in Chapter 3, is used to represent the plant more realistically.

The predictions of the stochastic model include not only the mean or expected value of the variables, but also the covariance matrix for these variables. A prediction thus consists not of a single value for a single variable, but rather a prediction of a distribution for the variable. The mean and the covariance are used to characterize the probability distribution.

The stochastic model in Chapter 3 was derived by assuming that the deviations caused by disturbance noise and measurement noise are small enough so that it is reasonable to consider the model linearized about the expected state. If the resultant linear time varying model is accepted as accurate, then the probability distributions for the random vectors at

any time remain Gaussian, and these probability distributions are completely specified by the means and covariances. This is useful because the means and covariances are easily computed, while Gaussian distributions are easily interpreted.

Aside from the fact that the chosen stochastic structure is easy to work with, there is another justification for its use. The stochastic model is judged by a hypothesis test to determine if it is statistically consistent with the process data. The hypothesis test is used following identification of the parameters of the stochastic model as described in Chapter 3. Thus the assumptions on the noise structure which were originally imposed are justified on the basis of statistical tests.

The use of the stochastic model for predicting plant behavior will now be discussed. The first step in calculating the predictions is to determine the nominal deterministic trajectory. This is the state trajectory which results from integrating the nonlinear differential equations of the deterministic model, given in Section 3.2. The inputs to the model are determined from the deterministic control, as described in Chapter 4. The nominal state trajectory which results is taken as the mean or expected state trajectory. This assumption is equivalent to assuming that using a stochastic model linearized about the trajectory, rather than a nonlinear stochastic model, gives small errors.

The covariance matrix for the states is derived by considering the behavior of small deviations from the nominal trajectory. The deviations are propagated by the linear time varying model derived by linearizing about the nominal trajectory. The model, as derived in Chapter 3, is

$$\tilde{\underline{x}}_{K+1} = A_K \tilde{\underline{x}}_K + G \underline{v}_K \quad (5.2-1)$$

where A_K is the transition matrix for the state deviations for time K to time $K+1$, $\tilde{\underline{x}}_K$ or $(\underline{x}_K - \underline{x}_K^*)$ is a deviation from the nominal trajectory \underline{x}_K^* , \underline{v}_K is a zero mean, white Gaussian noise process with covariance I , and G is a matrix with parameters identified by the maximum likelihood technique.

The covariance of state deviations can easily be determined. The deviations $\tilde{\underline{x}}_K$ are a zero mean random process, since \underline{v}_K and $\tilde{\underline{x}}_0$ are zero mean and uncorrelated. The covariance is thus propagated by

$$\Gamma_{K+1} = A_K \Gamma_K A_K' + GG' \quad (5.2-2)$$

where

$$\Gamma_k = \mathcal{E} [\tilde{\underline{x}}_k \tilde{\underline{x}}_k'] \quad (5.2-3)$$

The initial condition for the above equation is the covariance matrix Γ_0 , the covariance of the state at the time the prediction calculation is made. This covariance matrix is calculated as part of the on-line state estimator. This state estimator, a Kalman filter, is keeping current values for the expected values and covariances of the states. The behavior of the covariance under prediction conditions is then found by running equation (5.2-2) forward to give the predicted covariance of the states at a future time.

The deviation of the state from the nominal trajectory, described by $\tilde{\underline{x}}_K$, has a Gaussian probability distribution under the assumptions which have been made. The probability density function is

$$p(\underline{x}_K) = [(2\pi)^{K_1} |\det \Gamma_K|]^{-1/2} \exp\{-\frac{1}{2} \underline{\tilde{x}}_K' \Gamma_K^{-1} \underline{\tilde{x}}_K\} \quad (5.2-4)$$

The geometry of the distribution can be understood by noting that the contours of constant probability density are ellipsoids given by

$$\underline{\tilde{x}}_K' \Gamma_K^{-1} \underline{\tilde{x}}_K = E \quad (5.2-5)$$

The probability that the state lies within certain ellipsoids can be calculated by noting that E is Chi-squared with K_1 degrees of freedom, where K_1 is the dimension of $\underline{\tilde{x}}_K$. Table 3.6-1 shows the probability distribution for E for some values of K_1 . More detailed data can be readily obtained from established tables of Chi-squared distributions [28].

As an example of the behavior of the state covariance and its interpretation, Figure 5.2-1 shows an ellipse of probability .995 or 99.5% for a two state vector. This is based on the covariance Γ_0 taken from a Kalman filter operating on an actual data record from the simulated plant. The origin of the ellipse is the zero deviation case or the nominal state. The stochastic model estimates that the actual state lies somewhere in the ellipse with probability .995, and it lies outside the ellipse with probability .005. In the general case, ellipsoids of any specified probability can be found by solving equation (5.2-5) for the ellipsoid.

To summarize the behavior of the stochastic model, it is possible to predict not only the nominal state, but also to predict the covariances of deviations about the nominal state. These covariances, together with the Gaussian assumption, determine the probability distributions for the state estimates. Since the probability distributions are known, the

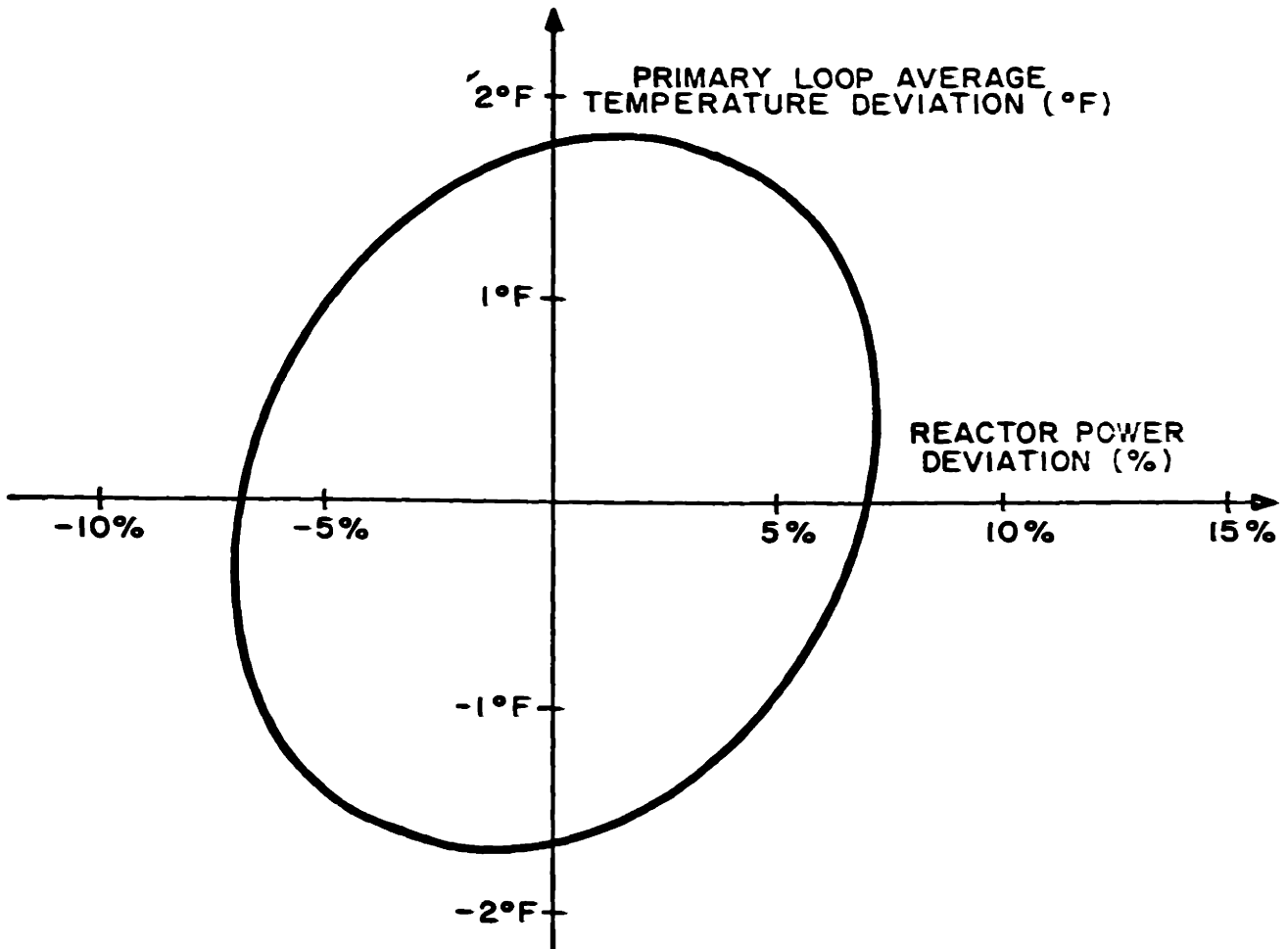


FIGURE 5.2-1 An Interpretation of State Covariance

probability of the predicted state lying within certain bounds can be determined. Thus the stochastic model can be used to give a well-defined interpretation of the amount of uncertainty in the process.

5.3 Modification of the Constraints

The control developed in Chapter 4 takes the plant through a minimum time load change - subject to specified and calculated state constraints. The deterministic model is used for the control calculations, and the nominal trajectory lies within the constraints. However, if the stochastic model is considered, there is a high probability that the constraints will be violated. Thus it is desirable to modify the control so that the stochastic model predictions indicate a low probability of violating the constraints. This is easily accomplished by adjusting the constraints to more restrictive values, and then calculating the deterministic control of the load change based on these adjusted constraints. For this new nominal trajectory the stochastic model predicts a low probability of violating the original constraints. Thus the overall control takes account of the uncertainty, as defined by the stochastic model, by adjusting the state constraints.

The amount by which the constraints are adjusted is now considered. In Section 5.2 an equation was developed for propagating the predicted state covariance matrix Γ_K . The variance of any particular component of the state can be determined from Γ_K . The corresponding diagonal element of Γ_K is the variance of the marginal distribution (see Papoulis [49]).

thus the covariance matrix Γ_K contains the information needed to determine the marginal distribution of a particular state variable.

The primary loop average temperature T_{AV} is the variable considered here, since it provides the limiting constraint on the states during the load change. The marginal distribution of this variable, from the state covariance matrix, is

$$\text{var}(T_{AV})_K = [\Gamma_{22}]_K \quad (5.3-1)$$

that is, the second diagonal element of Γ_K . This marginal distribution of T_{AV} is considered in defining the amount of the adjustment for the constraint. The three standard deviation bounds are used.

$$3\sigma = 3 \sqrt{\text{var}(T_{AV})_K} \quad (5.3-2)$$

The probability is 99.7 percent that T_{AV} will lie within these bounds around the nominal predicted value at time K as determined by prediction calculations before the start of the load change.

The state constraint for the primary loop average temperature is made more conservative by the amount of the three standard deviation bound. Figure (5.3-1) shows this adjustment. The adjusted constraint is then used for the actual control. The new nominal predicted trajectory misses the adjusted constraint by the amount 3σ . The stochastic deviations about this trajectory have a high probability, more than 99.8 percent, of missing the actual constraints at any time K. This is true because the entire 3σ band lies inside the actual constraint and the deviations outside the 3σ bands on one side also lie within the actual

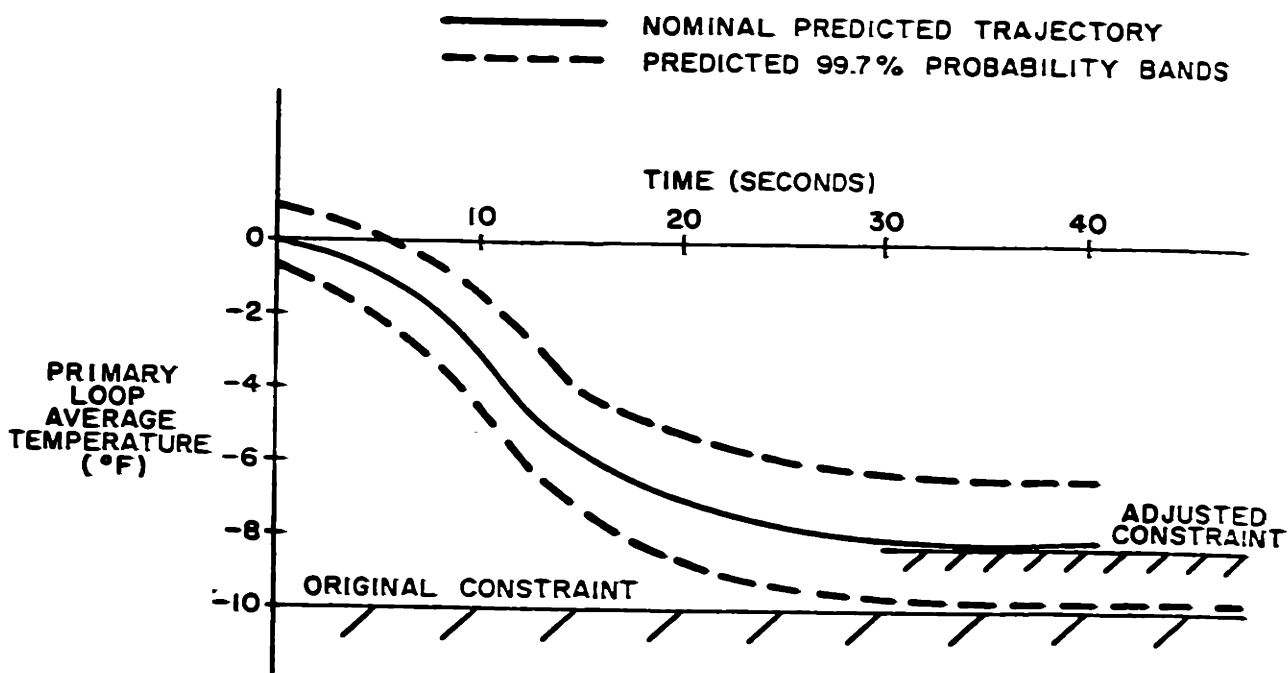


FIGURE 5.3-1 Adjustment of the Constraints

constraint. Thus the control scheme copes with uncertainty by adjusting the constraints which are used in the control calculations.

5.4 Prediction of Measurement Bands

The control developed in this study is capable of large fast load changes. Such a control can only be implemented if there are means to quickly detect abnormal or unexpected performance. One of the ways this is accomplished is to predict measurement bands based on the stochastic model which give a band within which the measurements from the plant should lie during the load change. The measurements of reactor power and primary loop average temperature are considered. The measurement bands are used for monitoring purposes by the computer. The bands are also displayed along with realized plant measurements, to provide for visual monitoring by the plant operator.

The calculation of the measurement bands is now considered. The bands describe deviations from the expected or nominal measurements. These measurement deviations are commonly called residuals. The residuals are related to the deviations of the state from the nominal and also to the measurement noise. The residuals are determined from the equation

$$\underline{r}_k = C_k \tilde{\underline{x}}_k + \underline{w}_k \quad (5.4-1)$$

where \underline{r}_k is the deviation from the nominal measurements, $\tilde{\underline{x}}_k$ is the deviation of the state from nominal, and where \underline{w}_k is the measurement noise.*

*The stochastic model is discussed more fully in Section 3.3.

The predicted covariance of the residuals is

$$R_K = C_K \Gamma_K C_K' + W \quad (5.4-2)$$

where Γ_K is the covariance matrix for the predicted state at time K, and where W is the covariance matrix of the measurement noise. The prediction of the performance of the measurements at a future time K is specified by the expected value determined by the deterministic prediction and by the covariance matrix R_K .

The predicted measurement bands are determined from the covariance of the residuals. The marginal distributions of the components of the residuals have variances determined by the diagonal elements of R_K . These marginal distributions are used for the prediction bands. The three standard deviation band about the nominal trajectory is used as the measurement band. This band has the following interpretation: a chosen measurement - reactor power for example - at a future time K should lie within the bands with a 99.7% probability.

The calculation procedure for the bands will now be considered in more detail. The calculation of the performance bands involves calculating two nominal trajectories, before and after the adjustment of the constraints. The nonlinear model is linearized about these trajectories, and the linear time varying stochastic model is used to calculate the predicted measurement residual covariances. This entire calculation takes about 20 seconds on an off-line 360-50 computer. The calculations were simplified before putting them on the on-line EAI 640 control computer. The calculation time was reduced to 5 seconds on this computer by taking advantage of the approximately asymptotic behavior of the covariance early in the load

change, as well as by noting the negligible variation between the covariance matrix about the original and the adjusted nominal trajectories. Additional programming efficiencies could reduce this time further. These results show that the display of predicted plant performance prior to the load change is clearly a practical technique.

The predicted measurement bands for a load change are displayed, as shown in Figure 5.4-1. The reactor power and the primary loop average temperature were chosen for this display, however other plant variables could have been chosen. The load change in the example is a 40% increase, with a large moderator temperature feedback effect and a small Xenon effect.

The usefulness of the predicted performance bands is enhanced by the display of the actual realized measurements as well as the predicted bands. This display is shown in shown in Figure 5.4-2. The display gives a reassurance or a warning of plant behavior, as the behavior of the plant is visually compared to the predictions made at the start of the load change.

An experiment was performed to illustrate the use of the measurement bands to visually detect plant variation. For this experiment the computer monitoring of the bounds was suppressed. A variation was made in the simulated plant by decreasing the moderator feedback coefficient by a factor of ten. The digital computer used the stochastic model, based on the former plant behavior, to make the predictions. However, as Figure 5.4-3 shows, the plant measurements differ from the predictions. Thus the variation in the plant can be detected by observing plant measurements and comparing them with predicted measurement bands. The computer does this

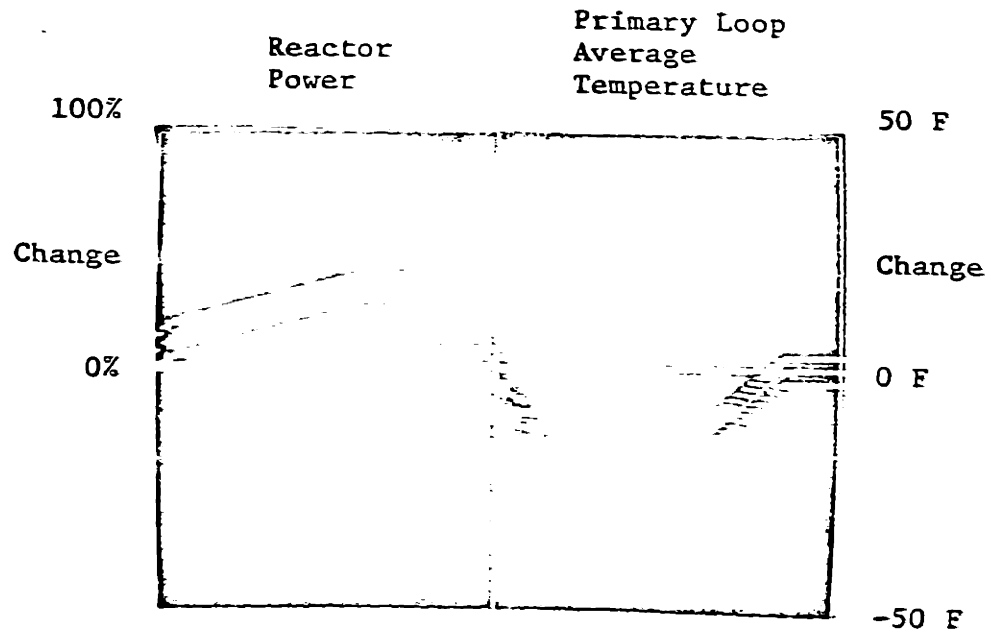


FIGURE 5.4-1 Prediction of Measurement Performance Bands

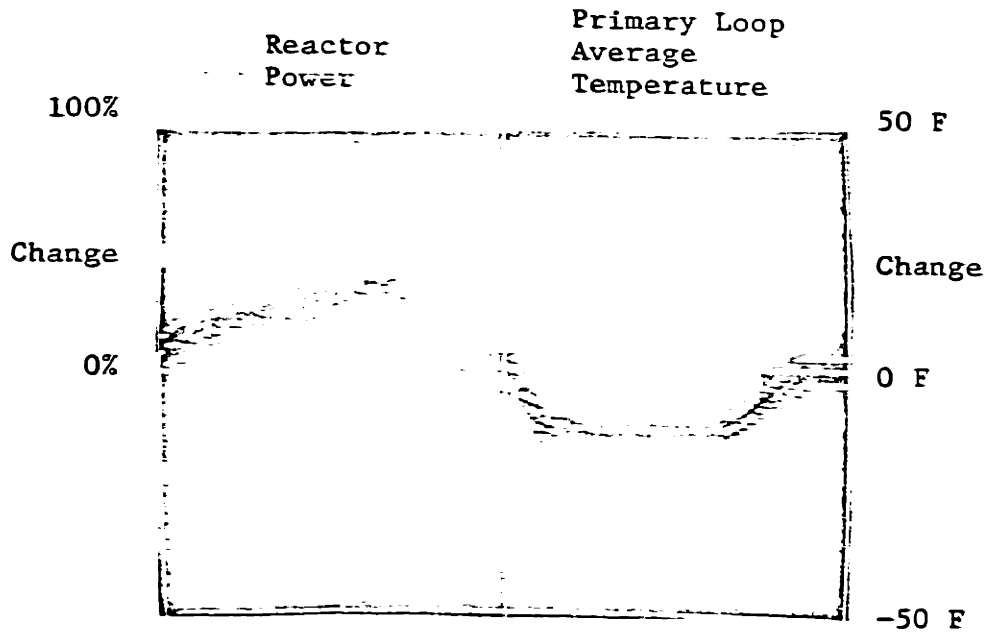


FIGURE 5.4-2 Display of Actual vs. Predicted Measurements During Normal Load Changes

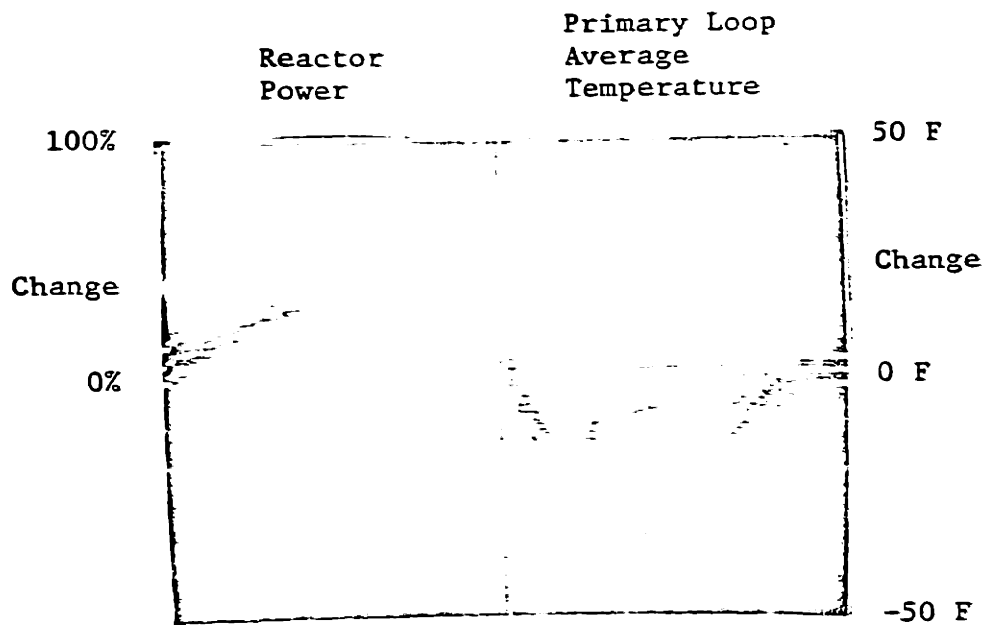


FIGURE 5.4-3 Display of Actual vs. Predicted Measurements Following a Plant Variation

and it also displays the bands and measurements so the operator can also monitor the plant performance.

To sum up, the results presented here demonstrate the value of predicting and displaying bands of normal measurement performance prior to the start of a load change. A demonstration is presented of the superposition of the actual measurements onto the display. The plant operator or a computer can monitor the performance of the plant during the load change by comparing the measurements with the predictions. In the event of abnormal behavior the load change can be aborted. Thus a practical means of detecting and dealing with unexpected performance has been developed.

5.5 On-line Hypothesis Testing

In the previous section a technique was developed which determined if a plant was not performing as expected during a load change. The method was to test whether some plant measurements, reactor power and primary loop average temperature, deviated from the nominal predictions by an amount greater than a calculated measurement band. In this section another technique is developed for the same purpose. This technique, called a hypothesis test, has some advantages over the bounds test.

The hypothesis test operates on all the data taken during the load change to determine whether the plant behavior is consistent with the stochastic model, while the bounds test merely applies a test to data points as they occur. The hypothesis test tends to give an early warning of plant variation or model error well before the bounds tests have been violated.

Thus the hypothesis test is a valuable tool for determining if the plant is or is not performing as expected during the load change.

The hypothesis test is derived in Section 3.6. The basic principles are reviewed here. Under ideal circumstances if the stochastic model actually represents the process, the difference between the plant measurements and the measurement predictions of an on-line Kalman filter should be uncorrelated in time. That is, these differences or residuals satisfy the equations:

$$\mathcal{E} (\underline{r}_K \underline{r}_L^T) = 0, K \neq L \quad (5.5-1)$$

$$\mathcal{E} (\underline{r}_K \underline{r}_K^T) = R_K \quad (5.5-2)$$

If the above equations do not hold, that is, if the residuals are correlated, then the actual process contains dynamic effects which do not occur in the stochastic model. Thus the correlation or lack of correlation in the residuals is used as a test to judge the correctness of the stochastic model.

The hypothesis test statistic was discussed in Section 3.6. This test statistic has a known probability distribution when the stochastic model is correct. In the event of a plant variation, the test statistic becomes large and it lies so far out in the tails of the theoretical distribution that the hypothesis of a correct model must be rejected. The reason that the hypothesis test statistic reacts in this way is that it is very sensitive to correlation in the residuals of the Kalman filter which occur in the event the model does not fit the process.

In the demonstration the hypothesis test is calculated every second

during the load change, starting after the first ten seconds of data. The performance of the hypothesis test statistic for a number of load changes is shown in Figure 5.5-1. This represents the case where the stochastic model is a good representation of plant behavior. The observed values of the hypothesis test statistic, recorded here at the end of the load changes, all lie within the 99.9% portion of the probability distribution. This may appear to be a very lenient limit. However, the performance of the test statistic when the stochastic model does not fit the plant is so dramatic that the limit on normal values can be lenient.

Figure 5.5-2 shows the performance of the hypothesis test following plant variation. These plant variations consist of changing the value of the moderator feedback coefficient by a factor of two in one case (run A) and a factor of five in the other (run B). The hypothesis test statistic values at the end of the load changes are shown. A short model parameter adaptation is performed between each load change. This adaptation, described in Section 5.6, succeeds in producing a model consistent with the plant performance, according to the hypothesis test, after four load changes. The important point in terms of the present discussion is the very large values that the hypothesis test statistic has in the event of plant variation. This abnormal behavior is evident early in the load change by monitoring the current value of the test statistic. The hypothesis test statistic thus gives a clear early warning in the event that the stochastic model does not match the observed plant performance.

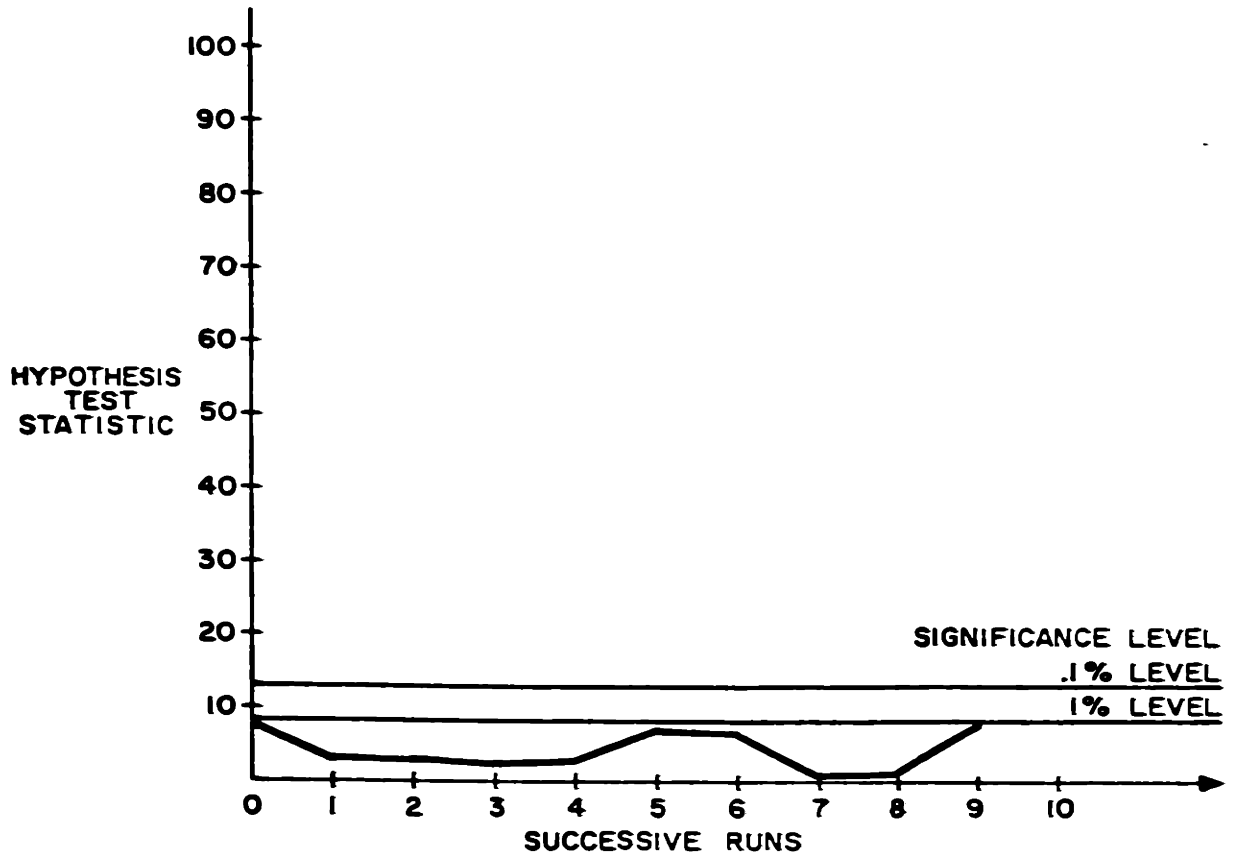


FIGURE 5.5-1 Hypothesis Test Performance Under Normal Conditions

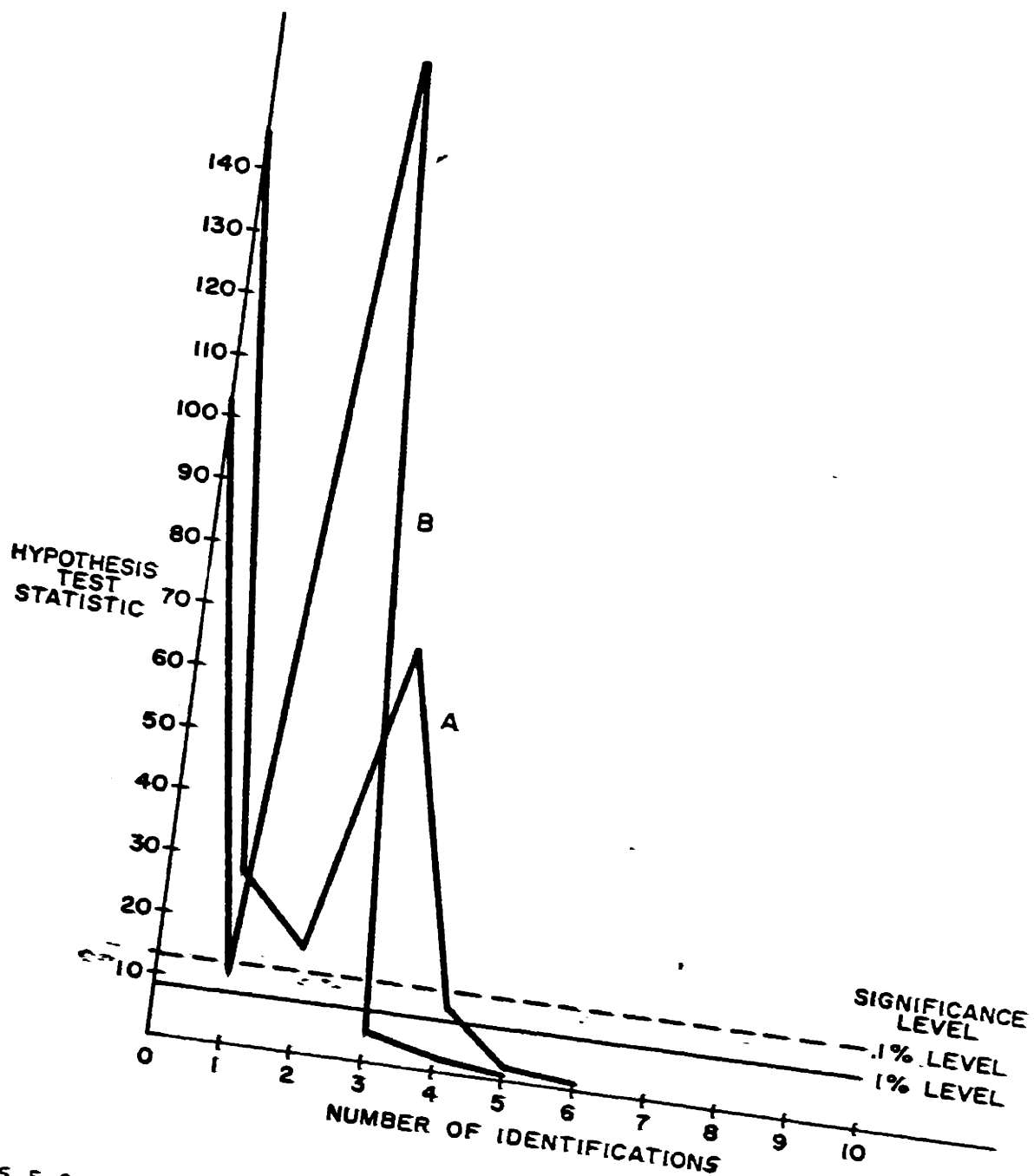


FIGURE 5.5-2 Hypothesis Test Performance Following Plant Variation

5.6 Parameter Adaptation

Two methods have been described which determine whether the stochastic model is consistent with the observed performance of the plant. These methods, a bounds test and a hypothesis test, allow the control computer to terminate the load change in the event that the plant behavior is not consistent with the model. In this event it is desirable to quickly adapt the model parameters, based on the data taken during the abortive load change, and to resume the load change using the updated model.

If there were no rush, the model parameters could be re-identified using the maximum likelihood identification procedures of Chapter 3, which were used for the original model identification. However, this would require on the order of an hour on the relatively slow on-line control computer. In an actual plant it is expected that this would be done, since the unmodeled variations in plant behavior would be slow effects which could be coped with by occasional re-identification of the model.

In the demonstration performed as part of this study, it was assumed that a rapid approximate technique for adapting the parameters was desired, which can be considered as a temporary model fix to expedite the load change. The time required for parameter adaptation was reduced considerably by using a simple technique. The assumption is made that the noise model is still valid and that the variation can be handled by identifying the parameters in the deterministic portion of the model. A least squares technique, described in Section 3.4, was used in the demonstration. This ad-hoc technique was found to produce adapted models

which still satisfy the hypothesis test and which are statistically consistent with the observed plant performance. Thus for the cases tested, for plant parameter changes, the rapid approximate methods can be used to update the model on-line, to produce models which once again are consistent with the plant performance. If the amount of disturbance noise or measurement noise of the actual plant had changed, this method would probably not be adequate, and a re-identification of the noise model parameters would be necessary.

The performance of the rapid approximate parameter adaptation technique is illustrated by Figures 5.5-2 and 5.6-1 which represent the same set of experiments. The hypothesis test statistic, Figure 5.5-2, and the search procedure cost, Figure 5.6-1, both take on large values in the case of model performance which does not match plant performance. The model parameters are updated between successive load changes, using the rapid approximate method, and after four load changes the model is consistent with the plant.

From the preceding discussion it is evident that a good model fit does not occur after a single application of the rapid approximate method, but rather it requires several load changes. However, one fact which is not clear from Figures 5.5-2 and 5.6-1 is that the first adaptation after a single load change produces a significant improvement in the model. This is shown in Figure 5.6-2, which shows the predicted and realized plant performance after a single parameter adaptation. Figure 5.6-2 shows the same load change as Figure 5.4-3, which is for a plant with a moderator temperature coefficient changed by a factor of ten from the value in effect

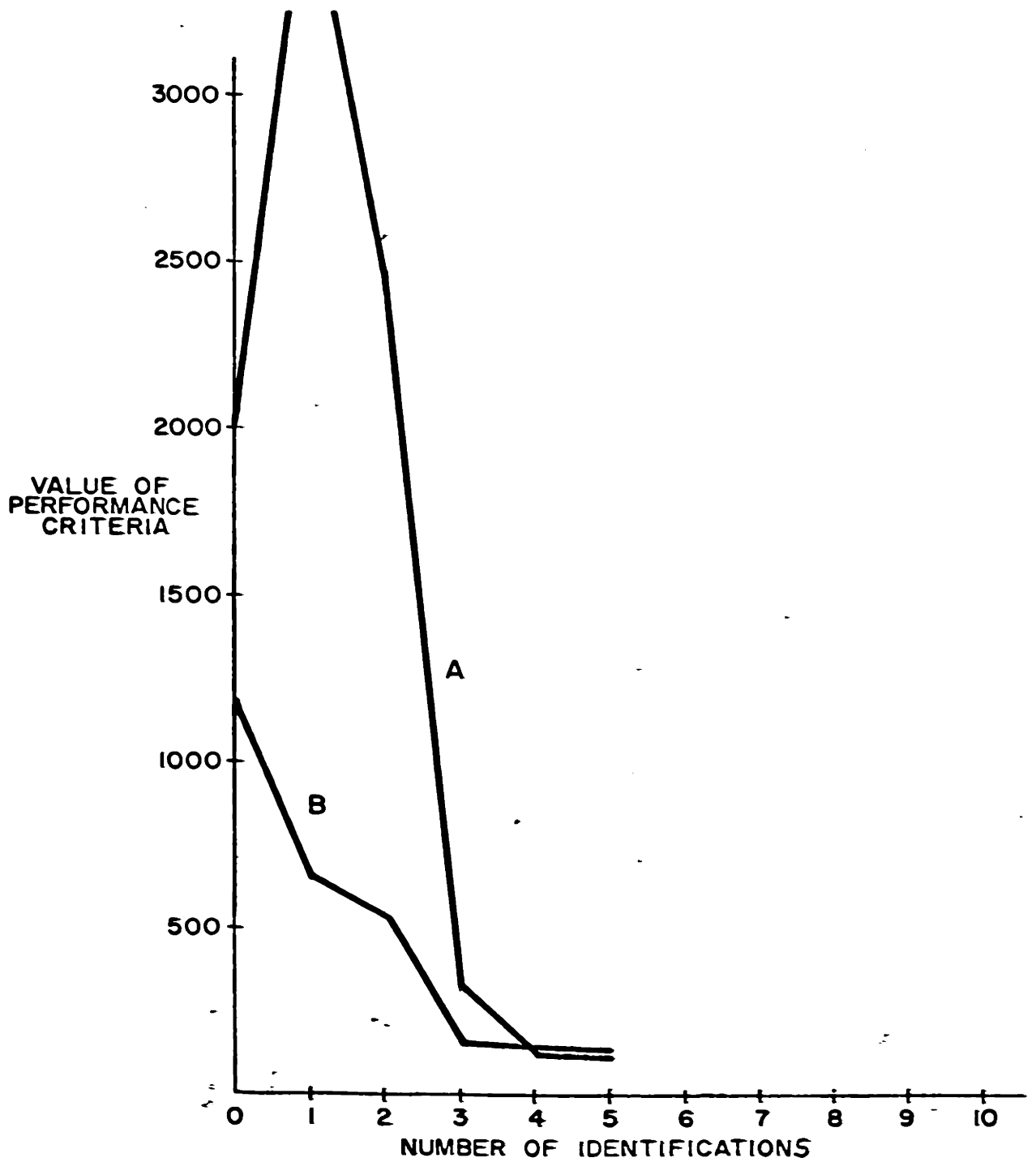


FIGURE 5.6-1 Least Squares Cost Performance Following Plant Variation

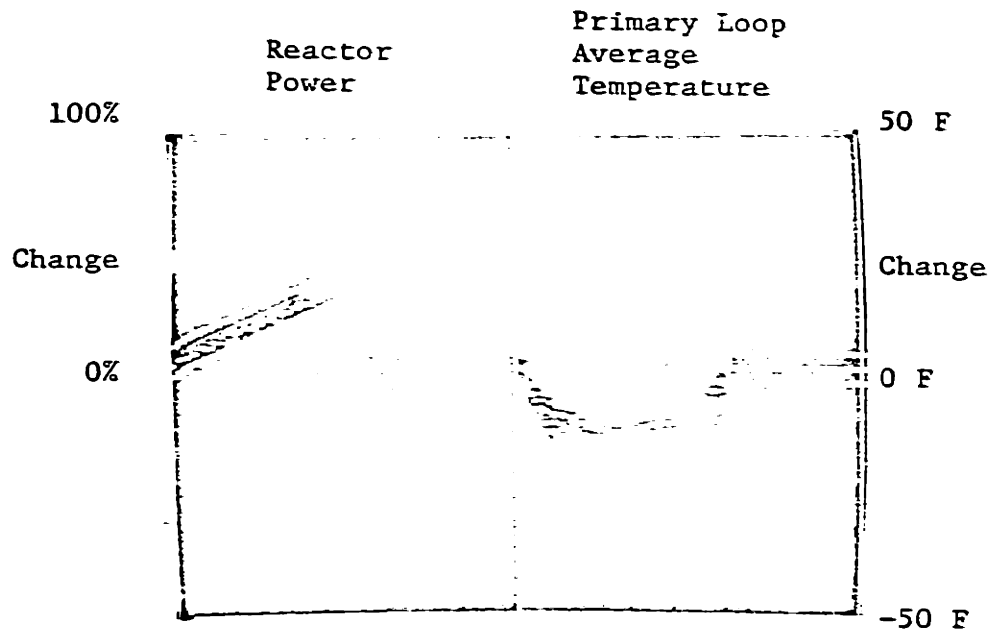


FIGURE 5.6-2 Display of Actual vs. Predicted Measurements Following Plant Variation and Model Adaptation

when the model was identified originally. Figure 5.4-3 shows the predicted and realized performance before any adaptation, and Figure 5.6-2 shows the same after a single application of the rapid-approximate parameter adaptation. This required about five minutes on the on-line control computer, but this could probably be reduced by an order of magnitude by programming efficiencies and by use of a faster computer.

The results of this study show that adaptation of the model to cope with plant variation is practical. The use of rapid and approximate methods to adapt the parameters as a method of quickly updating the model for use in immediate control has been demonstrated. The technique for the update of the model when time is not of the essence should be to re-identify the parameters of the complete stochastic model, as described in Chapter 3. Thus methods have been developed and demonstrated which cope with the problem of plant variations.

CHAPTER 6

SUMMARY

6.1 Problem Restatement

This study addresses the problem of control of the nuclear power plant during fast and large load changes. The control must take the plant through the load change smoothly - within certain constraints. Some of these constraints are explicit, such as the constraints on primary loop pressure deviations. Other constraints are implied by a combination of several variables, such as the constraints due to the combination of Xenon effects and available control reactivity. The control must make the load change rapidly, yet do so within the constraints.

The problem of control is further complicated by the variations which occur in the plant. Slow physical variations have the effect of slow changes in the plant dynamic behavior, while fast variations due to several factors make the short term behavior uncertain. A viable control must operate in the presence of these normal plant variations.

The plant variables are rapidly changing during a large, fast load change. For this reason it is essential to detect quickly any deviation from expected behavior so that the load change can be terminated before the plant variables reach deviation limits and initiate a plant shutdown. Furthermore, some means must be provided to reassure a plant operator during normal load changes that the rapid changes in the variables are normal. All these considerations are part of the load change problem.

6.2 Results of this Study

The nuclear power plant is considered at high power levels. A control of the plant during load changes is developed and tested in simulation. The control coordinates the turbine and the reactor during the load change, in order to maintain smooth plant operation during fast large load changes. The emphasis of the control is on maintaining the plant within certain constraints. These constraints are given or are calculated to keep the plant variables within acceptable limits, so that automatic plant shutdown limits will not be approached. The constraints include power rate of change, primary loop pressure, pressurizer level, primary loop average temperature, and constraints due to available control capabilities. Observing all the constraints guarantees smooth operation.

The techniques developed in this study were tested on a detailed simulation of a nuclear power plant. The high-order simulation included disturbances and measurement noise, as well as numerous nonlinear effects. The simulation was treated as an actual plant. Measurements were taken via analog to digital conversion at one second intervals. The measurements used were reactor power, primary loop average temperature*, turbine power, rod group position, and plant load set point. Control actions were via digital to analog conversion, also at one second intervals. The controls manipulated in this way were the reactor rod group speed and the turbine load set point.

The calculation of the control actions to coordinate the reactor and the turbine requires a plant model. This must be a low order model to be

*The average of two temperatures in the primary loop, one each at the reactor inlet and outlet.

useful in on-line control. This model of the plant is formed by representing the major dynamic phenomena, including the coupling between the reactor and the remainder of the plant. The reactor itself is represented by a nonlinear dynamic model which includes the effects of delayed neutron precursors, the Xenon effects, and temperature effects from the fuel and the moderator. The deterministic model of the plant is augmented with a noise model, representing the effects of random disturbances, model errors, and measurement noise. The overall model is thus a stochastic model.

Parameters of the deterministic and the noise parts of the stochastic model are identified from measurement data records. A maximum likelihood method is used for the identification. This method finds the parameters which maximize a certain probability function. The maximum likelihood method is a general technique which allows identification of both the deterministic and the noise parameters of a general state variable stochastic model.

The stochastic model is considered to be hypothetical until statistical evidence establishes that the model is consistent with the plant. A hypothesis test is formed which is sensitive to model error. The hypothesis test makes use of the measurement error residuals of a Kalman filter. An important property of the Kalman filter is used - the property that the residuals are uncorrelated in time if the model is correct. The hypothesis test is very sensitive to correlation of these residuals, and it proves to be very effective in detecting model error. The hypothesis is used to validate the identification, and also to detect plant variation.

The stochastic model is used to predict the plant performance prior to each load change. Both a nominal plant state trajectory and the covariance of the states about the trajectory are predicted. The predictions are used for two purposes. One use is to modify the state constraints, to make them more conservative, so that the stochastic model predicts a very low probability of violating the original constraints. The other use is to predict measurement bands, within which the plant measurements are expected to lie with high probability. These measurement bands are displayed before the load change begins, and the actual measurements are superposed on the display during the load change. This display is intended to provide a reassurance to the plant operator during normal load changes, and a visual warning of any unexpected behavior. The same data is used by the computer to monitor the load change.

In the event of an unacceptable plant variation, as detected by the hypothesis test or by the measurement bands test, the load change is stopped. The model parameters are then adapted based on the data taken during the abortive load change.

In summary, the results of this study demonstrate the practicality of large, fast and smooth load changes for a nuclear power plant. A coordinated control is developed which maintains smooth plant operation throughout large and rapid load changes. The control is based on a model. This model has its parameters identified and adapted to make the model a best fit to measured plant data. The model is stochastic, and both the noise and the deterministic model parameters are identified. The stochastic model is used in a variety of ways to permit control in the

presence of uncertainty. The validity of the stochastic model is checked to detect plant variation. The result of all these techniques is a control which not only provides large, fast load changes in a smooth manner, but which also can operate in the presence of variation and uncertainty.

6.3 Extensions

A subset of the results could be applied, if desired, to reduce the computer calculation time. The computer used in this study was dedicated to the load change control, while an actual plant computer must typically perform many other tasks. Thus some reduction in the scope of the control might be made for the initial plant implementation. For example, the strategy of not disturbing the primary loop average temperature during load change might be chosen as the standard strategy. By restricting the control to this strategy, the control and prediction calculations are considerably reduced. An approach like this is feasible to implement on currently available process control computer systems.

The control results of this study could be extended by considering different choices of constraints and goals for the control. For example, the desired primary loop average temperature could be a chosen function of load. This requires a minor extension of the control equations, which would still be based on the same concepts and the same model. The coordinated control in this case would still eliminate the undesirable fast transients during the load change, while producing the desired transition in the primary loop average temperature.

The techniques developed in this study could also be extended to other types of processes. In general, the features of the problem which are important are:

1. The desirability of large and fast state changes without violating some state constraints.
2. The presence of disturbances and measurement noise.
3. The possibility of plant variations.

As one example, the problems of chemical batch processing are similar to those encountered in this study, and the economic advantages of faster processing are obvious and easily calculated.

The several separate parts of this study could also be applied in various extensions. For example, as part of this study methods were developed for identifying a stochastic model of a plant given input-output measurements. The stochastic model was used, among other purposes, for constructing a Kalman filter for the process. This procedure could be considered as a separate result, available for extension to other processes - the automatic design by the computer of the Kalman filter for a process.

Another separate result which could find extended application is the hypothesis test. There are many problems where it is appropriate to use a Kalman filter to provide estimates of the plant states. In these cases, the hypothesis test can be applied to the residuals of the Kalman filter, to provide a statistical test of the validity of the filter. In this study the hypothesis test was used during load changes utilizing all the measurement data during the load change. This technique could easily be

extended to make a continuous hypothesis test. This would require using a finite memory or a weighted memory procedure, so that the hypothesis of recent valid behavior of the filter would be tested.

In summary, extensions of this study could take many forms. The separate results of stochastic model parameter identification and the uses of the model could find application in other processes in addition to nuclear power plants. The results which are specific to nuclear plant control could be used in the form developed here or the techniques could be modified, if desired, for plant application. The overall results of this study thus provide a basis for modern control of nuclear power plants and other processes which have similar control problems.

REFERENCES

1. Aanstad, D. J. "Dynamic Response and Data Constants for Large Steam Turbines." IEEE Course Text 70M29-PWR, New York: IEEE, 1970, pp. 40-49.
2. Anderson, W. N., et al. "Consistent Estimates of the Parameters of a Linear System." Annals of Mathematical Statistics, Vol. 40, pp. 2064-2075, 1969.
3. Ash, M. "Application of Dynamic Programming to Optimal Shutdown Control." Nucl. Sci. and Engr., Vol. 24, pp. 77-86, 1966.
4. Astrom, K. J. "On the Achievable Accuracy in Identification Problems." IFAC Symp. on Identification in Automatic Control Systems, Prague: September 1967.
5. Astrom, K. J., and P. Eykhoff. "System Identification, A Survey," IFAC Symp. on Identification and Process-Parameter Estimation, Prague: June 1970.
6. Athans, M., and P. Falb. Optimal Control. New York: McGraw Hill, 1966.
7. Balakrishnan, A. V. "On a New Computing Technique in Optimal Control and Its Application to Minimal-Time Flight Profile Optimization," Journal of Optimization Theory and Applications, Vol. 4, pp. 1-21, 1969.
8. Bensen, A. R. Control of Generation in the U. S. Columbia River Power System. Portland, Oregon: Bonneville Power Administration, 1966.
9. Birta, L. G., and P. J. Trushel. "An Optimal Control Algorithm Using the Davidon-Fletcher-Power Method with the Fibonacci Search," American Institute of Chemical Engineers Journal, Vol. 16, pp. 363-366, March, 1970.
10. Bjarlo, T. J., et al. "Digital Plant Control of the Holden BWR by a Concept Based on Modern Control Theory," Nucl. Sci. and Engr., Vol. 39, pp. 231-240, 1970.
11. Box, M. J. "A New Method of Constrained Optimization and a Comparison with Other Methods," British Computer Journal, Vol. 8, pp. 42-52, August 1965.

12. Brownlee, K. A. Statistical Theory and Methodology in Science and Engineering. (2nd ed.), New York: John Wiley and Sons, 1966.
13. Bryson, A. E., and Y. C. Ho. Applied Optimal Control. Waltham, Massachusetts: Blaisdell Publishing Company, 1969.
14. Bucy, R. S. "Recent Results in Linear and Nonlinear Filtering," Symp. on Stochastic Problems in Control, JACC, Ann Arbor, Michigan, 1968.
15. Busby, E. L., J. W. Skooglund, and K. L. Williams. "System Response to Severe Contingencies Including Control Systems--Transmission Line Protection and Load Management Relaying," IEEE Course Text 70M29-PWR. New York: IEEE, 1970, pp. 221-229.
16. Ciechanowicz, W., and S. Bogumil. "On the On-Line Statistical Identification of Nuclear Power Reactor Dynamics," Nucl. Sci. and Engr., Vol. 31, pp. 474-483, 1968.
17. Connecticut Yankee. System Description Documentation (SD-CYW-300). Pittsburgh, Pennsylvania: Westinghouse Electric Corporation, Atomic Power Division.
18. Cramer, H. Mathematical Methods of Statistics. Princeton, New Jersey: Princeton University Press, 1946.
19. Davidon, W. C. "Variable Metric Method for Minimization," Report ANL-5990, Argonne, Illinois: Argonne National Laboratory, 1959.
20. Denham, W. F. "Steepest-Ascent Solution of Optimal Programming Problems," Ph.D. Thesis (Applied Mathematics), Harvard, 1963.
21. Duncombe, E., and D. E. Rathbone. "Optimization of the Response of a Nuclear Reactor Plant to Changes in Demand," IEEE Trans., Vol. AC-14, pp. 277-281, June 1969.
22. El-wakil, M. M. Nuclear Power Engineering. New York: McGraw Hill, 1962.
23. Engenberger, M. A. "A Simplified Analysis of the No-Load Stability of Mechanical-Hydraulic Speed Control Systems for Steam Turbines," IEEE Course Text 70M29-PWR. New York: IEEE, 1970, pp. 101-118.
24. Fisher, R. A. "The Mathematical Foundations of Theoretical Statistics," Philosophical Transactions of the Royal Society, Series A, Vol. 222, pp. 306-368, 1922.
25. Fletcher, R., and M. J. D. Powell. "A Rapidly Converging Descent Method for Minimization," Brit. Computer Journal, Vol. 6, pp. 163-168, 1963.

26. Gyftopoulos, E. P. "Point Reactor Kinetics and Stability Criteria," Third U. N. Conference on Peaceful Uses of Atomic Energy, Geneva: 1964.
27. Habegger, L. J. "The Use of the Kalman Filter for the Estimation of Nuclear Reactor Parameters," Ph.D. Thesis (Nuclear Engineering), Purdue University, 1968.
28. Hald, A. Statistical Tables and Formulas. New York: John Wiley and Sons, 1952.
29. Hildebrand, F. B. Introduction to Numerical Analysis. New York: McGraw Hill, 1956.
30. Ho, Y. C., and R. C. K. Lee. "A Bayesian Approach to Problems in Stochastic Estimation and Control," IEEE Trans., Vol. AC-9, pp. 333-339, October 1964.
31. Jacobson, D. H., and W. Oksman. "An Algorithm that Minimizes Homogeneous Functions of N Variables in N+2 Iterations and Rapidly Minimizes General Functions," Technical Report No. 618, Cambridge, Massachusetts: Harvard University, Division of Engineering and Applied Physics, October 1970.
32. Jazwinski, A. H. "Adaptive Filtering," Automatica, Vol. 5, pp. 475-485, 1969.
33. -----, Stochastic Processes and Filtering Theory. New York: Academic Press, 1970.
34. Kalman, R. E. "Linear Stochastic Filtering Theory--Reappraisal and Outlook," Symp. on System Theory, Polytech. Institute of Brooklyn, New York, N.Y., April, 1965.
35. Kalman, R. E. and R. S. Bucy. "New Results in Linear Filtering and Prediction Theory," ASME Journal of Basic Engrg., Vol. 83, pp. 95-108, March 1961.
36. Kashyap, R. L. "Maximum Likelihood Identification of Stochastic Linear Systems," IEEE Trans., Vol. AC-15, February, 1970.
37. Kendall, M. G., and A. Stuart. The Advanced Theory of Statistics. Volume 2: "Inference and Relationship," New York: Hafner Publishing Company, 1961.
38. Kimbark, E. W. Power Systems Stability. Volume 3: "Synchronous Machines," New York: Dover Publishing Company, 1968.

39. Klopfenstein, A. "Response of Steam and Hydroelectric Generating Plants to Generation Control Tests," AIEE Trans. Power Apparatus and Systems, Vol. 78, pp. 1371-1381, December 1959.
40. Kushner, H. J. "Approximations to Optimal Nonlinear Filters," IEEE Trans., Vol. AC-12: 546-556, October 1967.
41. Lamarsh, J. R. Nuclear Reactor Theory. Reading, Massachusetts: Addison-Wesley, 1966.
42. Lee, R. C. K. Optimal Estimation, Identification and Control. Cambridge, Massachusetts: M.I.T. Press, 1964.
43. Lewins, J., et al. "Energy Optimal Xenon Shutdown," Nucl. Sci. and Engr., Vol. 31, pp. 272-281, 1968.
44. Lipinski, W. C. "Optimal Digital Computer Control of Nuclear Reactors," Report ANL-7530, Argonne, Illinois: Argonne National Laboratory, 1969.
45. Marciniak, T. J. "Time Optimal Digital Control of Zero-Power Nuclear Reactors," Report ANL-7510, Argonne, Illinois: Argonne National Laboratory, 1968.
46. Mehra, R. K. "On the Identification of Variances and Adaptive Kalman Filtering," IEEE Trans., Vol. AC-15, pp. 175-184, April 1970.
47. Monta, K. "Time Optimal Digital Computer Control of Nuclear Reactor," Journal of Nuclear Science and Technology, (Japan), Part I, 3, 227, June 1966; Part II, 3, 418, October, 1966, Part III, 4, 51, February, 1967.
48. Nishimura, T. "Error Bounds of Continuous Kalman Filters and the Application of Orbital Determination Problems," IEEE Trans., Vol. AC-12, pp. 268-275, June 1967.
49. Papoulis, A. Probability, Random Variables, and Stochastic Processes. New York: McGraw Hill, 1965.
50. Partain, C. L. and R. E. Bailey. "An Application of Time Optimal Control Theory to the Nuclear Reactor Startup Problem," JACC Preprints, New York: Lewis Winner Publishing Co., 1967.
51. Redfield, J. A., V. Prescop, and S. G. Margolis. "Pressurizer Performance During Load Drop Tests at Shippingport: Analysis and Test," Transactions American Nuclear Society, Vol. 10, No. 1, p. 323, June 1967.

52. Roberts, J. J., and H. P. Smith. "Time Optimal Solution to the Reactivity-Xenon Shutdown Problem," Nucl. Sci. and Engr., Vol. 22, pp. 470-478, 1965.
53. Roberts, J. J., R. F. Fleming, and H. P. Smith. "Experimental Application of the Time-Optimal Xenon Shutdown Program," Nucl. Sci. and Engr., Vol. 27, pp. 573-580, 1967.
54. Rosztoczy, Z. R., and L. E. Weaver. "Optimal Reactor Shutdown Program for Minimum Xenon Buildup," Nucl. Sci. and Engr., Vol. 20, pp. 318-323, 1964.
55. Sage, A. P., and G. W. Masters. "Identification and Modeling of Nuclear Reactors," IEEE Trans. on Nuclear Science, Vol. NS-14, No. 1, pp. 279-285, February 1967.
56. Sage, A. P., and J. L. Melsa. "Applications of Modern Control Theory to Nuclear Reactor Systems," Electrical Engineering Transactions (Australia), Vol. EE5, No. 1, pp. 61-72, March 1969.
57. Sakrison, D. J. "The Use of Stochastic Approximation to Solve the System Identification Problem," IEEE Trans., Vol. AC-12, pp. 563-567, October 1967.
58. Schweppe, F. C. Uncertain Dynamic Systems (to be published), Prentice Hall, New York, 1972.
59. Speyer, J. L., and A. E. Bryson. "Optimal Programming Problems with a Bounded State Space," AIAA Journal, Vol. 6, pp. 1488-1491, August 1968.
60. Thie, J. Reactor Noise. New York: Rowman and Littlefield, 1963.
61. United States Atomic Energy Commission, "Current Status and Future Technical and Economic Potential of Light Water Reactors," Report WASH 1082, Washington, D.C.: U.S. Government Printing Office, 1968.
62. Van Wylan, G. J. Thermodynamics. New York: John Wiley and Sons, 1959.
63. Von Neumann, J., et al. "The Mean Square Successive Difference," Annals of Mathematical Statistics, Vol. 12, pp. 153-162, 1941.
64. Weaver, L. E. Reactor Dynamics and Control. New York: American Elsevier, 1968.
65. Wishner, R. P., U. A. Tabaczynski, and M. Athans. "A Comparison of Three Nonlinear Filters," Automatica, Vol. 5, pp. 487-496, 1969.

APPENDIX A
THE NUCLEAR PLANT SIMULATION

The analog simulation described here was used in lieu of a plant for experimental testing. A number of parts of a pressurized water nuclear plant were individually simulated, and these parts were connected as in an actual plant to provide the overall coupled performance. The result may not match plant performance exactly, but it does provide similar behavior. The simulation includes a number of nonlinear effects, disturbance effects, and measurement noise effects to make the performance more realistic.

The simulation was constructed on an EAI-680 analog computer. There were 64 amplifiers included, of which 23 were integrators. The nonlinearities were produced by 2 dividers, a function generator and 4 limiters. The disturbance and measurement noise originated from a noise diode. The simulation was connected to an EAI-640 digital computer, which treated the simulation as if it were an actual plant. The digital computer was used for the prediction, adaptation and control tasks. The data from the simulated plant were acquired by analog to digital conversion at one second intervals.

In forming the simulation, the first level of approximation was in the choice of the time period of interest. Simulations of nuclear reactors and turbine-generators are often used in accident or line fault studies, where fast transients due to abnormal operation are of interest. In this

study phenomena which occur faster than about one second are considered to be instantaneous. On the other hand, phenomena which occur over a long time span are considered to be parameter changes. Table A-1 lists some of the transient phenomena associated with nuclear power plants and the time period which they occur.

The second level of approximation was to lump the various distributed phenomena in the plant into simpler lumped model forms. This approximation was somewhat subjective and it involved consideration of the analog computer capabilities as well as consideration of retaining accuracy. Table A-2 gives a description of the complexity of this simulation.

The specific parts of the plant in the simulation are:

- the reactor
- the pressurizer
- the heat exchanger
- the turbine
- analog control systems for the pressurizer, turbine, and rod control

These parts are discussed in the remainder of this appendix. The overall simulation structure is given in Figure A-1 to show the interconnection of the parts of the plant. The physical simulation facility is shown in Figure A-2.

The model of the reactor kinetics is now considered. The well known point kinetic model of the reactor kinetics is used [41]. The effects which are simulated are:

TABLE A-1

Time Periods of Common Nuclear Power Plant Phenomena

<u>Time Period</u>	<u>Phenomena</u>
days - months	fuel depletion, corrosion and fouling of heat exchanger and turbine.
hours	isotope buildup of I^{135} , Xe^{135} spatial oscillations.
seconds to minutes	load change effects on pressure, temperature, energy transfer, reactor kinetics, Xenon transients at high power.
less than a second	local reactor power excursions. power system transients.

TABLE A-2
A Description of Simulation Complexity

<u>Subsystem</u>	<u>Simulation</u>
Neutron Kinetics including Xenon Effects	Nonlinear, 4 states
Primary Loop Energy Transfer	Linear, 4 states
Steam Generator	Linear, 4 states
Pressurizer including Analog Control	Nonlinear, 4 states
Rod Control including Analog Control	Nonlinear, 4 states
Turbine including Analog Control	Linear, 3 states

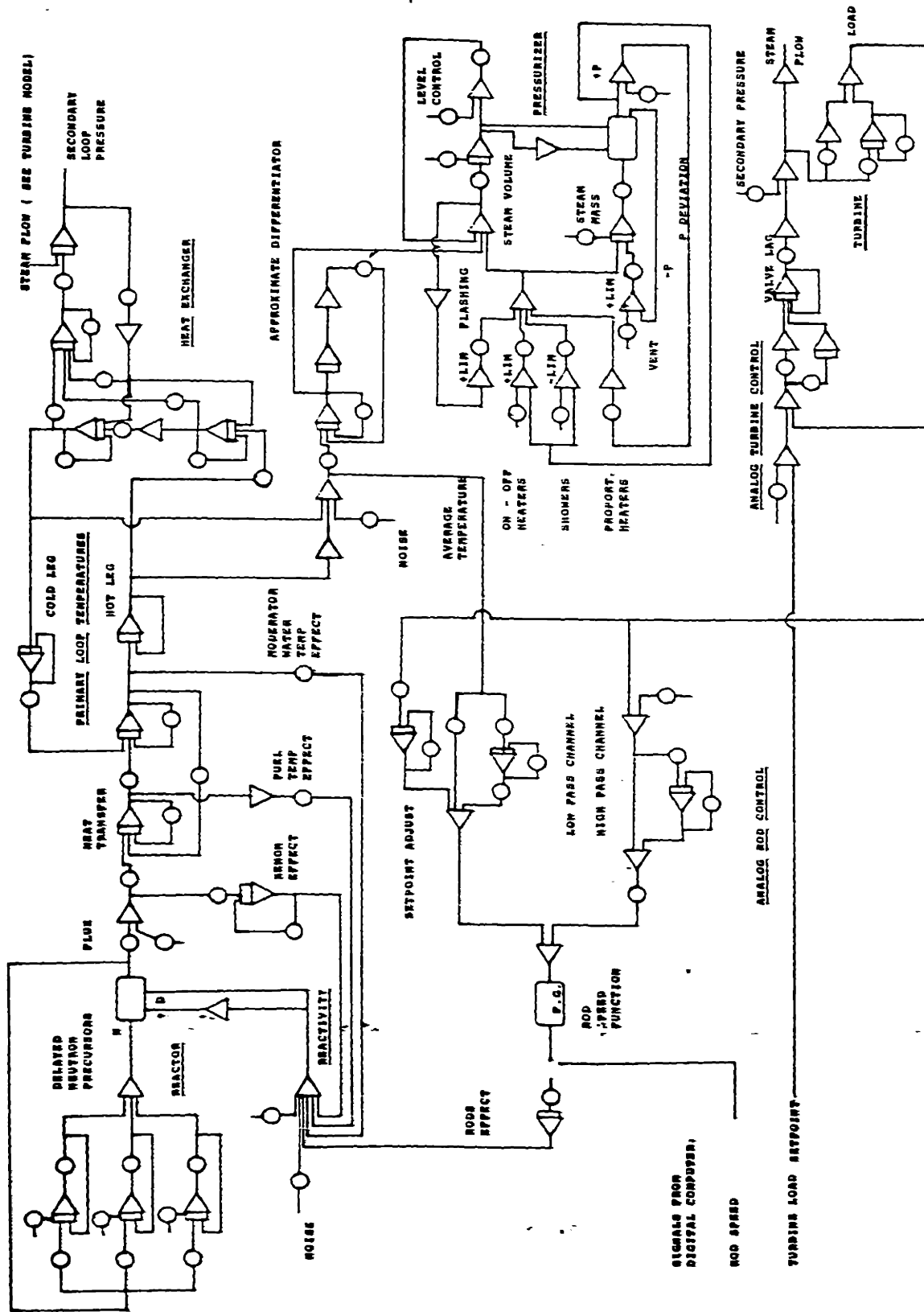


FIGURE A-1 Overall Simulation



FIGURE A-2 Physical Simulation Facility

fission

delayed neutron precursor isotopes

Xenon reactivity effect

moderator feedback reactivity

fuel feedback reactivity

control rod effect reactivity

The nomenclature is:

n neutron flux

c_i concentration of delayed precursor i

β_i fraction of fission neutrons which form precursor i

λ_i delay constant for precursor i

Λ prompt lifetime

The slowest three delayed neutron precursor groups are retained in the simulation. The first group neglected has a time constant of approximately 3 seconds. The point kinetic model is:

$$\frac{dn}{dt} = \frac{\rho - \beta}{\Lambda} n + \sum_{i=1}^3 \lambda_i c_i \quad (\text{A-1})$$

$$\frac{dc_i}{dt} = \frac{\beta_i}{\Lambda} n - \lambda_i c_i \quad i=1,2,3 \quad (\text{A-2})$$

$$\beta = \sum_{i=1}^3 \beta_i \quad (\text{A-3})$$

If the net reactivity $\rho \ll \beta$, then the prompt jump approximation holds and the first equation is approximately

$$\rho = \frac{\Lambda}{\beta - \rho} \sum_{i=1}^3 \lambda_i c_i \quad (\text{A-4})$$

The modeled reactivity effects are:

$$\begin{aligned} \rho_D &= \alpha_D \Delta T_M && \text{fuel effect} \\ \rho_M &= \alpha_M \Delta T_W && \text{moderator effect} \\ \rho_R &= \alpha_R \Delta R && \text{rod effect} \\ \rho_X &= \alpha_X \Delta X && \text{Xenon effect} \end{aligned}$$

where:

ΔT_M is change in metal temperature
 ΔT_W is change in water temperature
 ΔR is change in rod position
 ΔX is change in Xenon concentration

The dynamic equation of the Xenon is:

$$\frac{dX}{dt} = \lambda_I I - \lambda_X X - \sigma_{ax} nX \quad (\text{A-5})$$

where:

λ_I is decay constant for I^{135} , the precursor to Xe^{135}
 λ_X is the decay constant for X^{135}
 σ_{ax} is the absorption cross section of Xenon

The direct creation of Xenon by fission is a relatively small effect which has been neglected. The iodine concentration, a very slow changing effect,

is a constant in the simulation. This approximation reflects the fact that short term experiments were of interest. A simulation valid for long term experiments over a period of hours would include the buildup and decay of iodine according to:

$$\frac{dI}{dt} = \gamma_I \Sigma_f n - \lambda_I I \quad (A-6)$$

where:

γ_I is the fractional yield of I^{135}

Σ_f is the fission cross section

The control rods are generally manipulated by an analog control system. The simulation had the capability for either digital or analog rod control, with the choice determined by the state of a relay under computer or manual control. The block diagram with the analog rod control transfer functions is shown in Figure A-3. The basic operation is that the set point for the primary loop average temperature T_{av} is a function of steady state load. The rod control responds to deviations in T_{av} from this set point. The control also responds if a load mismatch between reactor and turbine load is detected. The simulation model is the same as the actual rod control, with a function generator used to represent the rod speed nonlinearity.

The heat transfer to the primary loop is now considered. The residence time of water in the core is less than two seconds. The heat transfer to this water was modeled as a two state process:

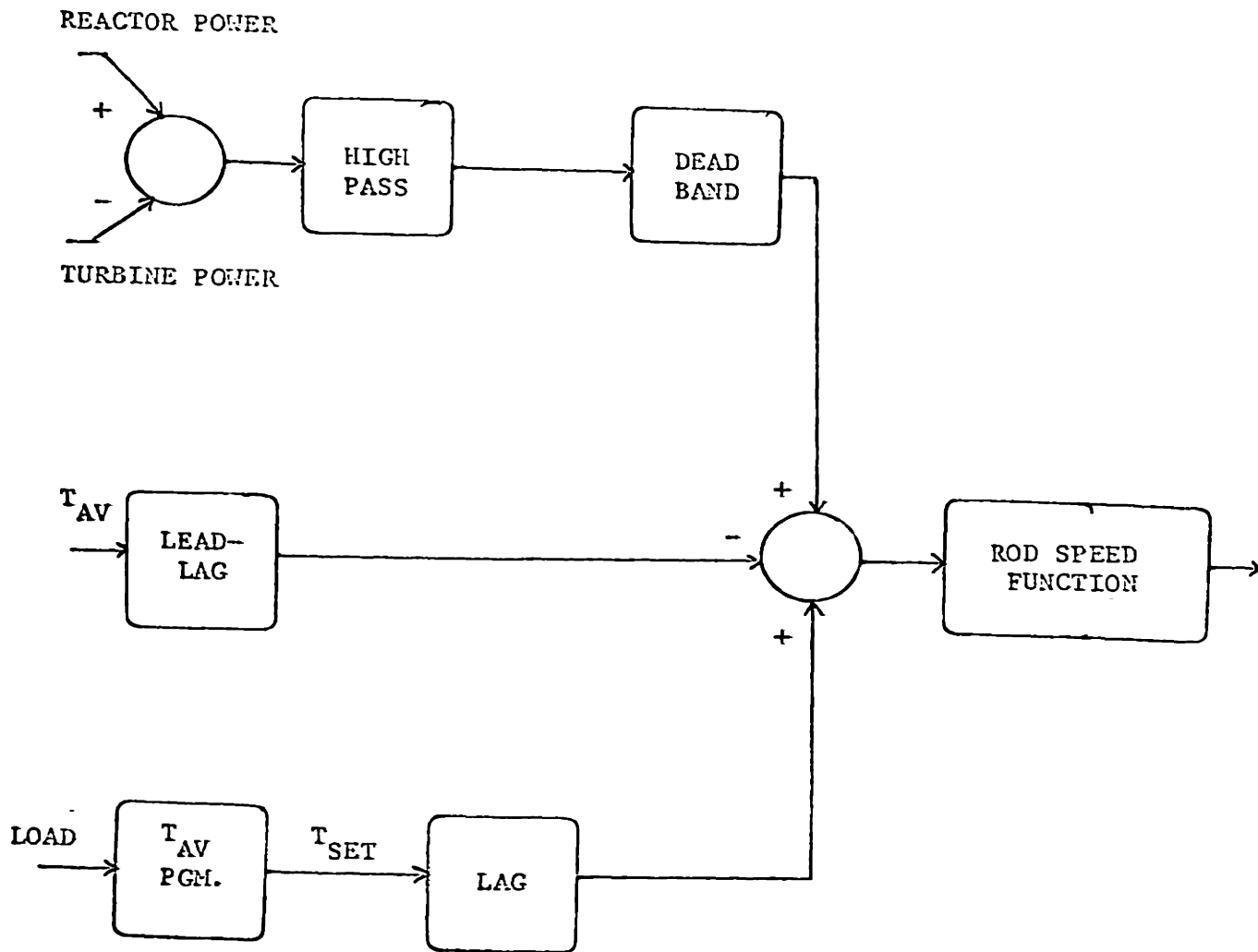


FIGURE A-3 Analog Rod Control

$$\frac{dT_W}{dt} = - \left(\frac{F_W}{V_W} + \frac{ShL}{V_W \rho_W c_W} \right) T_W + \frac{F_W}{V_W} T_{W_{in}} + \frac{ShL}{V_W \rho_W c_W} T_M \quad (A-7)$$

$$\frac{dT_M}{dt} = \frac{-ShL}{V_M \rho_M c_M} T_M + \frac{ShL}{V_M \rho_M c_M} T_W + \frac{P}{V_M \rho_M c_M} \quad (A-8)$$

The subscript M refers to the metal in the core fuel; the subscript W refers to the water in the core. The other parameters are:

V volume

ρ density

c heat capacity

F flow

L length of core

S effective core heat transfer area per unit length of core

h heat transfer coefficient

P thermal power generated in core

The pressurizer on the primary loop is now considered. The purpose of the pressurizer is to counteract the changes in pressure due to change in water volume as temperature changes. The pressurizer includes sprays, heaters and vent valves as control elements. The phenomena of flashing and condensation play a major role in the pressurizer behavior. A simulation of the pressurizer based on the physical phenomena, thermodynamic data, and the analog control system was developed. The simulation used for the pressurizer in this study is:

A. Expansion flow

$$f_T = \alpha_W \frac{d T_{AV}}{dt} \quad (A-9)$$

T_{AV} = average of hot and cold leg temperature

α_W = coefficient of expansion (8 ft³/°F for this study)

B. Liquid mass balance

$$\frac{dM_W}{dt} = f_T + f_C - f_{WS} \quad (A-10)$$

M_W = mass in pressurizer (water)

f_C = charging flow

f_T = expansion flow

f_{WS} = water to steam flow

C. Steam mass balance

$$\frac{dM_S}{dt} = f_{WS} - f_V \quad (A-11)$$

f_V = vent flow

D. Controlled flows

Vent flow:

f_V is zero when $P < P_2$ and f_V increases with very high gain if $P > P_2$, where P_2 is a set limit.

Water to steam flow:

$$f_{WS} = f_H - f_D + f_F \quad (A-12)$$

Heaters: f_H = Heater contribution, on when $P < P_3$, a set limit

Condensation: f_D = condensation flow, which changes from a small number for $P < P_1$, a set limit, to a large number for $P > P_1$. This accounts for wall condensation as well as showers.

Flashing: f_F = flashing, which rises with very high gain during steam volume increases.

The pressurizer level control is a very slow control. The primary system is (in the absence of accidents) a constant mass system which will have level transients during temperature transients.

The simulation of the heat exchanger or steam generator is now considered. The steam generator is a shell and tube heat exchanger. The steaming causes the void fraction on the secondary side to vary up the generator. This void fraction, which is sensitive to secondary loop pressure, affects the heat transfer between the primary and secondary loops. The level in the steam generator is sensitive to the pressure on the secondary side, due to the effect on voids. This affects the feed-water rate somewhat, due to the level control system. However, in practice this control is adjusted to be quite slow due to the assumption that the secondary loop is constant mass, and therefore, level transients are ignored unless they persist (control action) or exceed specified bounds (emergency action).

Figure A-4 shows a block diagram of the steam generator model. The equations for the blocks are:

A. Primary side inlet lump

$$\frac{dT_{11}}{dt} = - \left(\frac{F_1}{V_{11}} + \frac{SK_1 L}{V_{11} \rho_W c_W} \right) T_{11} + \frac{F_1}{V_{11}} T_H + \frac{SK_1 L}{V_{11} \rho_W c_W} T_2 \quad (A-13)$$

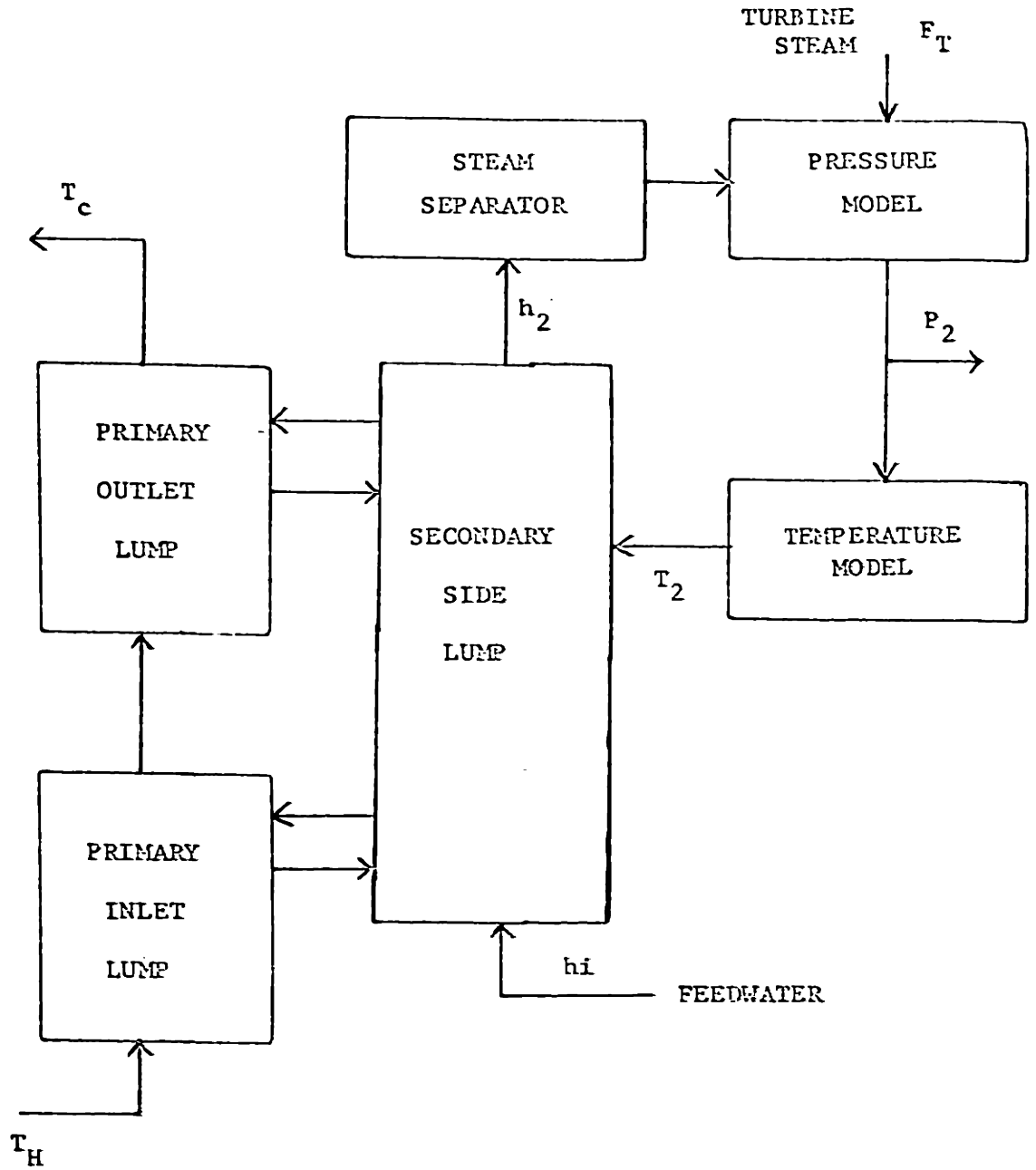


FIGURE A-4 Block Diagram of Heat Exchanger

where

T_{11} is the lumped temperature

T_H (inlet) hot leg temperature

T_2 secondary side lump temperature

$\left(\frac{V_{11}}{F_1}\right)$ primary lump residence time, is on the order of 3 seconds

$\left(\frac{SK_1L}{V_{11} W c_W}\right)$ overall heat transfer coefficient, where K_1 is conventional heat transfer coefficient

B. Primary side outlet lump

$$\frac{dT_{12}}{dt} = - \left(\frac{F_1}{V_{12}} + \frac{SK_2L}{V_{12} \rho_W c_W} \right) T_{12} + \frac{F_1}{V_{12}} T_{11} + \frac{SK_2L}{V_{12} \rho_W c_W} T_2 \quad (A-14)$$

T_{12} is the outlet of the primary loop side, also called T_c or cold leg temperature

C. Secondary side, energy balance

$$\frac{dh_2}{dt} = - \frac{F_2}{V_2} h_2 + \frac{F_2}{V_2} h_i - \frac{SKL}{V_2 \rho_W} (2T_2 - T_{11} - T_{12}) \quad (A-15)$$

h_2 is specific enthalpy in the secondary lump

h_i is feedwater enthalpy

D. Secondary side, steam separation

$$h_2 = h_f + x h_{fg} \quad (A-16)$$

$$x = \frac{h_2 - h_f}{h_{fg}} \quad (A-17)$$

$$F_s = F_2 \rho_W x \quad (A-18)$$

E. Secondary side, pressure

$$\tau \frac{dP_2}{dt} = F_S - F_T \quad (A-19)$$

F_T is steam flow to turbine

τ is time constant of pressure response

F. Secondary side, temperature in generator lump

The Clapeyron equation [62], at saturation, gives

$$\frac{dP}{dT} = \frac{h_{fg}}{T(v_g - v_f)} \quad (A-20)$$

The turbine model used in this study is one proposed by Aansted [1]. This model is shown in Figure A-5. The throttle valves are modeled as a linear relationship. The pressure P in the steam generator and the valve open area A both affect the steam flow to the turbine f_T . The analog control system for the turbine accepts inputs from the load dispatcher and from a speed control regulation system. In this study the load set point, one of the major plant inputs from the control point of view, is the load dispatcher input of the simulation. The speed or frequency control is not used in this study.

The details of variable scaling are presented in Table A-3. In general, the major variables are scaled in powers of 10 from their common engineering units. Simulation variables all have internal simulation values of magnitude less than 1.0.

The major simulation details are shown in Figure A-1. The variables and parameters labeled on the drawings are actually scaled by various

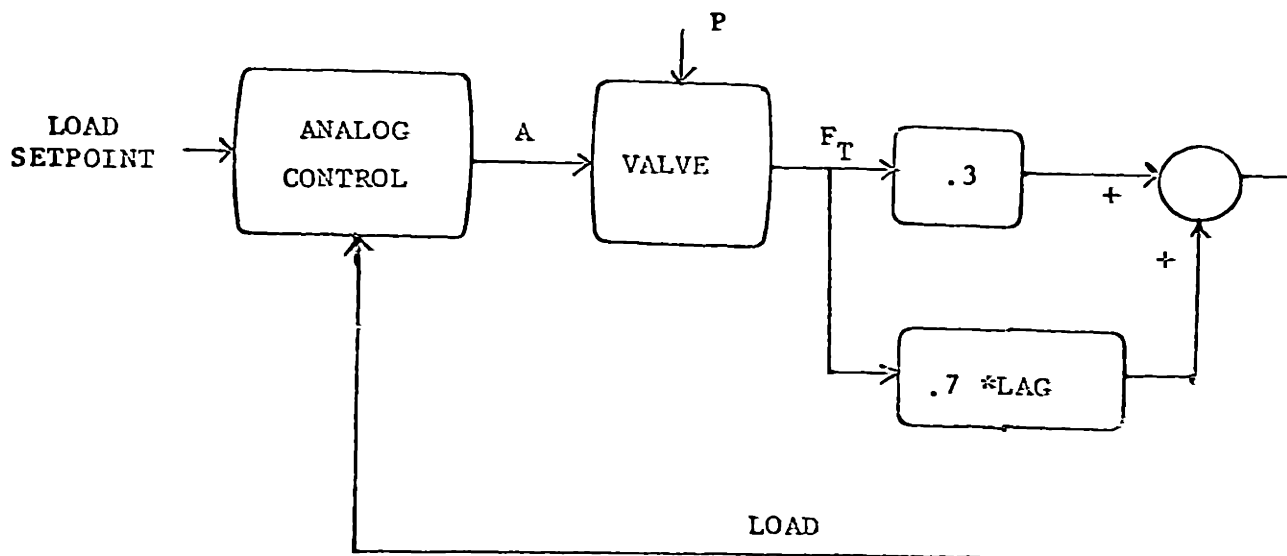


FIGURE A-5 Turbine Model

TABLE A-3
Simulation Variable Scaling

Note: All time scaling is 1.0, that is a real time simulation was used.

<u>Variable</u>	<u>Description</u>	<u>Full Scale Value</u>
H	Reactor Power	30,000 M.W.T.
ρ	Reactivity	.01 $\Delta K/K$
ΔT	Temperatures (Deviation)	100°F, 1000°F
Δh	Enthalpy (Deviation)	100 btu/lb.
f_T	Total Surge	100 ft ³ /sec.
V	Pressurizer Volume	1000 ft ³
Δf_{ws}	Water-Steam Flow (Deviation)	1000 ft ³ /sec.
P_1	Primary Pressure	10000 psi
ΔL	Load (Deviation)	1000 MW
ΔP_2	Secondary Pressure (Deviation)	1000 psi

factors which are omitted from the drawings for clarity.

It could be argued that a less noisy simulation would result if the scaling were "optimized". However, this would not only involve more effort, it would also be placing over-reliance on the deterministic aspect of the simulation. In fact, the process is subject to disturbances and the measurements are noisy, and it was necessary to add noise to the simulation to produce similar noisy effects. Thus, there was no point in complicating the problem by using awkward yet less noisy scaling.

Several responses of the plant are discussed in Chapter 2, and the measurement records are given there. The simulation appears to perform as a plant would, in terms of similar transients.

APPENDIX B
THE KALMAN FILTER

The problem under consideration is to find an optimal estimate of the state of a linear system. There are various criteria which could be used to define the optimal estimate, such as minimum variance linear estimate, maximum likelihood estimate and other criteria. There is one estimator, the Kalman filter [35], which is optimal under a number of these criteria for certain reasonable models of the disturbance and measurement noise of the process. This filter is easily operated in an on-line computer system, since the filter equations are simple. Thus the Kalman filter has assumed a great importance in modern system control over the last decade, due to its desirable theoretical properties and its ease of implementation.

Of the various derivations of the Kalman filter, one of the simplest uses the minimum variance linear estimate as the criterion. That is, the estimate is to be the result of a linear system operating on the data, and it is to be the estimate with minimum variance of all such linear estimates. This derivation, which is presented in this appendix, does not assume a probability distribution for the noise; it merely requires known means and covariances. However, if the noise is assumed to be Gaussian, then an additional result can be claimed: that the conditional probability distributions of the estimates given the data are known. This is true because for Gaussian distributions the minimum variance linear

estimate is also the conditional mean estimate [58]. The knowledge of the mean and covariance then specify the conditional distribution, since it is Gaussian. Thus although the derivation presented here does not require the assumption of Gaussian noise, such an assumption greatly extends the theoretical interpretations of the resulting Kalman filter. Of course, in an application the final test of the assumption is to test the performance of the filter. This was done to some extent in this thesis by means of a hypothesis test.

The derivation of the Kalman filter using the minimum variance linear estimate criterion is now considered. A process is assumed of the form:

$$\tilde{\underline{x}}_{K+1} = A_K \tilde{\underline{x}}_K + \underline{v}_{K+1} \quad (B-1)$$

$$\tilde{\underline{z}}_K = C_K \tilde{\underline{x}}_K + \underline{w}_K \quad (B-2)$$

where

$\tilde{\underline{x}}_K$ is an N dimensional vector of states

$\tilde{\underline{z}}_K$ is an M dimensional vector of plant measurements

\underline{v}_K is an N dimensional vector of zero mean white noise,
independent of all states and all other noise vectors

\underline{w}_K is an M dimensional vector of zero mean white noise,
independent of all states and all other noise vectors

The covariances of the noise vectors are taken as

$$\text{Cov}(\underline{v}_K) = V \quad (B-3)$$

$$\text{Cov}(\underline{w}_K) = W \quad (B-4)$$

The noise is assumed stationary here, although this is not needed in the derivation.

The covariance of the state is taken as:

$$\text{Cov}(\tilde{\underline{x}}_K) = \Gamma_K \quad (\text{B-5})$$

Thus the covariance of the measurements is:

$$\text{Cov}(\tilde{\underline{z}}_K) = C_K \Gamma_K C_K' + W \quad (\text{B-6})$$

The mean of the state at time K, before considering the measurements at time K, is:

$$\mathcal{E}(\tilde{\underline{x}}_K) = \hat{\underline{x}}_{-K|K-1} \quad (\text{B-7})$$

Thus the mean of the measurements, before observing the measurements, is:

$$\mathcal{E}(\tilde{\underline{z}}_K) = C_K \hat{\underline{x}}_{-K|K-1} \quad (\text{B-8})$$

The vector

$$\begin{bmatrix} \tilde{\underline{x}}_K \\ \tilde{\underline{z}}_K \end{bmatrix}$$

is considered. This has mean and covariance, a-priori

$$\mathcal{E} \begin{bmatrix} \tilde{\underline{x}}_K \\ \tilde{\underline{z}}_K \end{bmatrix} = \begin{bmatrix} \hat{\underline{x}}_{-K|K-1} \\ C_K \hat{\underline{x}}_{-K|K-1} \end{bmatrix} \quad (\text{B-9})$$

$$\text{Cov} \begin{bmatrix} \tilde{x}_K \\ \tilde{z}_K \end{bmatrix} = \begin{bmatrix} \Gamma_K & \Gamma_K C_K' \\ C_K \Gamma_K & C_K \Gamma_K C_K' + W \end{bmatrix} \quad (\text{B-10})$$

The assumed form of the estimate is linear.

$$\hat{x}_{K|K} = \hat{x}_{K|K-1} + K_K (\tilde{z}_K - C_K \hat{x}_{K|K-1}) \quad (\text{B-11})$$

The criterion of minimum variance is satisfied if the estimate error is uncorrelated to the data. Any other estimate, giving an estimate error correlated to the data, adds at least a positive semidefinite matrix to the covariance [58].

The criterion of uncorrelated estimate error and measurement gives the equation:

$$0 = \mathcal{E} [(\tilde{x}_K - \hat{x}_{K|K}) (\tilde{z}_K - C_K \hat{x}_{K|K-1})'] \quad (\text{B-12})$$

Expanding

$$0 = \mathcal{E} [(\tilde{x}_K - \hat{x}_{K|K-1} - K_K (\tilde{z}_K - C_K \hat{x}_{K|K-1})) (\tilde{z}_K - C_K \hat{x}_{K|K-1})'] \quad (\text{B-13})$$

where \tilde{z}_K is as given by equation (B-2). It is noted that $\hat{x}_{K|K-1}$ is viewed as a given constant for this one step estimation problem, so that this expression reduces to

$$0 = \Gamma_K C_K' - K_K (C_K \Gamma_K C_K' + W) \quad (\text{B-14})$$

So the minimum variance linear estimator of equation (B-11) is determined by

$$K_K = \Gamma_K C_K' (C_K \Gamma_K C_K' + W)^{-1} \quad (\text{B-15})$$

Other forms of the Kalman filter result from various matrix identities [58]. The covariance of the a-posteriori estimate is given by:

$$P_K = \Gamma_K - \Gamma_K C_K' (C_K \Gamma_K C_K' + W)^{-1} C_K \Gamma_K \quad (B-16)$$

or by a matrix identity

$$P_K = (\Gamma_K^{-1} + C_K' W^{-1} C_K)^{-1} \quad (B-17)$$

The a-priori estimate at time $K+1$ is found by propagating the model equation (B-1)

$$\hat{x}_{K+1|K} = \mathcal{E}(\tilde{x}_{K+1}) = A_K \hat{x}_{K|K} \quad (B-18)$$

$$\Gamma_{K+1|K} = A_K P_K A_K' + V \quad (B-19)$$

The Kalman filter consists of propagating the estimates using equations (B-18) and (B-19) and updating the estimates using equations (B-11), (B-15) and (B-16). Both the estimated states and the covariance of the estimates are calculated.

BIOGRAPHICAL NOTE

Robert Moore was born in 1942 in Chicago, Illinois. He attended The University of Michigan, where he received degrees of Bachelor of Science in Electrical Engineering (1964) and in Engineering Mathematics (1964). He worked as a part time computer programmer during his undergraduate education. From 1964 to 1966 Mr. Moore was a graduate student at the Massachusetts Institute of Technology, where he received his Master of Science in Electrical Engineering (1965) and (professional) Electrical Engineer Degree (1966). From 1966 to 1968 he worked as an Application Development Engineer in the Digital Systems Division of The Foxboro Company. In 1968 Mr. Moore returned to M.I.T. to pursue the Ph.D. degree. His major area was automatic control and his minor area was management.

END
PLEIA